

BODE IDEAL CUTOFF ANALYSIS FOR PREDICTION  
OF PILOT OPINION RATINGS

By

JOUNGUK KIM

Bachelor of Science  
Pusan National University  
Pusan, Korea  
1982

Master of Science  
Oklahoma State University  
Stillwater, Oklahoma  
1988

Submitted to the Faculty of the  
Graduate College of the  
Oklahoma State University  
in partial fulfillment of  
the requirements for  
the Degree of  
DOCTOR OF PHILOSOPHY  
December, 1993

BODE IDEAL CUTOFF ANALYSIS FOR PREDICTION  
OF PILOT OPINION RATINGS

Thesis Approved:

*Robert L. Swain*

Thesis Advisor

*Pat M. Wood*

*R. J. Lowery*

*Martin T. Hagan*

*Thomas C. Collins*

Dean of the Graduate College

## ACKNOWLEDGMENTS

I would like to express my deepest gratitude to Dr. R. L. Swaim, Chairman of my doctoral committee and my thesis advisor, for suggesting the problem, providing guidance and many hours of valuable time during my research. I also thank Dr. R. L. Lowery, Dr. P. M. Moretti, and Dr. M. T. Hagan, my doctoral committee members, for their interest and assistance.

I extend my appreciation to my mother who supported me for making my graduate study at O.S.U. possible. I thank my wife and two sons who endured difficult times. This work is dedicated to them.

## TABLE OF CONTENTS

Chapter	Page
I. INTRODUCTION . . . . .	1
1.1 Problem Statements . . . . .	1
1.2 Objectives and Scope . . . . .	2
II. LITERATURE REVIEWS . . . . .	4
2.1 Mathematical Pilot Model . . . . .	4
2.2 Pilot Opinion Ratings . . . . .	6
III. THEORIES . . . . .	19
3.1 Representation of Human Behavior . . . . .	19
3.2 Optimal Control Model . . . . .	21
3.3 Time Domain Performance . . . . .	27
3.4 Pilot Transfer Function . . . . .	28
3.5 Bode Ideal Cutoff Analysis . . . . .	32
IV. IMPLEMENTATION . . . . .	45
4.1 Descriptions of the Numerical Simulation . . . . .	45
4.2 Application of the Kleinman Data . . . . .	46
4.2.1 Velocity Control Example . . . . .	48
4.2.2 Acceleration Control Example . . . . .	56
4.3 Application of the Neal-Smith Data . . . . .	61
4.3.1 Neal-Smith Tracking Task . . . . .	61
4.3.2 Results and Discussions . . . . .	68
V. SUMMARY AND CONCLUSIONS . . . . .	90
REFERENCES . . . . .	92
APPENDIX - MATLAB PROGRAM FOR OPTIMAL CONTROL MODEL . . . . .	94

## LIST OF TABLES

Table		Page
2.1.	Frequency Domain Approach . . . . .	7
2.2.	Time Domain Approach . . . . .	9
4.1.	Input Parameters of Velocity Control Example . . . . .	50
4.2.	Time Domain Performance of Velocity Control Example . . . . .	50
4.3.	Input Parameters of Acceleration Control Example . . . . .	57
4.4.	Time Domain Performance of Acceleration Control Example . . . . .	57
4.5.	Neal-Smith Configurations . . . . .	64
4.6.	Input Parameters for Neal-Smith Pitch Tracking Task . . . . .	67
4.7.	Group Summary . . . . .	74
4.8.	Summary of Effects of Perceptual Time Delay (2D) . . . . .	88

## LIST OF FIGURES

Figure	Page
1.1. The Cooper-Harper Rating Scale . . . . .	3
2.1. Block Diagram of the Optimal Control Model . . . . .	6
2.2. Neal-Smith Pilot/Vehicle Model Structure . . . . .	12
2.3. Neal-Smith Control Strategy in Tracking Task . . . . .	12
2.4. Neal-Smith Results . . . . .	13
2.5. Control Theoretical Model of Optimal Human Behavior . . . . .	13
2.6. Human Optimal Control Model . . . . .	14
2.7. Hess Results . . . . .	14
2.8. Schmidt Results (Arnold Configurations) . . . . .	15
2.9. Schmidt Results (Neal-Smith Configurations) . . . . .	16
2.10. Model Comparison (Bacon-Schmidt) . . . . .	17
2.11. Bacon-Schmidt Results (Neal-Smith Configurations) . . . . .	17
2.12. Multi-Loop Flight Path Tracking Task (Anderson-Schmidt) . . . . .	18
2.13. Anderson-Schmidt Results . . . . .	18
3.1. General Loop Structure of the Man-Machine System . . . . .	20
3.2. Block Diagram of Optimal Control Model . . . . .	27
3.3. Optimal Pilot Transfer Function . . . . .	29
3.4. Standard Feedback Control Structure . . . . .	33
3.5. Implications of the Integral Allowing Reshaping. . . . .	37
3.6. Desired Shape of Open Loop Transfer Function . . . . .	38
3.7. Improper Adding of the High Frequency Rolloff . . . . .	39
3.8. The Bode Ideal Cutoff . . . . .	40

Figure	Page
3.9.	Interpretation of the Bode Ideal Cutoff . . . . . 42
3.10.	Important Factors of the Ideal Cutoff . . . . . 43
3.11.	Correlation of Time Domain and Frequency Domain Loop Structure . . . . 44
4.1.	Computation Flow of the Optimal Control Model . . . . . 47
4.2.	Phase Plot of the Pade Approximation for 0.2 sec Delay . . . . . 48
4.3.	Magnitude Plot of Open Loop Response (Velocity Control) . . . . . 53
4.4.	Phase Plot of Open Loop Response (Velocity Control) . . . . . 53
4.5.	Closed Loop Response (Velocity Control) . . . . . 54
4.6.	Comparison of Kleinman Model and Approximated Model. . . . . 54
4.7.	Magnitude Plot of Pilot Transfer Function (Velocity Control) . . . . . 55
4.8.	Phase Plot of Pilot Transfer Function (Velocity Control) . . . . . 55
4.9.	Magnitude Plot of Open Loop Response (Acceleration Control) . . . . . 58
4.10.	Phase Plot of Open Loop Response (Acceleration Control) . . . . . 59
4.11.	Closed Loop Response (Acceleration Control) . . . . . 59
4.12.	Magnitude Plot of Pilot Transfer Function (Acceleration Control) . . . . . 60
4.13.	Phase Plot of Pilot Transfer Function (Acceleration Control) . . . . . 60
4.14.	Neal-Smith Pitch Tracking Task (Classical Model) . . . . . 61
4.15.	Neal-Smith Tracking Performance Standard . . . . . 62
4.16.	Neal-Smith Tracking Task (OCM) . . . . . 67
4.17.	POR/Feedback Correlation . . . . . 70
4.18.	POR/Sensor Noise Cutoff Frequency Correlation . . . . . 70
4.19.	Feedback/Tracking Error Correlation . . . . . 71
4.20.	Limitation of Human Sensing (Gain) . . . . . 71
4.21.	Limitation of Human Sensing (Phase) . . . . . 72
4.22.	Interpretation of High Frequency Performance of OCM (Phase) . . . . . 72
4.23.	POR of Neal-Smith Configurations . . . . . 73

Figure	Page
4.24. Interpretation of POR Criteria . . . . .	73
4.25. Results of POR (Group 1) . . . . .	75
4.26. Magnitude Plot of Pilot and Vehicle Transfer Function (Group 1) . . . . .	76
4.27. Magnitude Plot of Open Loop Transfer Function (Group 1) . . . . .	76
4.28. Phase Plot of Vehicle Transfer Function (Group 1) . . . . .	77
4.29. Phase Plot of Pilot Transfer Function (Group 1) . . . . .	77
4.30. Phase Plot of Open Loop Transfer Function (Group 1) . . . . .	78
4.31. Results of POR (Group 2) . . . . .	79
4.32. Magnitude Plot of Vehicle Transfer Function (Group 2) . . . . .	79
4.33. Magnitude Plot of Pilot Transfer Function (Group 2) . . . . .	80
4.34. Magnitude Plot of Open Loop Transfer Function (Group 2) . . . . .	80
4.35. Phase Plot of Vehicle Transfer Function (Group 2) . . . . .	81
4.36. Phase Plot of Pilot Transfer Function (Group 2) . . . . .	81
4.37. Phase Plot of Open Loop Transfer Function (Group 2) . . . . .	82
4.38. Results of POR (Group 3) . . . . .	83
4.39. Magnitude Plot of Vehicle and Pilot Transfer Function (Group 3) . . . . .	83
4.40. Magnitude Plot of Open Loop Transfer Function (Group 3) . . . . .	84
4.41. Phase Plot of Vehicle and Pilot Transfer Function (Group 3) . . . . .	84
4.42. Phase Plot of Open Loop Transfer Function (Group 3) . . . . .	85
4.43. Magnitude Plot of Open Loop Transfer Function with 0.2 sec Delay (2D). . . . .	87
4.44. Magnitude Plot of Pilot Transfer Function . . . . .	89
4.45. Phase Plot of Pilot Transfer Function . . . . .	89



## NOMENCLATURE

Matrices	<b>Bold upper case alphabet</b>
Vectors	<b>Bold low case alphabet</b>
Scalar	Plain alphabet
$(.)^{-1}$	Inverse of $(.)$
$(.)^T$	Transpose of $(.)$
$(\dot{.})$	Derivative of $(.)$
$ (\cdot) $	Absolute value of $(.)$
$\angle(\cdot)$	Angle of $(.)$
$E\{(\cdot)\}$	Expectation value of $(.)$

## CHAPTER I

### INTRODUCTION

#### 1.1 Problem Statement

In the past decade there has been increasing attention in the integrated optimal control, frequency domain approach for the analysis of pilot/vehicle systems in handling quality research [1-4]. This approach has been focused on attempts to bridge the gap between the crossover model and the optimal control model (OCM) of the pilot/vehicle system. What makes this attempt attractive for handling quality research is its systematic procedure for providing an explicit form of the pilot transfer function and frequency domain parameters of the pilot/vehicle system such as bandwidth, stability margins, sensor noise constraints and feedback over a prescribed frequency band. In general, these frequency domain parameters are more useful to the flight control designer than the statistical descriptions in the time domain.

The optimal control approach to modeling a pilot in the loop was successfully done by Kleinman et al. in 1970 [5, 6]. A pilot transfer function can be automatically developed from the optimal control model which is based on optimal control and estimation theory. However, there is no guideline to characterize this optimal pilot transfer function related to handling qualities using the optimal control approach in the frequency domain. Most of the research has been contributed in duplicating results of the classical frequency domain approach using this optimal control model for various tasks.

This thesis presents the concept of the Bode ideal cutoff to analyze pilot/vehicle systems in the frequency domain based on the optimal control model. The Bode ideal cutoff takes into account the pattern of the pilot transfer function for a given aircraft

dynamics and a task. Specifically, it provides the absolute standard, maximum available feedback at a pilot working band, which can be used to define the ideal feedback at a working band with the high frequency stability and constraints. The goal of this work is to correlate the values of the frequency domain performance of pilot/vehicle systems with pilot opinion ratings (POR) as determined by the Cooper-Harper rating system [7] (Figure 1.1.).

## 1.2 Objectives and Scope

This research is focused on the relationship between the time domain performance and the frequency domain performance. The major objectives are:

- (1) To develop pilot transfer functions from the optimal pilot model using a 4<sup>th</sup> order Pade approximation for the perceptual (reaction) time delay element. (The approximation is valid for frequencies less than 30 rad/sec.)
- (2) To compare pilot transfer functions with the classical crossover model.
- (3) To characterize pilot transfer functions using the Bode ideal cutoff.
- (4) To find important parameters that effect the pilot opinion ratings in the frequency domain.
- (5) To relate the values of the frequency domain performance with the Cooper-Harper rating system.

In this study, two simple vehicle dynamics [6] and the 51 Neal-Smith configurations for the pitch attitude tracking task [8] are tested using the above objectives.

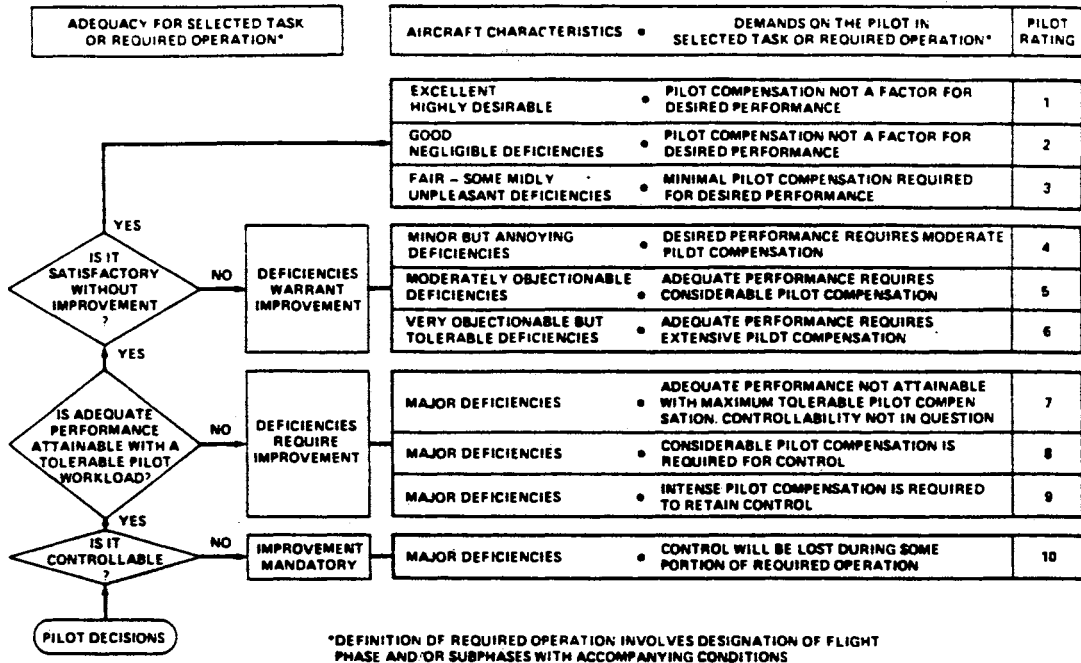


Figure 1.1. The Cooper-Harper Rating Scale [7]

## CHAPTER II

### LITERATURE REVIEW

#### 2.1 Mathematical Pilot Model

Hundreds of studies have been published on modeling the human operator from the viewpoint of analyzing the nonlinear characteristics of the human behavior in the man-machine system. These mathematical models of the human operator have been developed under two categories.

- (1) Classical control approach in the frequency domain
- (2) Modern control approach in the time domain

A detailed discussion of the models of the human operator is beyond the scope of this thesis. Classical and modern approaches for modeling the human operator are briefly reviewed.

Most of the classical approaches in the field of the manual control system were contributed in understanding the behavior of the human operator as a controller of single-input, single-output (SISO), linear, time-invariant systems. Conventionally, the mathematical model for describing the human controller can be characterized by the servo analytical techniques in the frequency domain. The advantage of the classical approach is that the results of the frequency domain performance are in a form very useful to the flight control designer. Much of this work based on a quasi-linearization technique was successfully done by McRuer et al. [9].

The quasi-linear models are very effective in analyzing the characteristics of the human operator performing a closed loop compensatory tracking or state regulation tasks. It is assumed that a well trained human operator performing such a task develops a

relatively stable control strategy to minimize some displayed errors with his inherent psycho-physical limitations. The response of the human operator is strongly dependent on the mental and physical conditioning of the operator as well as the type of the information presented to him. Therefore, it is very difficult to predict the behavior of the human operator with a simple transfer function for complex man-machine systems in general. However, a very large class of the experimental data can be explained by the following form.

$$G_p(s) = K_p \frac{(\tau_1 s + 1)}{(\tau_2 s + 1)} \left[ \frac{e^{-\tau s}}{\tau_h s + 1} \right] \quad (2.1)$$

where the bracketed term represents the human operator's limitation, perceptual time delay and neuromuscular dynamics. The remaining term represents the human's equalization characteristics to adapt his stable control strategy to match a given situation.

In the complex multi-loop systems, the subsequential loop closure technique has been implemented with some limited success [10]. However, it is very difficult to construct the loop structure of the pilot/vehicle system with such a classical pilot model as well as to define the pilot's compensation in the multi-loop systems.

The modern control approach to modeling the human controller is rooted in a significant work of Kleinman et al. [6] which is based on optimal control and estimation theory in the time domain. This approach also has the assumption that a well-motivated, well-trained human operator generates an optimal control input under a given situation subject to his inherent limitations and constraints, and his control task. Figure 2.1. shows a simplified block diagram of the optimal control model, at which the shadowed block represents the mathematical key elements of the human behavior. The advantage of the optimal control model is the capability of handling multi-input, multi-output (MIMO) systems with the state space technique. Also, the pilot transfer function can be automatically generated under a given task. Therefore, the optimal control model is a most

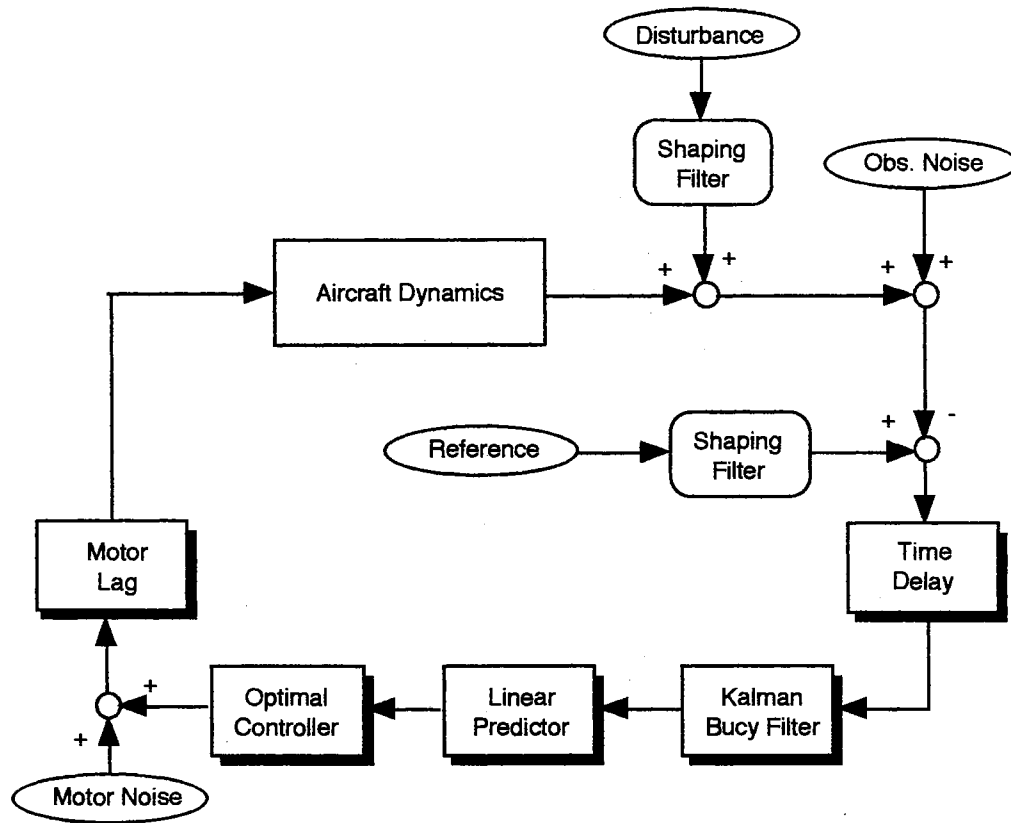


Figure 2.1. Block Diagram of the Optimal Control Model

powerful tool in the analysis of complex multi-variable man-machine systems. The optimal control model will be discussed in Chapter III in detail.

## 2.2 Pilot Opinion Ratings

Most of the field studies of handling qualities are closely related to the mathematical pilot model which can give critical effects in the prediction of the pilot opinion ratings. The frequency domain approach with a classical pilot model was done to find the correlation between the values of the pilot transfer function's parameters and the pilot opinion ratings. The time domain approach with an optimal control model is to correlate the value of the cost function with the pilot opinion ratings. Both approaches are summarized in TABLE 2.1 and TABLE 2.2, respectively.

TABLE 2.1

## FREQUENCY DOMAIN APPROACH

---

McRuer, Ashkenas, and Guerre (1960) [11]

Correlation: Pilot rating and parameters of the classical pilot model

Comments: The earliest documentation of the relationship between the pilot transfer function and pilot opinion

---

Graham, Krendel, McRuer, and Reisener (1965) [9]

Correlation: Pilot rating and quasi-linear model

Comments: Implicit internal model of the human operator

---

Anderson (1970) [12]

Correlation: Pilot rating and root mean square tracking performance and lead time constant of the classical pilot model

$$\text{POR} = R_1 + R_2 + R_3 + 1.0$$

Application: Longitudinal helicopter hover task

Comments: Computer implementation for the prediction of handling qualities  
"Paper Pilot"

---

Neal and Smith (1970) [8]

Correlation: Pilot rating and pilot's compensation of the classical pilot model and pilot/vehicle oscillation that resulted

Application: 51 basic short period configurations for the pitch tracking task

Assumption: "Pilot wants to acquire the target quickly and predictably, with minimum overshoot and oscillation."

Comments: "To acquire the target quickly and predictably" means that the pilot wants to keep the magnitude of closed loop transfer function relatively close to 0 dB.

"with minimum oscillation and overshoot" means that the pilot wants to minimize the closed-loop resonant peak.



TABLE 2.1 (Continued)

---

Neal and Smith (Continued)

Pilot control strategy is a tradeoff between good low frequency performance and minimum accompanying oscillations. (Figure 2.2.-2.4.)

---

Onstott (1972) [13]

Correlation: Pilot rating and pilot gain

Application: Roll tracking task

---

Adams and Moore (1976) [14]

Correlation: Pilot rating and lead time constant

Application: Lateral directional mode

---

The prediction of handling qualities with the classical pilot models has the following disadvantages:

- (1) The pilot loop structure depends on the given systems and control tasks. Specifically, it is very difficult to construct the appropriate pilot loop structure in the complex multi-loop systems.
- (2) There is no systematic procedure for selecting the values of the parameters in the classical pilot models.
- (3) Correlation between the pilot opinion ratings and the parameters of the classical pilot models is very difficult because different pilot models are applied to different vehicles and different control tasks.

TABLE 2.2

## TIME DOMAIN APPROACH

---

Kleinman, Baron, and Levison (1970) [6]

Correlation: Pilot rating and the value of the performance index of the optimal control model (Figure 2.5.-2.6.)

$$J = E \left\{ \lim_{T \rightarrow \infty} \frac{1}{T} \int_0^T [ \mathbf{x}^T(t) \mathbf{Q} \mathbf{x}(t) + u^T(t) r u(t) + \dot{u}^T(t) g \dot{u}(t) ] dt \right\}$$

Assumption: "Human pilot behaves optimally in some sense, subject to his psycho-physical limitations."

Comments: Original work of the optimal control model  
Linear quadratic Gaussian optimal control  
Pilot loop structure is automatically generated in SISO and MIMO systems.

---

Dillow and Picha (1975) [15]

Correlation: Pilot rating and the value of the performance index

$$POR = \sqrt{J}$$

Application: Longitudinal hover task of a V/STOL aircraft

---

Phatak, Weinert, Segall, and Day (1976) [16]

Comments: Different form of the optimal pilot model

---

Hess (1977) [17-18]

Correlation:  $POR = R(J)_s$

Assumption: (1) The performance index and model parameters in the optimal pilot modeling procedure yields a dynamically representative model of human pilot.  
(2) The variables selected for inclusion in the performance index are directly observable by the pilot.  
(3) The weighting coefficients in the index of performance are chosen as the squares of the reciprocals of maximum allowable

TABLE 2.2 (Continued)

---

Hess (Continued)

deviations of the respective variables, and these deviations are consonant with the task as perceived by the pilot.

- Application: 7 pitch attitude tracking tasks from McDonnell (1968)  
 2 longitudinal hover tasks from Duffy (1976)  
 5 pitch attitude tracking tasks from Arnold (1973)  
 5 longitudinal hover tasks from Miller and Vinje (1968) (Figure 2.7.)
- Comments: General pilot rating formulation
- 

## Schmidt (1979, 1980) [19]

- Correlation: Pilot rating and the value of the performance index
- Application: 14 Arnold configurations
- $$\text{POR} = \log_{10}(J) + 4$$
- 14 Neal-Smith high-order configuration dynamics
- $$\text{POR} = \log_{10}(J)$$
- Comments: The pilot rating/cost magnitude sensitivity, or the slope of regression, appeared to be greater due to aeroelastic (or other low damped) mode. (Figure 2.8.-2.9.)
- 

## Bacon and Schmidt (1982) [1]

- Application: 26 Neal-Smith configurations for pitch tracking
- Comments: Integrated optimal control, frequency domain approach for pilot/vehicle analysis  
 Duplicate the Neal-Smith criteria using the optimal control model (Figure 2.10.-2.11.)
- 

## Anderson and Schmidt (1985) [2]

- Application: 32 Smith configurations for the pitch tracking task  
 Approach and landing of high-order system (Figure 2.12.-2.13.)
- Comments: Integrated optimal control, frequency domain approach for multi-loop pilot/vehicle analysis

TABLE 2.2 (Continued)

---

Thompson and McRuer (1988) [3]

Application: Dander helicopter data for single and multi-axis tracking tasks

Comments: Comparison of the human optimal control and crossover model using the Pade approximation for the pure time delay of the human pilot

---

McRuer and Schmidt (1990) [4]

Correlation:  $POR = 7.7 + 3.7 \log_{10}(J)$

Application: Dander helicopter data for single and multi-axis tracking tasks

Comments: Correlation for the multi-axis problem in the time domain

---

Optimal control approach related to the prediction of the handling qualities has the following advantages compared to the classical approach.

- (1) Pilot loop structure can be automatically developed with a given vehicle and control tasks.
- (2) Optimal control model can treat MIMO systems naturally with a state space technique.
- (3) The main concept of the optimal control modeling can be directly related to the handling qualities. The value of performance index itself is the metric of the handling qualities.

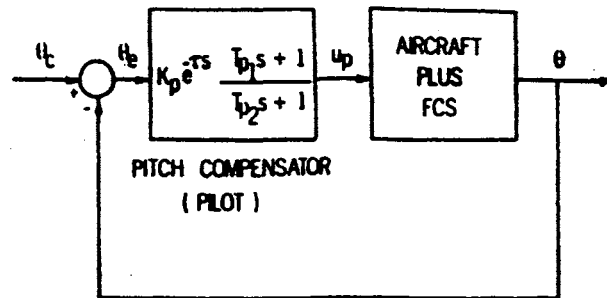


Figure 2.2. Neal-Smith Vehicle/Pilot Model Structure [8]

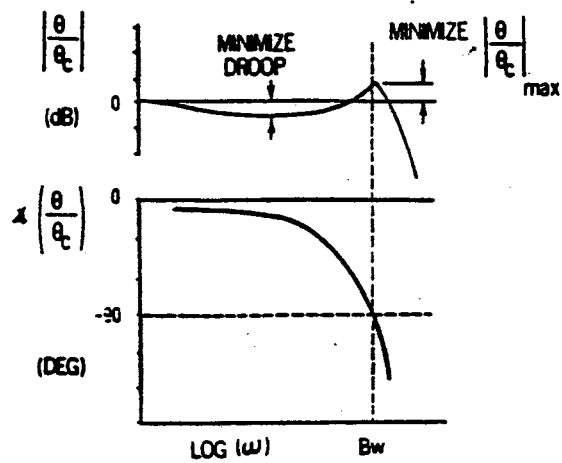


Figure 2.3. Neal-Smith Control Strategy in Tracking Task [8]



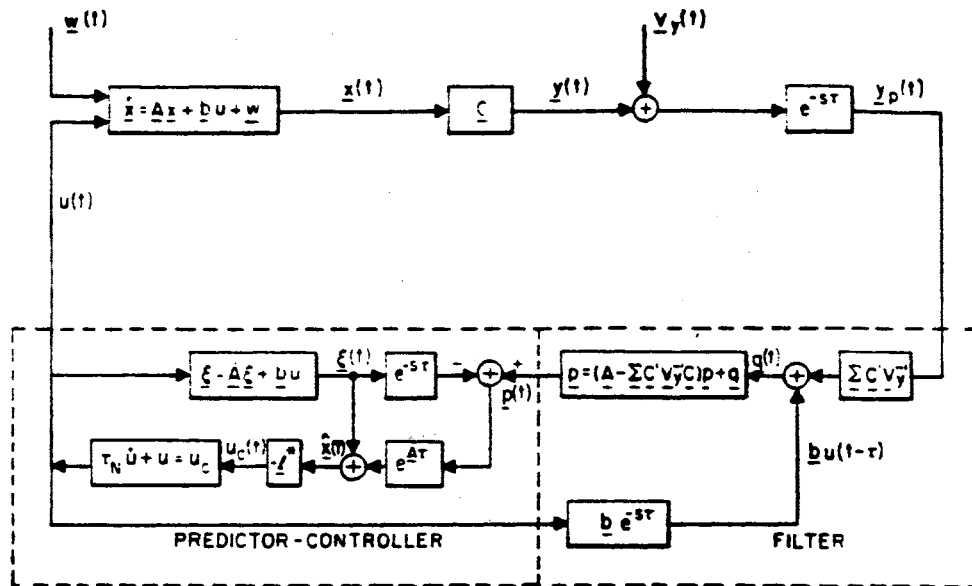


Figure 2.6. Human Optimal Control Model [6]

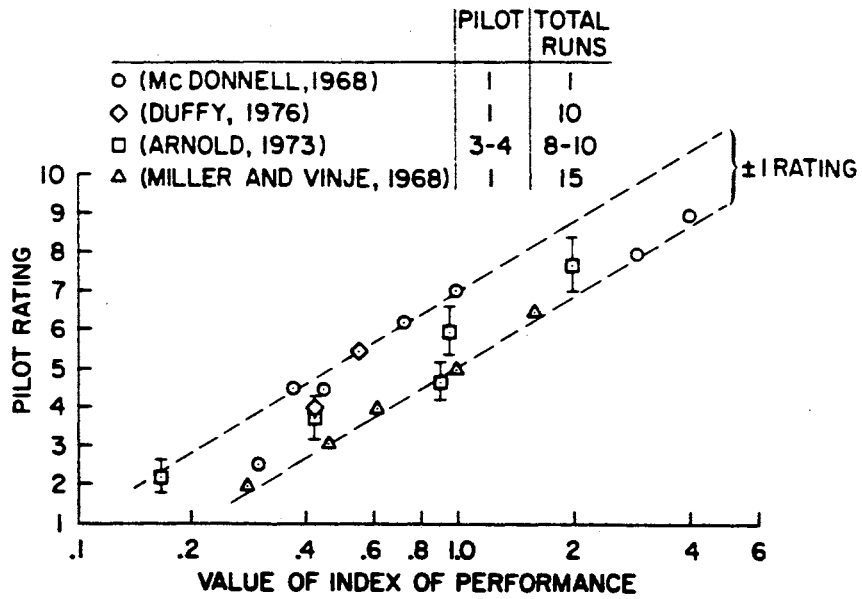


Figure 2.7. Hess Results [18]

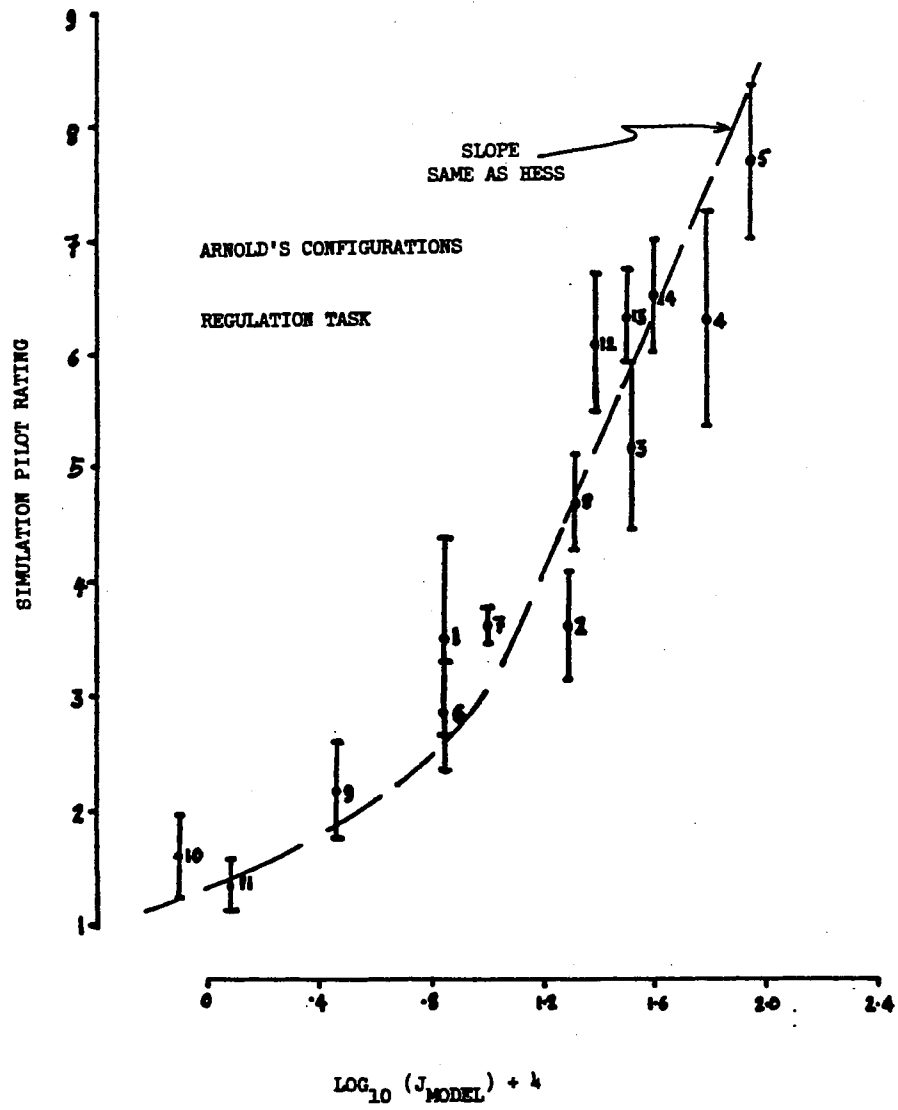


Figure 2.8. Schmidt Results (Arnold Configurations) [19]



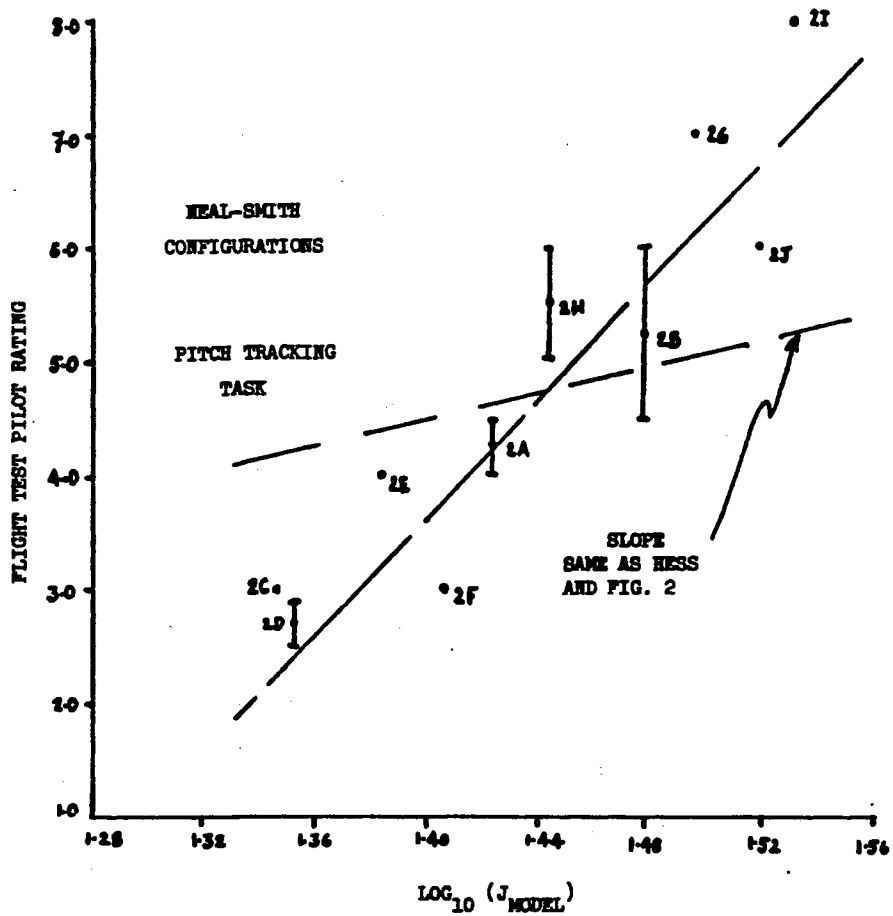


Figure 2.9. Schmidt Results (Neal-Smith Configurations) [19]

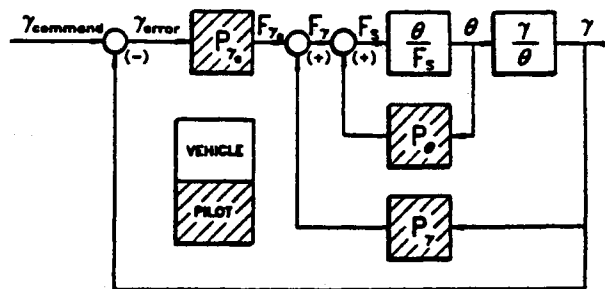


Figure 2.10. Model Comparison (Bacon-Schmidt) [1]

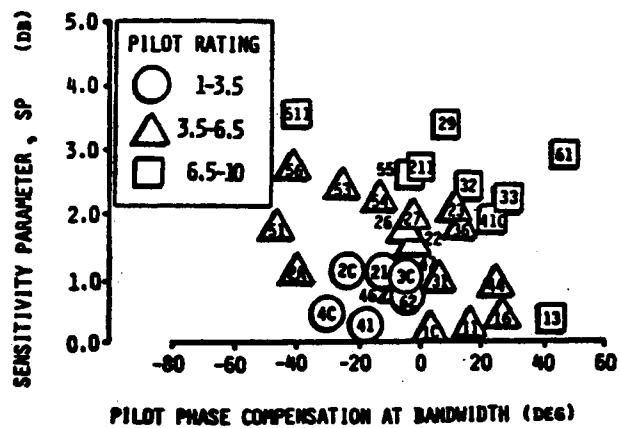


Figure 2.11. Bacon and Schmidt Results (Neal-Smith Configurations) [1]

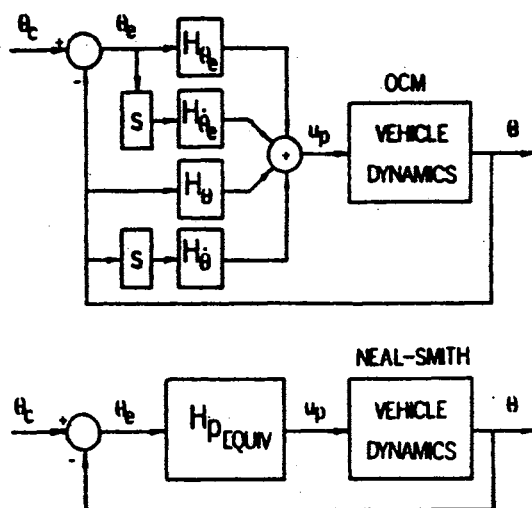


Figure 2.12. Multi-Loop Flight Path Tracking Task (Anderson and Schmidt) [2]

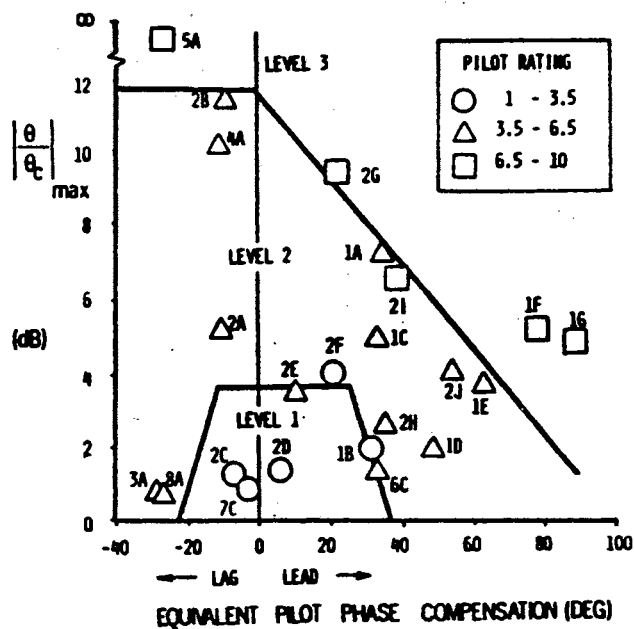


Figure 2.13. Anderson and Schmidt Results (LAHOS Configurations) [2]

## CHAPTER III

### THEORIES

#### 3.1 Representation of Human Behavior

The behavior of the human operator in the man-machine systems is very difficult to describe explicitly because the combined human sensing, data processing and actuating elements of the human operator are directly connected to the various display instruments and the actuators of the controlled system through the internal nerve pathway. In spite of this difficulty, the mathematical model of the human operator must have within its framework his inherent psycho-physical limitations in performing a given task with a controlled system. Conventionally, the characteristics of the human operator are categorized as the following three linear elements:

- (1) Perceptual time delay
- (2) Equalization and computational operation
- (3) Neuromuscular dynamics

The general loop structure of the man-machine system with the above elements is shown in Figure 3.1.

Major sources of the perceptual time delay are based on the human sensing nerve excitation, conduction and the data processing time in the central nerve system, which is basically dependent of a display array of the controlled system as well as the task requirements. Since these elements are internally combined in the human body, it is conveniently represented as a lumped equivalent time delay. In a simple tracking task, the perceptual time delay is generally accepted in the range of 0.15 to 0.25 seconds [20-22]. The equalization and computational operation of the human operator is the most important

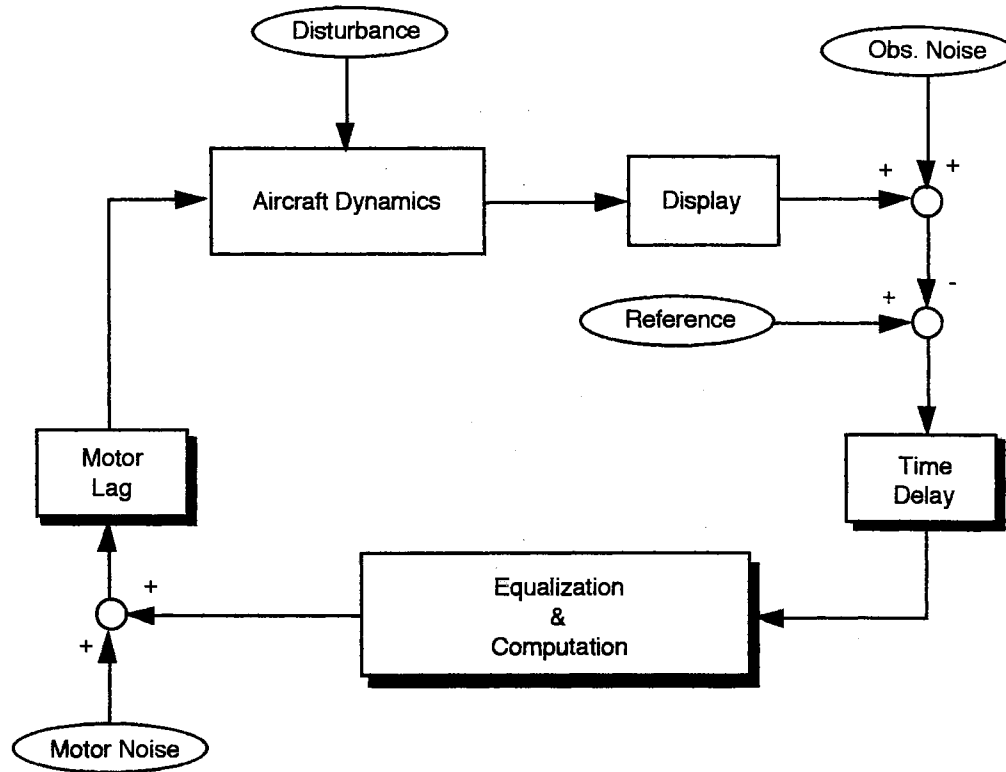


Figure 3.1. General Loop Structure of the Man-Machine System

key element of the human behavior, which stabilizes the response of the closed loop system and minimizes the error in the tracking tasks. In other words, this element generates the relatively stable, best control strategy to the neuromuscular system under the situation of the given task and conditionings of the human operator. Thus, this element is also strongly dependent on a controlled system and a given task.

Neuromuscular dynamics are modeled by the first order lag and detail discussion was done by McRuer et al. [22].

$$H_n(s) = \frac{1}{(\tau_n s + 1)} \quad (3.1)$$

The neuromuscular constant,  $\tau_n$ , depends on the task to perform in the man-machine

system. The adjustment required for the given situation is obscure because the neuromuscular mechanism is not well understood and the appropriate measurement of the variation is very difficult. A typical value of the neuromuscular constant is 0.1 second in the range of 0.1 to 0.6 seconds.

The remnant of the human operator is defined as a component of human response that is unpredictable in other than a statistical sense. The various sources of inherent human randomness can cause the errors in observing the system outputs and executing the control strategy through the neuromuscular system. Observation noise is described as the effects of the random perturbations in observing the system output through the display panel. Motor noise represents the random errors in executing the intended control strategy, and the fact that the pilot cannot generate the ideal control input under a given situation. Thus, the observation noise and motor noise in Figure 3.1. are represented as the lumped remnant of the human operator, which can be modeled as independent, zero-mean, Gaussian white noise [23].

### 3.2 Optimal Control Model [3, 5-6]

The basic function of the human operator in the man-machine system is to control a given dynamic system in some prescribed way. This is the situation of the typical tracking tasks in the pilot/vehicle system. It is assumed that the pilot has a single input for simplicity and extracts the information of the error and error rate with a single display. It is also assumed that the given vehicle dynamics, which may include the dynamics of the vehicle's actuator, sensor and control system, are represented by the linear, time invariant equations of motion:

$$\dot{\mathbf{x}}(t) = \mathbf{A} \mathbf{x}(t) + \mathbf{B} u(t) + \mathbf{F} \mathbf{w}(t) \quad (3.2)$$

where  $\mathbf{x}(t)$  is the state vector,  $u(t)$  is the scalar pilot's control input and  $\mathbf{w}(t)$  represents

external disturbances which is the zero-mean, Gaussian white noise with autocovariances

$$E\{ \mathbf{w}(t) \mathbf{w}^T(\sigma) \} = \mathbf{W} \delta(t-\sigma) \quad (3.3)$$

The two system outputs  $\mathbf{y}(t)$  are error,  $y_e(t)$ , and error rate,  $\dot{y}_e(t)$ , which are linear combination of the system states,  $\mathbf{x}(t)$ , and control input,  $u(t)$ .

$$\mathbf{y}(t) = \mathbf{C}\mathbf{x}(t) + \mathbf{D}u(t) \quad (3.4)$$

The pilot perceives the delayed system output,  $\mathbf{y}(t-\tau)$ , with observation noise,  $\mathbf{v}_y(t-\tau)$ , through the display panel.

$$\mathbf{y}_p(t) = \mathbf{y}(t-\tau) + \mathbf{v}_y(t-\tau) \quad (3.5)$$

where  $\tau$  is the perceptual time delay of the pilot and  $\mathbf{v}_y(t)$  is the zero-mean, Gaussian white noise with autocovariance,  $\mathbf{V}_y$

$$E\{ \mathbf{v}_y(t) \mathbf{v}_y^T(\sigma) \} = \mathbf{V}_y \delta(t-\sigma) \quad (3.6)$$

The intensity of the observation noise,  $\mathbf{V}_y = \text{diag} ( v_{y1}, v_{y2} )$ , is defined quantitatively as

$$v_{yi} = \frac{\rho_{yi} \pi}{f} \frac{\sigma_{yi}^2}{E(\sigma_{yi}, T_i)^2} \quad i = 1, 2 \quad (3.7)$$

where  $\rho_{yi}$  is the observation noise ratio and  $f$  is the attentional factor of the human operator for the multi-axis task which has the range  $0 \leq f \leq 1$ .  $\sigma_{yi}^2$  is the covariance of the system output, error and error rate, and  $T_i$  is the observation threshold which is based on the

human eye perceptual levels.

$$E(\sigma_{y_i}, T_i) = \text{erfc}\left(\frac{T_i}{\sigma_{y_i} \sqrt{2}}\right) = \text{Prob}(|y_i| > T_i) \quad (3.8)$$

The range of the above erfc function is from 0 to 1. For example, if the observation threshold is zero, erfc function is 1, which means there is no effects of the observation threshold in equation (3.7).

The assumption of the optimal control model is that the human operator chooses an optimal control input  $u^*(t)$  with the objective in the steady state which minimizes the performance index based on the perceptual observations  $y_p(\cdot)$  in equation (3.5)

$$J(u) = E\left\{ \lim_{T \rightarrow \infty} \frac{1}{T} \int_0^T [y^T(t) Q y(t) + u^T(t) r u(t) + \dot{u}^T(t) g \dot{u}(t)] dt \right\} \quad (3.9)$$

Equation (3.9) can be expressed simply as

$$J(u) = E\left\{ \sum_{i=1}^2 q_i y_i^2 + r u^2 + g \dot{u}^2 \right\} \quad (3.10)$$

The weightings in equation (3.10) are  $q_i \geq 0$ ,  $r \geq 0$  and  $g > 0$  and the third term in equation (3.9) results in the neuromuscular dynamics of the human operator. Neuromuscular dynamics,  $H_n(s)$  in equation (3.1), are not directly included in the performance index, but the weighting  $g$  on the control rate is adjusted to represent the neuromuscular first order lag.

The optimal control input,  $u^*(t)$ , can be determined by the estimated state of the system through the Kalman-Bucy filter (KBF) and linear predictor (LP), which is a typical Linear Quadratic Regulator (LQR) problem with the time delay and the observation noise.



By including the control input,  $u(t)$ , in the system state vector,  $\mathbf{x}_0(t)$ , and using  $\mu(t) = \dot{u}(t)$ , the LQR problem can be solved based on the estimated states with the performance index, equation (3.9).

$$\dot{\mathbf{x}}_0(t) = \mathbf{A}_0 \mathbf{x}_0(t) + \mathbf{B}_0 \mu(t) \quad (3.11)$$

$$\mathbf{y}(t) = \mathbf{C}_0 \mathbf{x}_0(t) \quad (3.12)$$

$$\mathbf{x}_0(t) = \begin{bmatrix} \mathbf{x}_0(t) \\ u(t) \end{bmatrix} \quad \mathbf{A}_0 = \begin{bmatrix} \mathbf{A} & \mathbf{B} \\ \mathbf{0} & 0 \end{bmatrix} \quad \mathbf{B}_0 = \begin{bmatrix} \mathbf{0} \\ 1 \end{bmatrix}$$

$$\mathbf{y}(t) = \begin{bmatrix} y_e(t) \\ \dot{y}_e(t) \end{bmatrix} \quad \mathbf{C}_0 = [ \mathbf{C} \quad \mathbf{D} ] \quad (3.13)$$

The solution of the optimal control input is:

$$\mu(t) = -\mathbf{L} \mathbf{x}_0(t) \quad (3.14)$$

$$\mathbf{L} = [ \mathbf{L}_1 \quad \mathbf{L}_2 ] = g^{-1} \mathbf{B}_0^T \mathbf{K}_0 \quad (3.15)$$

$$\mathbf{0} = \mathbf{A}_0^T \mathbf{K}_0 + \mathbf{K}_0 \mathbf{A}_0 + \mathbf{Q}_0 - \mathbf{K}_0 \mathbf{B}_0 g^{-1} \mathbf{B}_0^T \mathbf{K}_0 \quad (3.16)$$

$$\mathbf{Q}_0 = \begin{bmatrix} \mathbf{C}_0^T \mathbf{Q} \mathbf{C}_0 & \mathbf{0} \\ \mathbf{0} & r \end{bmatrix} \quad (3.17)$$

The weighting,  $g$ , on the control rate,  $\dot{u}(t)$ , is determined by the iteration so that

$$\mathbf{L}_2^{-1} = \tau_h \quad (3.18)$$

The KBF and LP generate the estimated states of the augmented system which is driven by the external disturbance,  $\mathbf{w}(t)$ , and the neuro-motor noise,  $v_u(t)$ .

$$\dot{\mathbf{x}}_1(t) = \mathbf{A}_1 \mathbf{x}_1(t) + \mathbf{B}_1 u_c(t) + \mathbf{F}_1 \mathbf{w}_1(t) \quad (3.19)$$

$$\mathbf{y}(t) = \mathbf{C}_1 \mathbf{x}_1(t) \quad (3.20)$$

$$\begin{aligned} \mathbf{x}_1(t) &= \begin{bmatrix} \mathbf{x}_1(t) \\ u(t) \end{bmatrix} & \mathbf{w}_1(t) &= \begin{bmatrix} \mathbf{w}(t) \\ v_u(t) \end{bmatrix} & \mathbf{y}(t) &= \begin{bmatrix} y_e(t) \\ \dot{y}_e(t) \end{bmatrix} \\ \mathbf{A}_1 &= \begin{bmatrix} \mathbf{A} & \mathbf{B} \\ \mathbf{0} & -L_2 \end{bmatrix} & \mathbf{B}_1 &= \begin{bmatrix} \mathbf{0} \\ L_2 \end{bmatrix} & \mathbf{F}_1 &= \begin{bmatrix} \mathbf{F} \\ L_2 \end{bmatrix} \\ \mathbf{C}_1 &= [\mathbf{C} \quad \mathbf{D}] & \mathbf{W}_1 &= \begin{bmatrix} \mathbf{W} & \mathbf{0} \\ \mathbf{0} & V_u \end{bmatrix} \end{aligned} \quad (3.21)$$

where  $v_u(t)$  represents the neuro-motor noise which is a zero-mean, Gaussian white noise with a autocovariance:

$$E\{v_u(t) v_u(\sigma)\} = V_u \delta(t-\sigma) \quad (3.22)$$

It is inserted to the neuromuscular dynamics with the commanded input,  $u_c(t)$ . The intensity of the neuro-motor noise,  $V_u$ , is defined as

$$V_u = \rho_u \pi \sigma_u^2 \quad (3.23)$$

It is noted that the covariance of commanded input,  $\sigma_u^2$ , is proportional to the neuro-motor noise intensity,  $V_u$ . The KBF estimates the delayed states of the augmented system,  $\hat{\mathbf{x}}_1(t-\tau)$ , which is the linear mean-square estimate of  $\mathbf{x}_1(t-\tau)$  based on observation  $y_p(\sigma)$  for

$\sigma < t$ .

$$\hat{\mathbf{x}}_1(t-\tau) = \mathbf{A}_1 \hat{\mathbf{x}}_1(t-\tau) + \mathbf{H}_1 [ \mathbf{y}_p(t-\tau) - \mathbf{C}_1 \hat{\mathbf{x}}_1(t-\tau) ] + \mathbf{B}_1 u_c(t-\tau) \quad (3.24)$$

$$\mathbf{H}_1 = \Sigma_1 \mathbf{C}_1^T \mathbf{V}_y^{-1} \quad (3.25)$$

$$\mathbf{0} = \mathbf{A}_1 \Sigma_1 + \Sigma_1 \mathbf{A}_1^T + \mathbf{F}_1 \mathbf{W}_1 \mathbf{F}_1^T - \Sigma_1 \mathbf{C}_1^T \mathbf{V}_y^{-1} \mathbf{C}_1 \Sigma_1 \quad (3.26)$$

The linear predictor generates the updated states of the augmented system,  $\hat{\mathbf{x}}_1(t)$ , from  $\hat{\mathbf{x}}_1(t-\tau)$  based on observations  $\mathbf{y}_p(\sigma)$  for  $\sigma < t$ .

$$\dot{\xi}(t) = \mathbf{A}_1 \xi(t) + \mathbf{B}_1 u_c(t) \quad (3.27)$$

$$\hat{\mathbf{x}}_1(t) = \xi(t) + e^{\mathbf{A}_1 \tau} [ \hat{\mathbf{x}}_1(t-\tau) - \xi(t-\tau) ] \quad (3.28)$$

Finally, the commanded optimal control,  $u_c(t)$ , is computed by

$$u_c(t) = -\mathbf{L}^* \hat{\mathbf{x}}_1(t) \quad (3.29)$$

$$\mathbf{L}^* = \begin{bmatrix} \mathbf{L}_2^{-1} \mathbf{L}_1 & \mathbf{0} \end{bmatrix} \quad (3.30)$$

The derivation of the optimal control mode is discussed in detail in Kleinman [5-6]. Figure 3.2. shows the key elements and variables of the optimal control model.

In summary, the element of equalization and computation in Figure 3.1. is replaced by the Kalman-Bucy filter, the linear predictor and the optimal control gain in Figure 3.2. The Kalman Bucy filter represents the estimation ability of the human operator from the delayed stochastic information and the linear predictor is the compensation for the

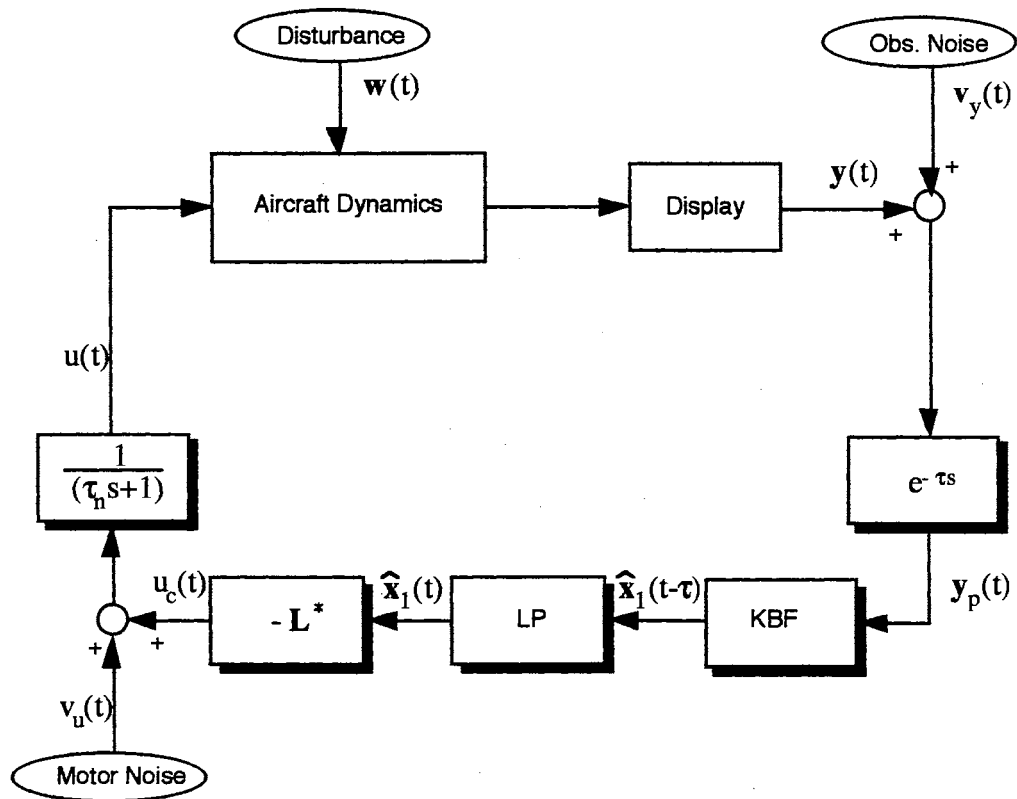


Figure 3.2. Block Diagram of the Optimal Control Model

perceptual time delay. The optimal control gain represents the relative stable control strategy of the human operator under the given situation. The advantage of the optimal control model is that the structure of the human operator in the feedback loop of the man-machine system is automatically generated through the systematic procedure.

### 3.3 Time Domain Performance [3, 5-6]

The time domain performance of the human operator is represented by the following statistical values of the mean squared estimate and the performance index. They are solved by the iterative method so that  $\sigma_{y_i}^2$  and  $\sigma_{uc}^2$  satisfy the equation (3.7) and (3.23), respectively. In the time domain, the handling qualities are directly related to the value of

the performance index,  $J$ , which is minimized by the optimal control  $u^*(t)$ .

$$\mathbf{E}_1 = E\{ \mathbf{e}_1(t) \mathbf{e}_1^T(t) \} = e^{\mathbf{A}_1 t} \Sigma_1 e^{\mathbf{A}_1^T t} + \int_0^t e^{\mathbf{A}_1 \sigma} \mathbf{F}_1 \mathbf{W}_1 \mathbf{F}_1^T e^{\mathbf{A}_1^T \sigma} d\sigma \quad (3.31)$$

where  $\mathbf{e}_1(t)$  is the estimation error which is defined as

$$\mathbf{e}_1(t) = \mathbf{x}_1(t) - \hat{\mathbf{x}}_1(t) \quad (3.32)$$

$$\begin{aligned} \hat{\mathbf{X}}_1 &= E\{ \hat{\mathbf{x}}_1(t) \hat{\mathbf{x}}_1^T(t) \} \\ &= \int_0^\infty e^{[\mathbf{A}_1 - \mathbf{B}_1 \mathbf{L}^T] \sigma} e^{\mathbf{A}_1 \tau} \mathbf{H}_1 e^{\mathbf{A}_1^T \tau} e^{[\mathbf{A}_1 - \mathbf{B}_1 \mathbf{L}^T]^T \sigma} d\sigma \end{aligned} \quad (3.33)$$

$$\mathbf{X}_1 = E\{ \mathbf{x}_1(t) \mathbf{x}_1^T(t) \} = \mathbf{E}_1 + \hat{\mathbf{X}}_1 \quad (3.34)$$

$$\mathbf{Y} = E\{ \mathbf{y}(t) \mathbf{y}^T(t) \} = \mathbf{C}_1 \mathbf{X}_1 \mathbf{C}_1^T \quad (3.35)$$

$$\mathbf{U}_c = E\{ u_c(t) u_c^T(t) \} = \mathbf{L}^* \hat{\mathbf{X}}_1 \mathbf{L}^{*T} \quad (3.36)$$

$$\hat{\mathbf{U}} = E\{ \hat{u}(t) \hat{u}^T(t) \} = \mathbf{L} \hat{\mathbf{X}}_1 \mathbf{L}^T + \begin{bmatrix} \mathbf{0} & \mathbf{L}_2 \end{bmatrix} \mathbf{E}_1 \begin{bmatrix} \mathbf{0} & \mathbf{L}_2 \end{bmatrix}^T \quad (3.37)$$

$$J = \text{trace}(\mathbf{Y}\mathbf{Q}) + \text{trace}(\hat{\mathbf{U}}\mathbf{g}) \quad (3.38)$$

### 3.4 Pilot Transfer Function [3]

The classical model of the human operator is represented by the simple transfer function which has a single input,  $y_e(t)$ , and a single output,  $u(t)$ . However, the optimal

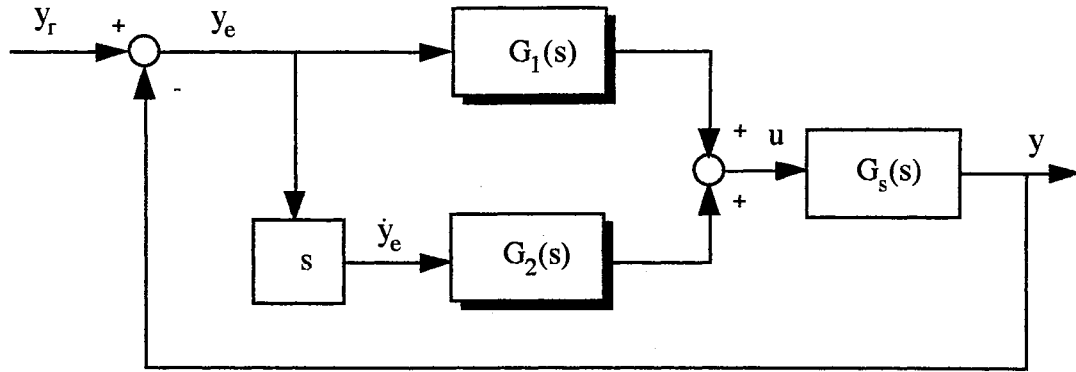


Figure 3.3. Optimal Pilot Transfer Function

control model has two inputs,  $y_e(t)$  and  $\dot{y}_e(t)$ . The loop structure of the optimal transfer function for SISO system is shown in Figure 3.3.

$G_1(s)$  and  $G_2(s)$  is based on the following matrix transfer function [6].

$$\begin{aligned} \mathbf{G}(s) &= [G_1(s) \quad G_2(s)] \\ &= \frac{-\mathbf{L}^*}{(\tau_h s + 1)} \left[ (s\mathbf{I} - \hat{\mathbf{A}}) \int_0^\tau e^{(s\mathbf{I} - \mathbf{A}_1)\sigma} d\sigma (s\mathbf{I} - \mathbf{A}_1 + \mathbf{B}_1\mathbf{L}^*) + s\mathbf{I} - \hat{\mathbf{A}} + \mathbf{B}_1\mathbf{L}^* \right]^{-1} \mathbf{H}_1 \end{aligned} \quad (3.39)$$

where

$$G_1(s) = \frac{u(s)}{y_e(s)} \quad G_2(s) = \frac{u(s)}{\dot{y}_e(s)} \quad \hat{\mathbf{A}} = \mathbf{A}_1 - \mathbf{H}_1\mathbf{C}_1 \quad (3.40)$$

Thus, the pilot transfer function has a form:

$$G_p(s) = G_1(s) + s G_2(s) \quad (3.41)$$

Frequency domain performance measures are based on the pilot transfer function  $G_p(s)$  and

the system transfer function  $G_s(s)$ .

Due to the combined elements of the human operator, perceptual time delay, Kalman-Bucy filter, linear predictor and the optimal control gain, the optimal pilot transfer function may not be represented by a simple transfer function. Using the representation of McRuer [6] with the Pade approximation for the perceptual time delay, the pilot transfer function can be expressed more effectively rather than using equation (3.39).

The delayed commanded control is defined by  $u_p(t)$ .

$$u_p(t) = u_c(t-\tau) \quad (3.42)$$

Equation (3.42) can be represented by the standard matrix form of the linear differential equation through the Pade approximation for the perceptual time delay.

$$\dot{\mathbf{x}}_p(t) = \mathbf{A}_p \mathbf{x}_p(t) + \mathbf{B}_p u_c(t) \quad (3.43)$$

$$u_p(t) = \mathbf{C}_p \mathbf{x}_p(t) + \mathbf{D}_p u_c(t) \quad (3.44)$$

The reconstruction of the human operator with the Pade approximation allows us to represent the combined KBF/LP/neuromuscular system by the standard matrix differential equation as

$$\dot{\mathbf{x}}_2(t) = \mathbf{A}_2 \mathbf{x}_2(t) + \mathbf{B}_2 [ \mathbf{y}(t) + \mathbf{v}_y(t) ] + \mathbf{E}_2 \mathbf{v}_u(t) \quad (3.45)$$

$$u(t) = \mathbf{C}_2 \mathbf{x}_2(t) \quad (3.46)$$

$$\mathbf{A}_2 = \begin{bmatrix} \mathbf{A}_1 - \mathbf{H}_1 \mathbf{C}_1 & -\mathbf{B}_1 \mathbf{D}_p \mathbf{L}^* & \mathbf{B}_1 \mathbf{C}_p & \mathbf{0} \\ -e^{\mathbf{A}_1 \tau} \mathbf{H}_1 \mathbf{C}_1 & \mathbf{A}_1 - \mathbf{B}_1 \mathbf{L}^* & \mathbf{0} & \mathbf{0} \\ \mathbf{0} & -\mathbf{B}_p \mathbf{L}^* & \mathbf{A}_p & \mathbf{0} \\ \mathbf{0} & -\mathbf{L}_2 \mathbf{D}_p \mathbf{L}^* & \mathbf{L}_2 \mathbf{C}_p & -\mathbf{L}_2 \end{bmatrix}$$

$$\mathbf{x}_2(t) = \begin{bmatrix} \mathbf{p}(t) \\ \hat{\mathbf{x}}(t) \\ \mathbf{x}_p(t) \\ \mathbf{u}(t) \end{bmatrix} \quad \mathbf{B}_2 = \begin{bmatrix} \mathbf{H}_1 \\ e^{\mathbf{A}_1 \tau} \mathbf{H}_1 \\ \mathbf{0} \\ \mathbf{0} \end{bmatrix} \quad \mathbf{E}_2 = \begin{bmatrix} \mathbf{0} \\ \mathbf{0} \\ \mathbf{0} \\ \mathbf{0} \end{bmatrix}$$

$$\mathbf{C}_2 = [\mathbf{0} \quad \mathbf{0} \quad \mathbf{0} \quad \mathbf{1}]$$

$$\mathbf{p}(t) = \mathbf{x}_1(t - \tau) \quad (3.47)$$

A state space realization for  $G_p(s)$  is associated with  $y_e(t)$  as an input and  $u(t)$  as an output of the human operator:

$$\dot{\mathbf{x}}_2(t) = \mathbf{A}_2 \mathbf{x}_2(t) + [\mathbf{B}_{21} + \mathbf{A}_2 \mathbf{B}_{22}] y_e(t) \quad (3.48)$$

$$\mathbf{u}(t) = \mathbf{C}_2 \mathbf{x}_2(t) + \mathbf{C}_2 \mathbf{B}_{22} y_e(t) \quad (3.49)$$

The second subscript indicates the number of the column matrix in the  $\mathbf{B}_2$  matrix of equation (3.47). The state space form of the human operator, equation (3.48) and (3.49), can be converted to the pilot transfer function,  $G_p(s)$ , by standard techniques. The order of  $G_p(s)$  will be  $2(n+m)+k+3$  where  $n$  is the order of the controlled system and  $m$  is the order of the shaping filter, and  $k$  is the order of the Pade approximation. The pilot transfer function has  $n+m+1$  exact and some approximate pole/zero cancellations.



### 3.5 Bode Ideal Cutoff Analysis

In 1940, Hendrick W. Bode published his work about four integrals which characterize the feedback control systems in the frequency domain [24]. It was realized that these integrals provided the analytical insight of the feedback control system as well as the design methodology [25-27] in the frequency domain which is called as the Bode ideal cutoff. In this thesis, the Bode ideal cutoff is used to relate the handling qualities with the frequency domain performance in the pilot/vehicle system and to take into account bandwidth and human sensing constraints, stability margins, and the feedback over a working band. Some of the feedback fundamentals and four Bode integrals will be discussed briefly.

Figure 3.4. represents a stable closed loop system consisting of a linear time invariant plant,  $\mathbf{G}$ , and a controller,  $\mathbf{K}$ , which is excited by command signals,  $\mathbf{r}$ , measurement noises,  $\mathbf{n}$ , and external disturbances,  $\mathbf{d}$ .  $\mathbf{P}$  is an optional prefilter which is used in shaping the command signals. It is assumed that the external disturbances are reflected to the output of the controlled system,  $\mathbf{y}$ , and all signals are multivariable. Also, the plant and the controller are linear time invariant systems which can be represented by the matrix transfer functions,  $\mathbf{G}(s)$  and  $\mathbf{K}(s)$ , respectively.

If the feedback control system shown in Figure 3.4. is stable, it can be characterized by the following equations:

(1) Input-output behavior

$$\mathbf{y} = \mathbf{GK} (\mathbf{I} + \mathbf{GK})^{-1} (\mathbf{r} - \mathbf{n}) + (\mathbf{I} + \mathbf{GK})^{-1} \mathbf{d} \quad (3.50)$$

$$\mathbf{u} = \mathbf{K} (\mathbf{I} + \mathbf{GK})^{-1} (\mathbf{r} - \mathbf{n} - \mathbf{d}) \quad (3.51)$$

$$\mathbf{e} = \mathbf{r} - \mathbf{y}$$

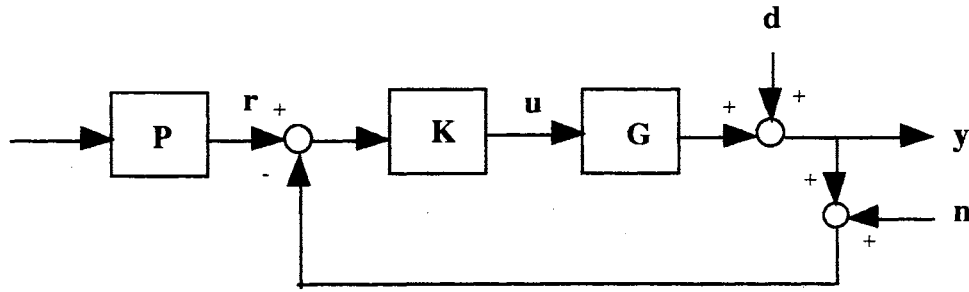


Figure 3.4. Standard Feedback Control Structure

$$= (\mathbf{I} + \mathbf{G}\mathbf{K})^{-1} (\mathbf{r} - \mathbf{d}) + \mathbf{G}\mathbf{K} (\mathbf{I} + \mathbf{G}\mathbf{K})^{-1} \mathbf{n} \quad (3.52)$$

(2) System sensitivity

$$\Delta \mathbf{H}_{cl} = (\mathbf{I} + \mathbf{G}'\mathbf{K})^{-1} \Delta \mathbf{H}_{ol} \quad (3.53)$$

where  $\Delta \mathbf{H}_{cl}$  and  $\Delta \mathbf{H}_{ol}$  represents changes in the closed loop and open loop system, respectively, which is caused by changes in the plant, i.e.,  $\mathbf{G}' = \mathbf{G} + \Delta \mathbf{G}$ .

Equations (3.50)-(3.53) explicitly show the fundamental characteristics of feedback control systems. Equation (3.52) provides the analytical insight that the loop's errors under the presence of command signals and external disturbances can be made small by making the sensitivity operator,  $(\mathbf{I} + \mathbf{G}\mathbf{K})^{-1}$ , small, and equation (3.53) shows that the closed loop sensitivity is improved under these same conditions, provided  $\mathbf{G}'$  does not stray far from  $\mathbf{G}$ . It is also shown in equation (3.50) that the output of the controlled system is not effected too much by the external disturbances with small sensitivity operator.

In the SISO systems, the scalar sensitivity,  $[1 + G(j\omega)K(j\omega)]^{-1}$ , has small magnitude, or equivalently that  $[1 + G(j\omega)K(j\omega)]$  have large magnitude, in the frequency range where the command signals, external disturbances and/or plant changes,  $\Delta G$ , are significant. Thus, good feedback controller design is focused on achieving high loop gains

in the prescribed frequency range under the stability boundaries and the constraints of the sensor noise. In spite of the simple statement of the feedback controller design, it is not a trivial work because the loop gain must satisfy certain performance tradeoffs and design limitations. Finding the appropriate tradeoff between the command/disturbance error reduction and the sensor noise error reduction is the main issue in the field of the feedback controller design. The conflict between these two objectives is shown in equation (3.52). For the example of the SISO systems, if the magnitude of  $G(j\omega)K(j\omega)$  is very large over a certain frequency range, the error due to the command and disturbance is relatively small. However, it also makes the errors due to the sensor noise relatively large because it is directly passed to the system output over the same frequency range, i.e.,

$$y = G(j\omega)K(j\omega) [1 + G(j\omega)K(j\omega)]^{-1} n \approx n \quad (3.54)$$

Also, large loop gains can make the control input,  $u$ , quite unacceptable in equation (3.51).

$$u = K(j\omega) [1 + G(j\omega)K(j\omega)]^{-1} (r - n - d) \approx G^{-1}(j\omega) (r - n - d) \quad (3.55)$$

It is shown that command, disturbances and sensor noise are actually amplified at the control input whenever the frequency range significantly exceeds the bandwidth of  $G(j\omega)$ , i.e., for  $\omega$  such that  $G(j\omega) \ll 1$  we get

$$G^{-1}(j\omega) \gg 1 \quad (3.56)$$

The Bode ideal cutoff derived from the Bode integrals will help us to calculate how much feedback is available with constraints of the sensor noise and stability margin in the prescribed frequency range. In the discussion to follow we define the open loop transfer function,  $L(s)$ , as the product of the plant transfer function,  $G(s)$ , and the controller

transfer function,  $K(s)$ , in the SISO systems.

$$L(s) = G(s)K(s) \quad (3.57)$$

where  $L$  has the magnitude,  $|L|$ , and the phase,  $\phi$ :

$$L = |L| e^{j\phi} \quad (3.58)$$

and the magnitude at low and high frequencies are denoted as

$$|L|_0 = |L(j\omega)|_{\omega=0} \quad (3.59)$$

$$|L|_\infty = |L(j\omega)|_{\omega=\infty} \quad (3.60)$$

If  $L(s)$  is minimum phase, four Bode integrals are follows:

- (1) The first integral says that the phase,  $\phi$ , of the open loop transfer function,  $L(s)$ , at one frequency is a weighted function of the log gain slope at all frequencies.

$$\phi(\omega_a) = \frac{1}{\pi} \int_{-\infty}^{\infty} \frac{d \ln |L|}{du} \ln \coth \left| \frac{u}{2} \right| du \quad (3.61)$$

where

$$u = \ln \left( \frac{\omega}{\omega_a} \right)$$

The weighting function,  $\ln \coth |u/2|$ , is a very strong weight on  $\omega_a$ , which is approximately one decade on either side of  $\omega_a$ ,

(2) The second integral says that negative feedback is always balanced by positive feedback given  $L(s)$  is stable and has more than one pole rolloff.

$$\int_0^{\infty} \ln |1 + L| d\omega = 0 \quad (3.62)$$

(3) The third integral says the open loop gain over the working band, which is normalized frequencies between 0 to 1, can be reshaped while maintaining the weighted phase outside the working band.

$$\int_{\omega=0}^{\omega=1} (\ln |L(j\omega)| - \ln |L|_{\infty}) d \arcsin \omega = - \int_{\omega=1}^{\omega=\infty} \frac{\phi}{\sqrt{\omega^2 - 1}} d\omega \quad (3.63)$$

This means that we can construct the desired loop gain freely over the working band while keeping the good high frequency performance. Figure 3.5. is a good example of the third integral. The flat gain,  $|L|_0$ , over the working band is a measure of the available feedback even though the gain is not necessary to be flat.

(4) The fourth integral says that in order to increase the loop gain,  $|L|_0$ , in the working band more negative phase is required in the same frequency range.

$$\int_{-\infty}^{\infty} \frac{\phi}{\omega} d\omega = \pi (\ln |L|_{\infty} - \ln |L|_0) \quad (3.64)$$

What the ideal shape of the open loop transfer function in the feedback control system is will be explained with the above four Bode integrals using the Nichols chart. Here the square stability margins is used to tolerate independent variations of  $x$  dB and  $y\pi$

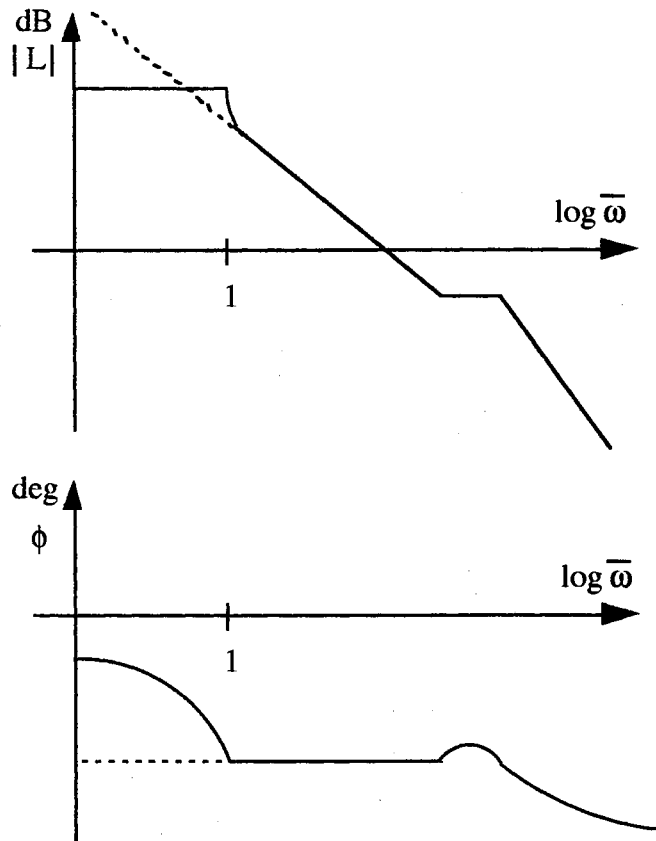


Figure 3.5. Implications of the integral allowing reshaping

radians in the change of gain and phase, respectively. In order to achieve a high loop gain in the working band,  $0 \leq \bar{\omega} \leq 1$ , we must keep the Nichols plot to the stability boundary as close as possible in Figure 3.5. This can be explained by the fourth integral.

The segment 1 and 2 of the Nichols plot, which is the function,  $|L|(\phi)$ , can be mapped onto the function  $L(j\omega)$ . The open loop transfer function of the two segments is [25]:

$$L(j\omega) = \frac{|L|_0}{[\sqrt{1 - \omega^2} + j\omega]^{\frac{2\phi}{\pi}}} \quad (3.65)$$



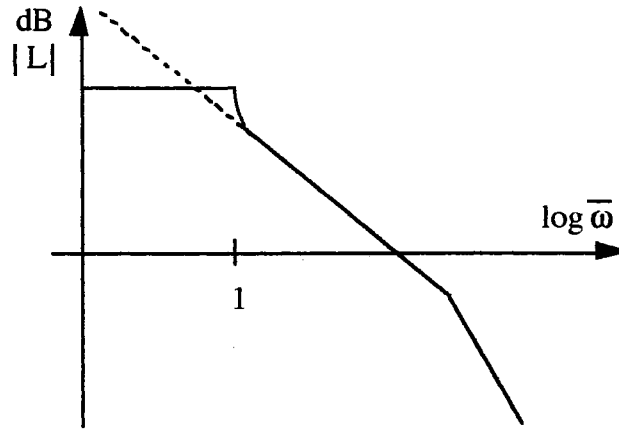


Figure 3.7. Improper adding of the High Frequency Rolloff

$$\min |L| = \max (\bar{\omega} \leq 1) \quad (3.66)$$

$$|L| \gg 1 \quad (\bar{\omega} \leq 1) \quad (3.67)$$

$$|L| = \left( \frac{\bar{\omega}}{\bar{\omega}_c} \right)^n 10^{\Lambda \left[ \frac{\pi}{20} \right]} \quad (\bar{\omega} > \bar{\omega}_c) \quad (3.68)$$

$$|\phi| \leq (1 - y) \pi \quad (\bar{\omega} \leq \bar{\omega}_c) \quad (3.69)$$

$$\phi_{\text{nmp}}(\bar{\omega}) \equiv \left| \phi_{\text{nmp}}(\bar{\omega}_c) \left( \frac{\bar{\omega}}{\bar{\omega}_c} \right) \right| \leq 1 \text{ radian} \quad (\bar{\omega} < \bar{\omega}_c) \quad (3.70)$$

where  $\bar{\omega}$  represents the normalized frequency with the working band frequency and  $n$  is the number of poles in the high frequency asymptote of  $|L|$  which is  $-6n$  dB/octave. Gain margin and phase margin is  $x$  dB and  $y\pi$  radians and  $\phi_{\text{nmp}}$  is the phase shift due to nonminimum phase sources. Figure 3.7. shows the ideal cutoff of the magnitude of the open loop transfer function and corresponding phase shape. Detailed ideal cutoff structure is shown in Figure 3.8. Note that the line with a slope of  $-12(1-y)$  dB/octave crosses the



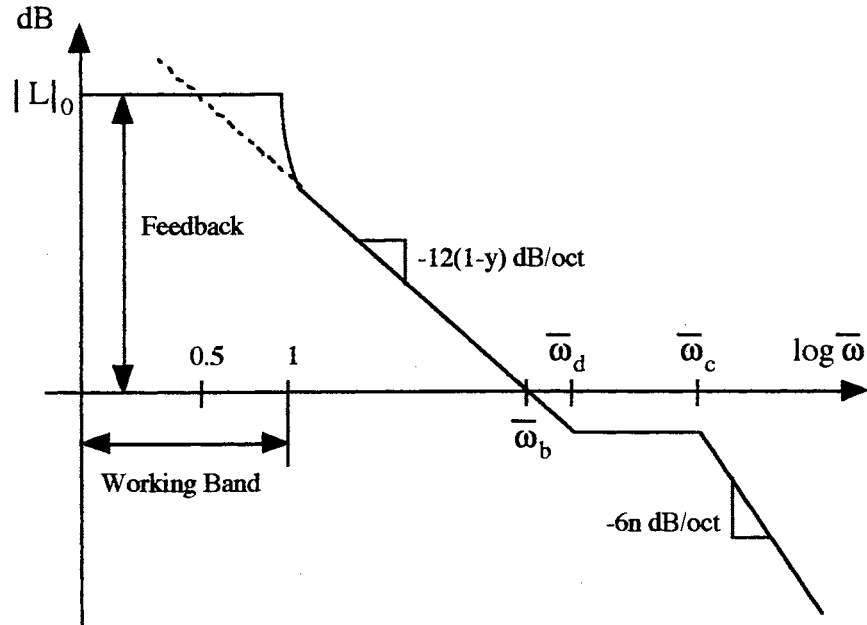


Figure 3.8. The Bode Ideal Cutoff

gain of  $|L|_0$  at  $\bar{\omega} = 0.5$ . The maximum available feedback in the working band under the high frequency constraints is represented by [25]:

$$L_{\max} = 20 \log_{10} |L|_0 = 12 (1 - y) (1 + \log_2 \bar{\omega}_d) - x \quad (3.71)$$

where

$$\bar{\omega}_d = \frac{2 (1 - y) \bar{\omega}_c}{n + \left| \phi_{\text{nmp}}(\omega_c) \right| \left( \frac{\pi}{2} \right)} \quad (3.72)$$

The Bode ideal cutoff allows us to calculate the maximum available feedback using equation (3.71) at the working band under the conditions of the high frequency rolloff, sensor noise attenuation and stability margins. High frequency constraints are related to the order of the controller and stability margin is set for the model uncertainty.

The pilot control strategy in the optimal control model is to adopt the control input,  $u^*(t)$ , which minimizes

$$J(u) = E\left\{ \lim_{T \rightarrow \infty} \frac{1}{T} \int_0^T [ \mathbf{y}^T(t) \mathbf{Q} \mathbf{y}(t) + u^T(t) \mathbf{r} u(t) + \dot{u}(t)^T(t) \mathbf{g} \dot{u}(t) ] dt \right\} \quad (3.9)$$

subject to his psycho-physical limitations. This objective function can be interpreted in the frequency domain as the pilot wanting to maximize the feedback in his working band for good tracking under the high frequency constraints such as stability margins, bandwidth, sensor noise attenuation and high frequency rolloff. In other words, the open loop transfer function of the optimal control model,  $G_p(s)G_s(s)$ , tends to construct the ideal cutoff pattern to reject the disturbances at his working band and to attenuate sensor noises at the high frequency range without violating the closed loop stability in the frequency domain. Equation (3.51) shows that large feedback gain at the working band can make the system tracking errors small in the presence of commands and disturbances.

$$\begin{aligned} \mathbf{e} &= \mathbf{r} - \mathbf{y} \\ &= (\mathbf{I} + \mathbf{GK})^{-1} (\mathbf{r} - \mathbf{d}) + \mathbf{GK} (\mathbf{I} + \mathbf{GK})^{-1} \mathbf{n} \end{aligned} \quad (3.51)$$

In the above two equations, equation (3.9) and equation (3.51), which defines the objective of the human pilot's behavior, we can find the strong relation between the value of performance index in the time domain and the feedback at working band in the frequency domain. Another important factor of the handling qualities is the speed of the closed loop system response. If the human is working in the relatively high frequency range,  $\bar{\omega} \leq \bar{\omega}_c$  in Figure 3.9., the closed loop system response will be fast. Sensor noise cutoff frequency is heavily dependent on the system dynamics. Figure 3.9. shows the interpretation of the

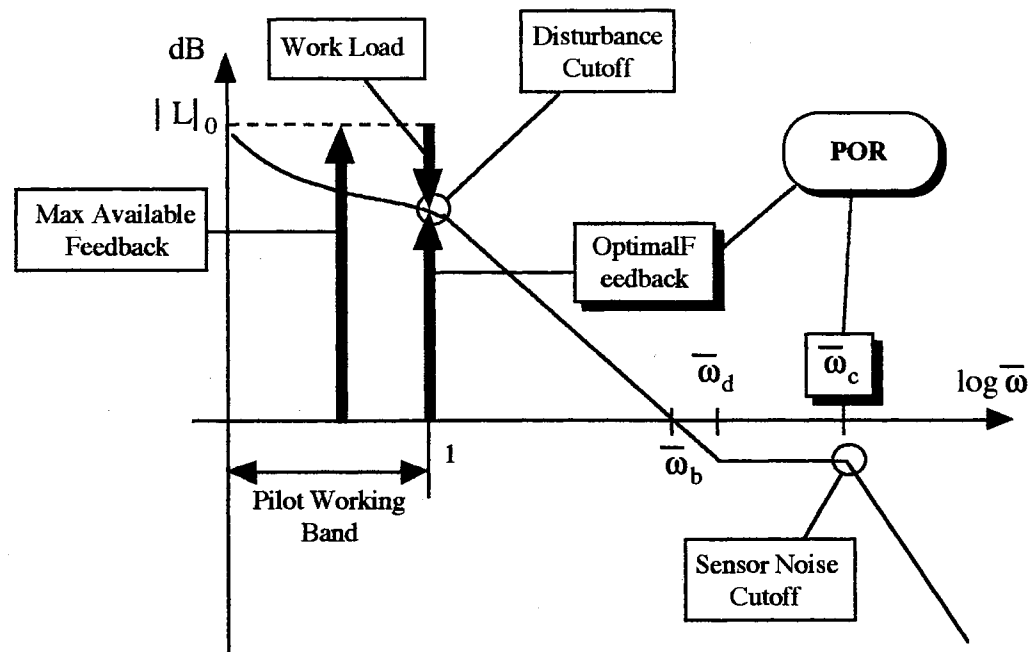


Figure 3.9. Interpretation of the Bode Ideal Cutoff

Bode ideal cutoff in the tracking task. Here, good tracking is related to the feedback at the working band and fast response is related to the sensor cutoff frequency.

Therefore, the pilot opinion rating will be predicted based on these two terms which are generated from the optimal control model automatically with the human limitations. It is also possible to use the maximum available feedback at the working band as the indication of the difficulty level of the task and/or the pilot work load.

The important factors of the open loop performance required in the ideal cutoff analysis are shown in Figure 3.10.

- (1)  $w_1 =$  Disturbance cutoff frequency (rad/sec)

It is defined by the shaping filter cutoff frequency to model the command signal.

Pilot working band is defined by  $0 \leq \omega \leq w_1$ .

- (2)  $w_2 =$  Gain crossover frequency (rad/sec)
- (3)  $x =$  Gain margin (dB)
- (4)  $y =$  Phase margin (deg)

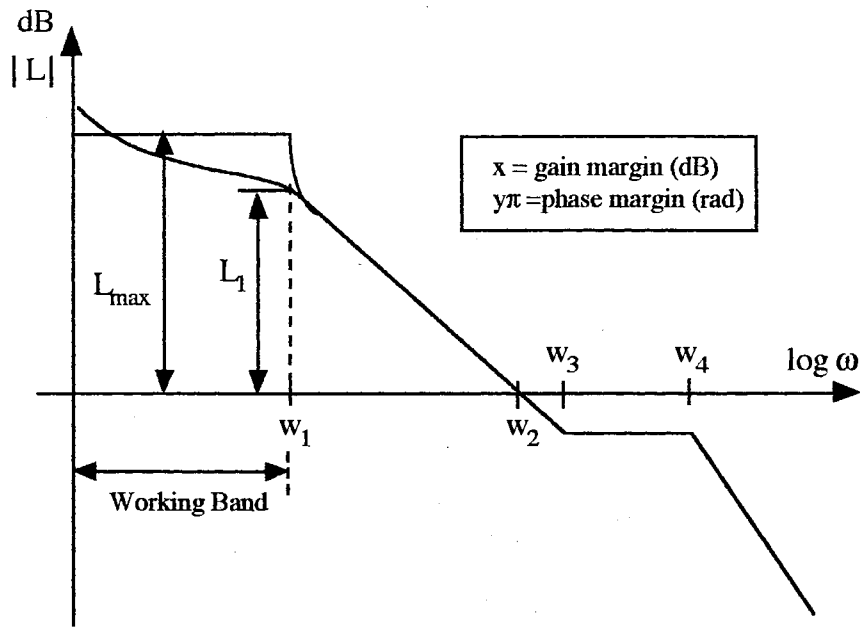


Figure 3.10. Important Factors of the Ideal Cutoff

- (5)  $\omega_4$  = Sensor noise cutoff frequency (rad/sec)

It is measured by the high frequency peak of the open loop transfer function.

- (6)  $\omega_3$  = Ideal Bode step frequency (rad/sec)

$$-x = -12(1-y) \log_2 \left[ \frac{\omega_3 - \omega_2}{\omega_2} \right] \quad (3.73)$$

- (7)  $L_1$  = Feedback at a disturbance cutoff frequency,  $\omega_1$

- (8)  $L_{\max}$  = Maximum available feedback (dB)

Using  $\omega_d = \omega_3 / \omega_1$ , it can be calculated by equation (3.71)

Figure 3.10. helps us to understand the relation between the optimal control model loop structure and the equivalent transfer function loop structure.

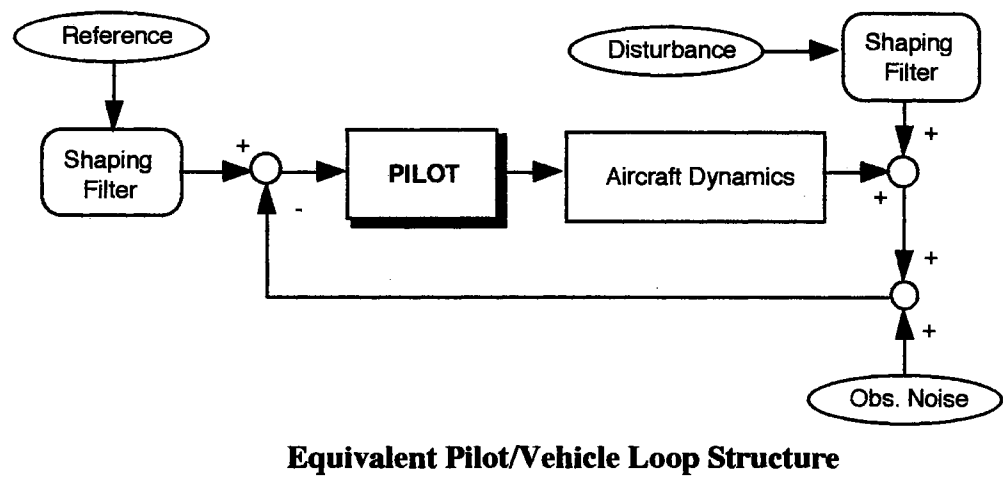
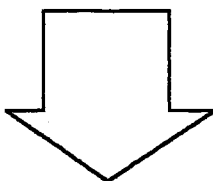
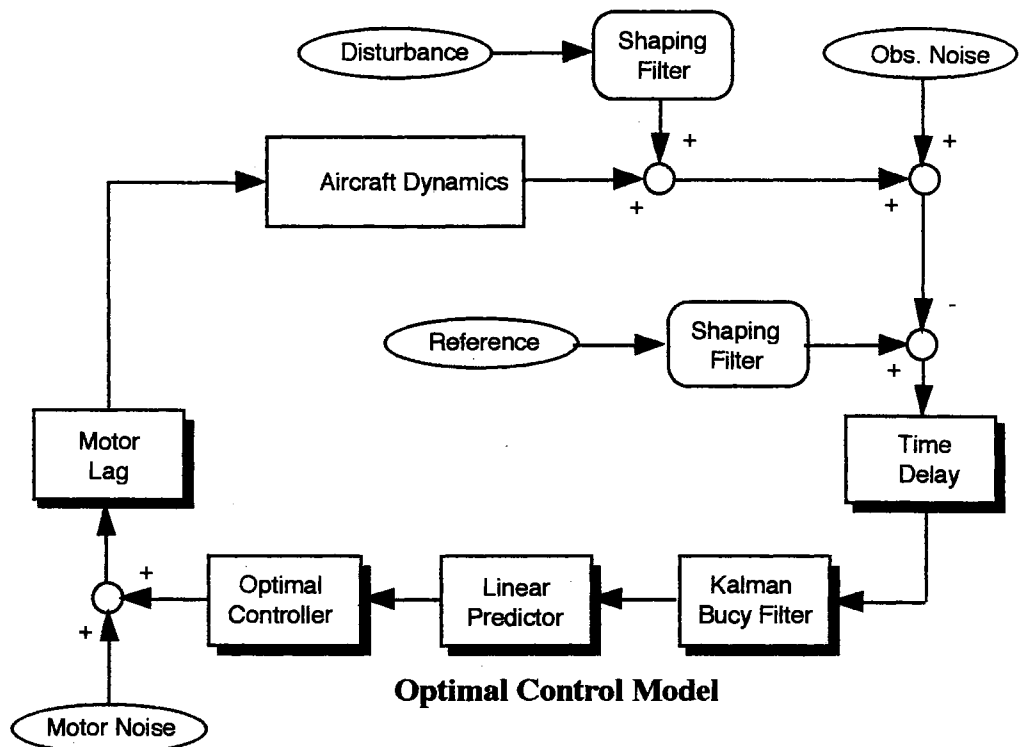


Figure 3.11. Correlation of Time Domain and Frequency Domain Loop Structure

## CHAPTER IV

### IMPLEMENTATION

#### 4.1 Descriptions of the Numerical Simulation

In order to implement the optimal control model, it is assumed that the following input parameters are given:

- (1) **A, B, C, D, F, W:** parameters of the linear vehicle system and the shaping filter.
- (2)  $q_i, r$ : weightings in the performance index
- (3)  $\tau_n, \tau, f, T_i$ : parameters of the human's limitation

Experimental data and equations in the manual control systems are [20-22]:

- (1)  $\tau_n = 0.1 - 0.6$  sec: neuromuscular time constant
- (2)  $\tau = 0.15 - 0.25$  sec: perceptual time delay
- (3)  $[T_1, T_2] = [0.05 \text{ deg}, 0.18 \text{ deg/sec}]$ : observation threshold
- (4) Observation noise

$$v_{yi} = \frac{\rho_{yi} \pi}{f} \frac{\sigma_{yi}^2}{E(\sigma_{yi}, T_i)^2} \quad i = 1, 2$$

$\rho_{yi} = 0.01$  : average noise to signal ratio

frequency power density = -20 dB

- (5) Neuro-motor noise

$$V_u = \pi \rho_u E\{u_c^2\}$$

$$\rho_u = 0.003$$

frequency power density = -25 dB

The algorithm for solving the human optimal control model is summarized in Figure 4.1. The human optimal control model can be assumed as the standard linear quadratic Gaussian optimal control problem, with the following distinctions [3]:

- (1) The performance index includes  $\dot{u}(t)$ . The LQR problem is solved by augmented system with neuromuscular mode.
- (2) The Kalman Bucy filter is used for estimating the states of the controlled system augmented with the neuromuscular mode.
- (3) The linear predictor is used since the observations are delayed.
- (4) The observation and motor noise intensities are defined as a ratio of the respective mean square outputs and inputs, equation (3.7) and (3.21). Iteration is required to achieve this ratio. In this thesis, bi-section method and  $x=f(x)$  method are used for the iteration of LQR problem and KBF/LP problem, respectively.
- (5) 4<sup>th</sup> order Pade approximation for the perceptual delay is used to obtain the pilot transfer function. This approximation is valid in the range of  $\omega \leq 30$  rad/sec .

(Figure 4.2.)

#### 4.2. Application of the Kleinman Data [6]

The performance of the optimal control model was successfully matched to the experimental data obtained from a set of simple dynamics by Kleinman et al [6]. Here two simple vehicle dynamics,  $k/s$  and  $k/s^2$ , among them are investigated to validate the representation of the pilot transfer function using the Pade approximation for the perceptual time delay. For  $k/s$  and  $k/s^2$  dynamics, a simulated first order noise spectrum having a break frequency of 2 rad/ sec was applied as a velocity disturbance to the vehicle.

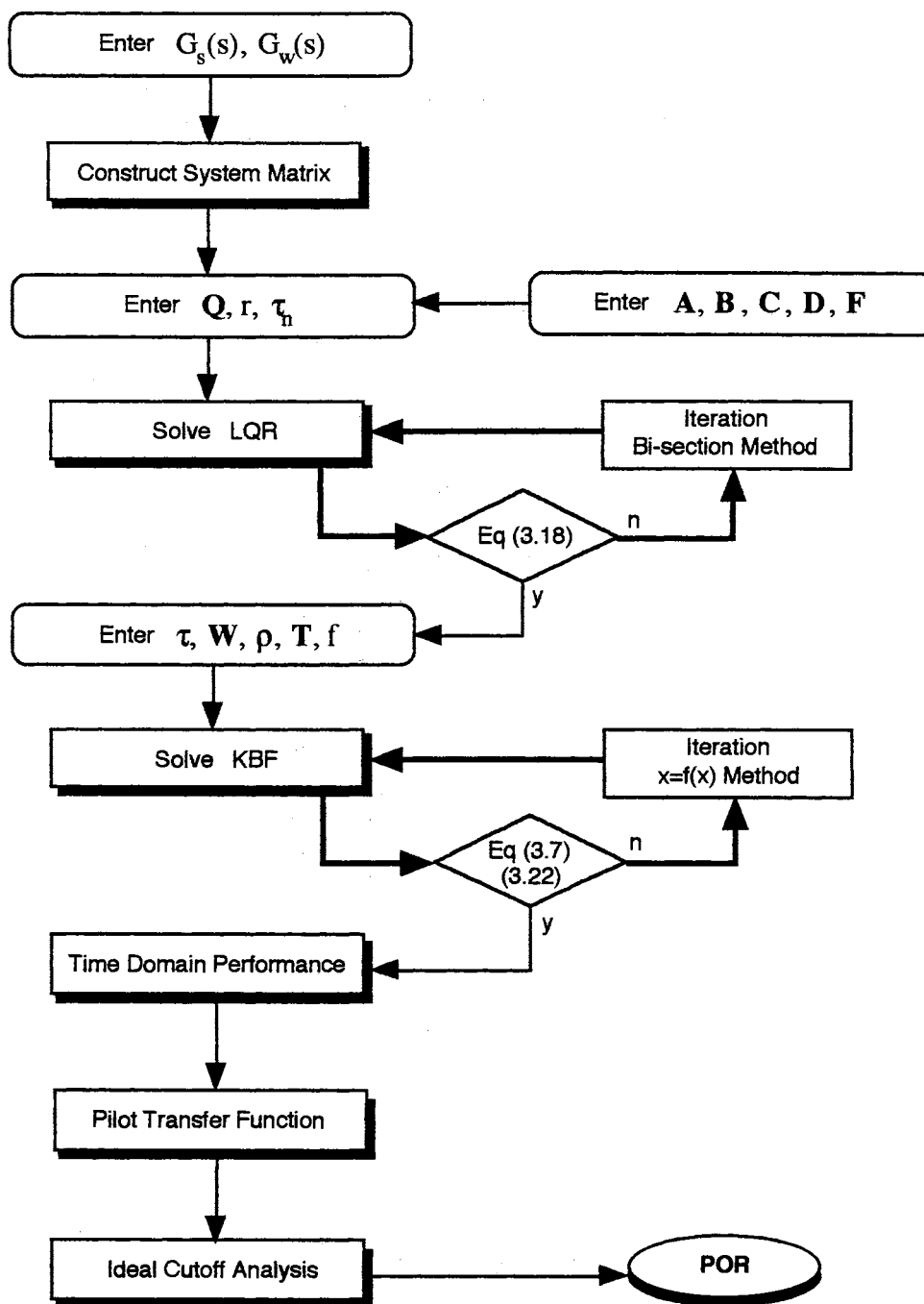


Figure 4.1. Computation Flow of the Optimal Control Model



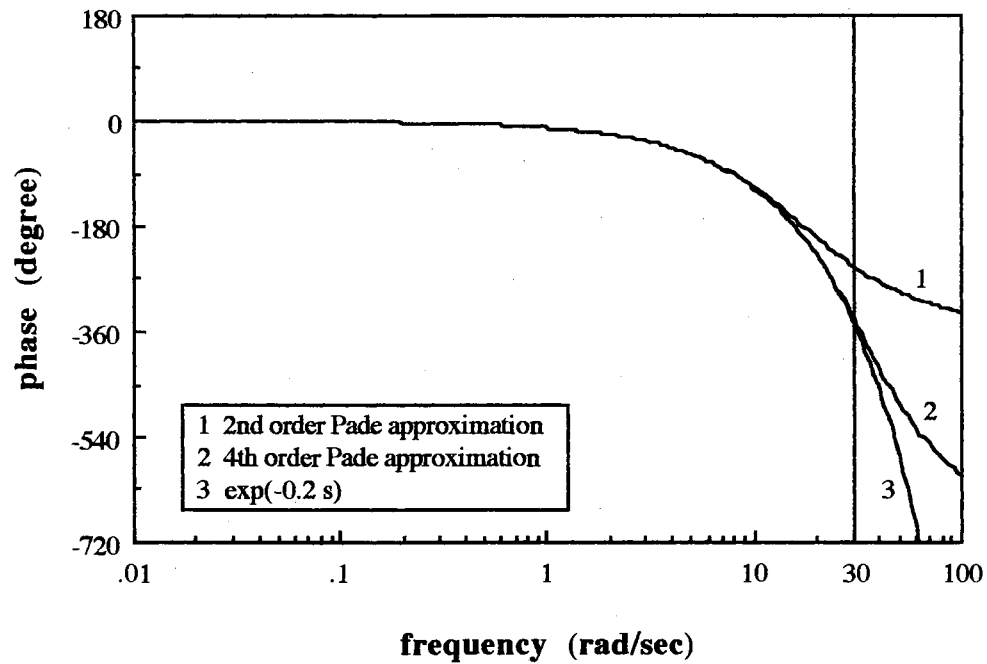


Figure 4.2. Phase Plot of the Pade Approximation for 0.2 sec Delay

#### 4.2.1. Velocity Control Example

The controlled system and the external disturbance are represented by:

$$\begin{aligned}
 y(s) &= G_s(s) [u(s) + G_w(s) w(s)] \\
 &= G_s(s)u(s) + G_s(s)G_w(s)w(s)
 \end{aligned} \tag{4.1}$$

where

$$G_s(s) = \frac{1}{s} \quad G_w(s) = \frac{1}{s+2} \tag{4.2}$$

The second canonical state space form is used for the systematic representation based on the white noise,  $w(t)$ , and the control input,  $u(t)$ , in equation (4.1)

$$\dot{x}_1(t) = x_2(t) \quad (4.3)$$

$$\dot{x}_2(t) = -2x_2(t) + w(t) \quad (4.4)$$

$$\dot{x}_3(t) = u(t) \quad (4.5)$$

$$y(t) = x_1(t) + x_3(t) \quad (4.6)$$

where  $w(t)$  is Gaussian white noise with a covariance  $W = 8.8$ .  $x_1(t)$  and  $x_3(t)$  are the system output due to the white noise and the control input, respectively. The error and error rate,  $y_e(t)$  and  $\dot{y}_e(t)$ , for the regulating task are defined as

$$y_e(t) = -y(t) = -x_1(t) - x_3(t) \quad (4.7)$$

$$\dot{y}_e(t) = -\dot{y}(t) = -x_2(t) - u(t) \quad (4.8)$$

The objective of the task is to minimize the following mean squared performance index

$$J(u) = E\{y_e^2\} + g E\{\dot{u}^2\} \quad (4.9)$$

The input parameters for solving the optimal control model and results of the time domain performance are shown in TABLE 4.1 and TABLE 4.2 respectively. In TABLE 4.2, (.) represents the experimental value of the Kleinman data [10]. Figure 4.3.-4.5. shows the frequency domain results using the 4<sup>th</sup> order Pade approximation. The magnitude of the approximated pilot transfer function is exactly the same as the Kleinman's model and its phase is compared with the Kleinman model in Figure 4.6.

TABLE 4.1

## INPUT PARAMETERS OF VELOCITY CONTROL EXAMPLE

W	$\tau_h$	$\tau$	$\rho_y$	$\rho_{\dot{y}}$	$\rho_u$	$q_1$	$q_2$	f	$T_1$	$T_2$
8.8	0.08	0.15	0.01	0.01	0.003	1	0	1	0	0

TABLE 4.2

## TIME DOMAIN PERFORMANCE OF VELOCITY CONTROL EXAMPLE

g	$\sigma_{y_e}^2$	$\sigma_{\dot{y}_e}^2$	$\sigma_u^2$	$\sigma_{\ddot{u}}^2$	$\sigma_{\ddot{u}}^2$	J
0.00016	0.12(0.13)	3.07(3.1)	3.86(4.2)	4.85	244	0.16

This approximation is valid in the frequency range less than 30 rad/sec.

The pilot transfer function is:

$$G_p(s) = \frac{181.967(0)(-2)(-3.26)(-6.43)(-12.50)(-12.67)[-0.96,40.31][-0.62,45.19]}{(0)(-1.99)(-2)(-6.50)(-12.50)(-12.50)[0.28,23.32][0.53,58.18](-78.55)} \quad (4.10)$$

where (a) represents  $(s+a)$  and  $[\zeta, \omega_n]$  represents  $(s^2+2\zeta\omega_n s+\omega_n^2)$ . The order of the pilot transfer function is 11, which matches the number of the state,  $\mathbf{x}_2(t)$ , in equation (3.47). The order of the pilot transfer function, N, can be calculated by the simple equation:

$$N = 2(n+m+1)+(\text{order of Pade approximation}) + 1 \quad (4.11)$$

where  $n$  and  $m$  are the order of the controlled system and the shaping filter, respectively.  $(n+m)$  represents the number of the minimum states of the system equation based on equation (3.2). In this example, the number of the states in the system equation, equation (4.3)-(4.5), is 3, but the number of the minimum states is 2. The number of zeros of the pilot transfer function should be less than the order of the pilot transfer function because the matrix  $C_2B_{22}$  is always zero in equation (3.49).

Equation (4.10) has 3 exact pole/zero cancellations which are the poles of the controlled system, (0), the shaping filter, (-2), and the neuromuscular dynamics, (-12.50). It also contains 2 close pole/zero cancellations, (-6.43)(-12.67)/(-6.50)(-12.50). These exact cancellations can be explained by the use of the  $A_1$  matrix in both the Kalman Bucy filter and the linear predictor. The numerator, [-0.96,40.31][-0.62,45.19], is the same as the numerator of the Pade approximation which represents the perceptual time delay. This can be converted to the time delay in the low frequency range:

$$\frac{(2)(0.96)}{(40.31)} = 0.048 \text{ sec}, \quad \frac{(2)(0.62)}{(45.19)} = 0.027 \text{ sec}$$

$(0.048+0.027)=0.075$  sec is half of the given time delay, 0.15 sec. The denominator, [0.28,23.32][0.53,58.18], is the shifted version of the Pade approximation due to the loop closure. These can also be converted to the time delay in the low frequency range:

$$\frac{(2)(0.28)}{(23.32)} = 0.024 \text{ sec}, \quad \frac{(2)(0.53)}{(58.18)} = 0.018 \text{ sec}$$

$(0.024+0.018)=0.042$  sec is another half of the Pade approximation. Thus, the total recovered time delay is  $(0.075+0.042)=0.117$  sec, which is recognized as the effective time delay of the human operator. If we cancel the exact and close pole/zeros and neglect

(-78.55) with the gain adjustment, the pilot transfer function can be represented as

$$G_p(s) = \frac{4.17(-3.26)}{(-1.99)} e^{-0.117s} \quad (4.12)$$

This reduced simple pilot model works very well only in the frequency range less than 3 rad/sec. (Figure 4.7.-4.8.) However, the peak of the pilot transfer function, which is related to the sensor noise attenuation explained in Section 3.5, cannot be explained in this model. It is a very significant factor in handling qualities. Thus, the high frequency approximation should be done outside of this peak, and it will be discussed in detail in Section 4.3.

$$G_p(s) = \frac{2271.50(-3.26)}{(-1.99)[0.27,23.32]} e^{-0.099s} \quad (4.13)$$

The magnitude and phase of the equation (4.13) are also shown in Figure 4.7.-4.8. This reduced model is much better than equation (4.12) from the point of view of high frequency approximation.

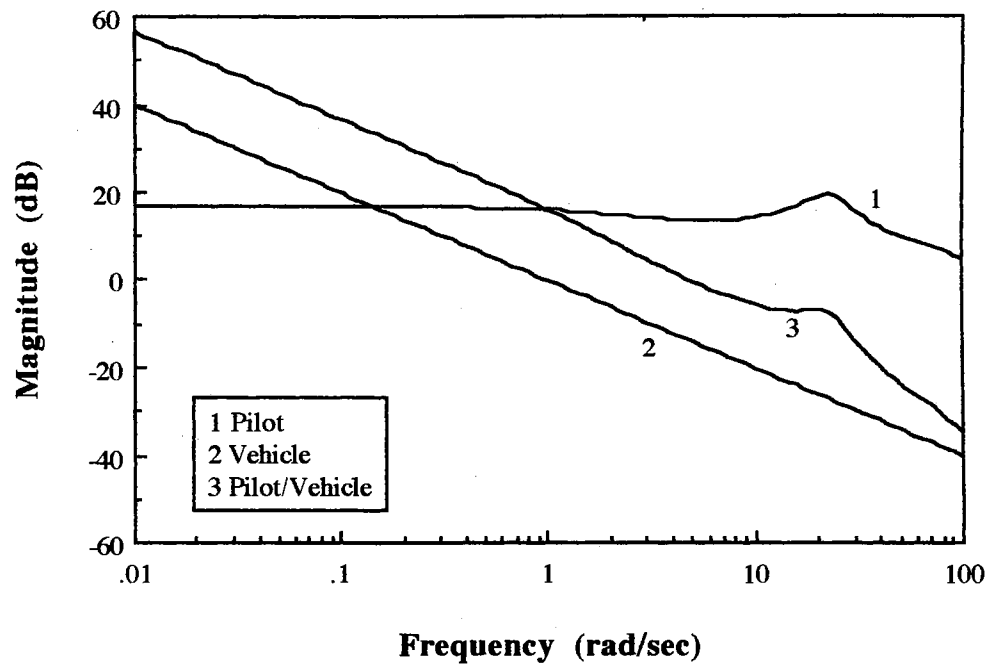


Figure 4.3. Magnitude Plot of Open Loop Response (Velocity Control)

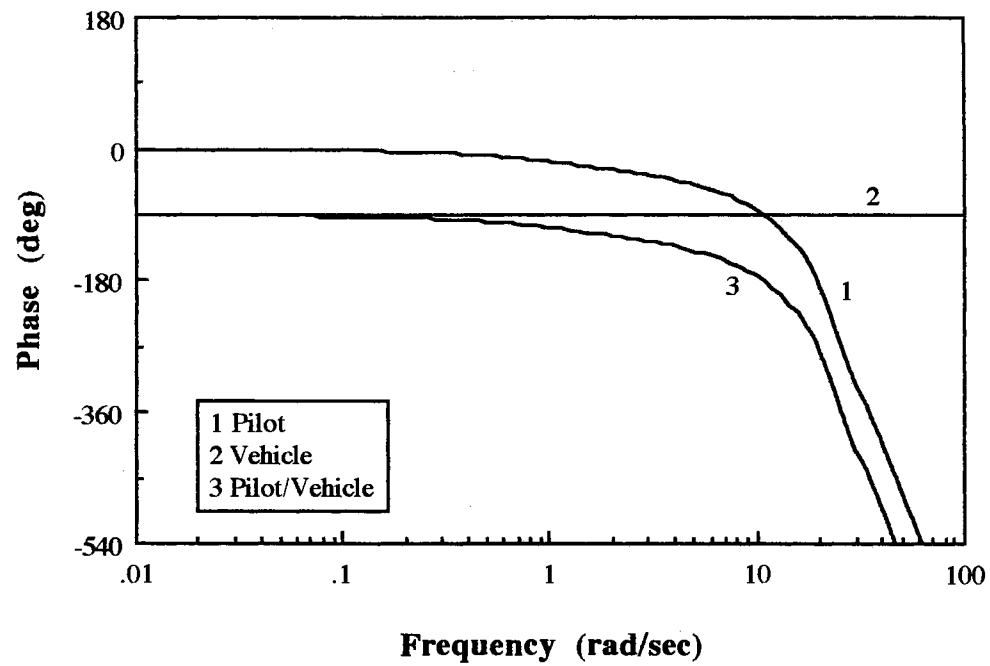


Figure 4.4. Phase Plot of Open Loop Response (Velocity Control)

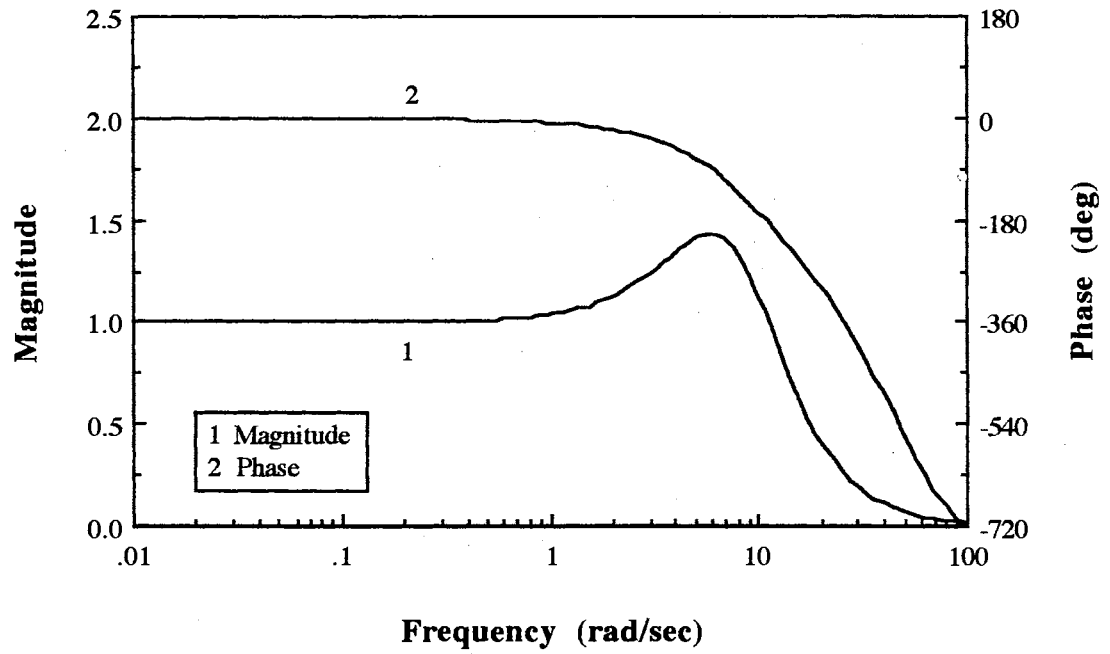


Figure 4.5. Closed Loop Response (Velocity Control)

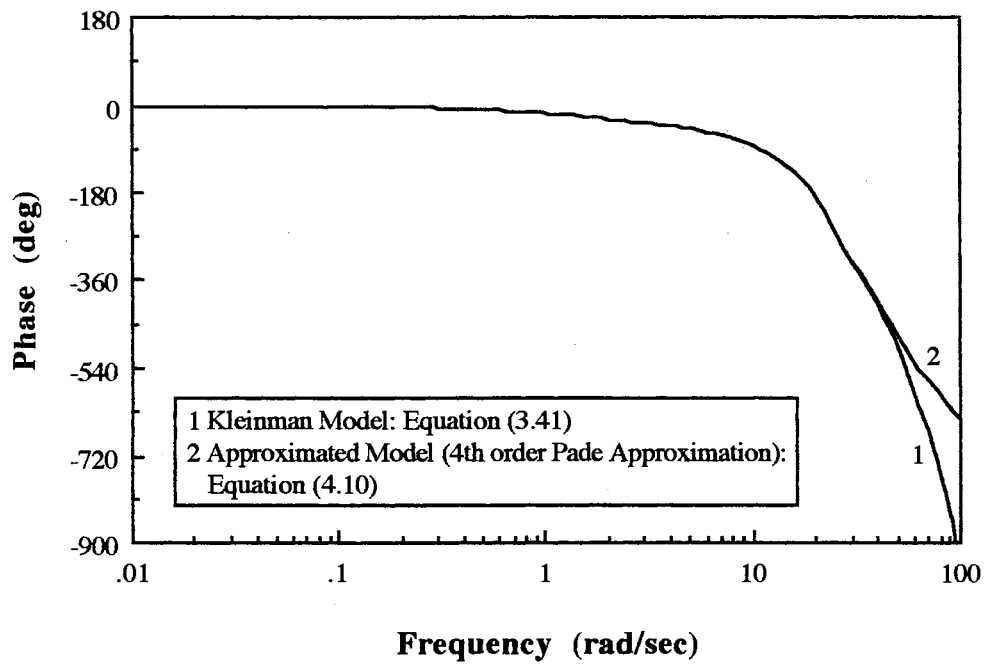


Figure 4.6. Comparison of Kleinman Model and Approximated Model

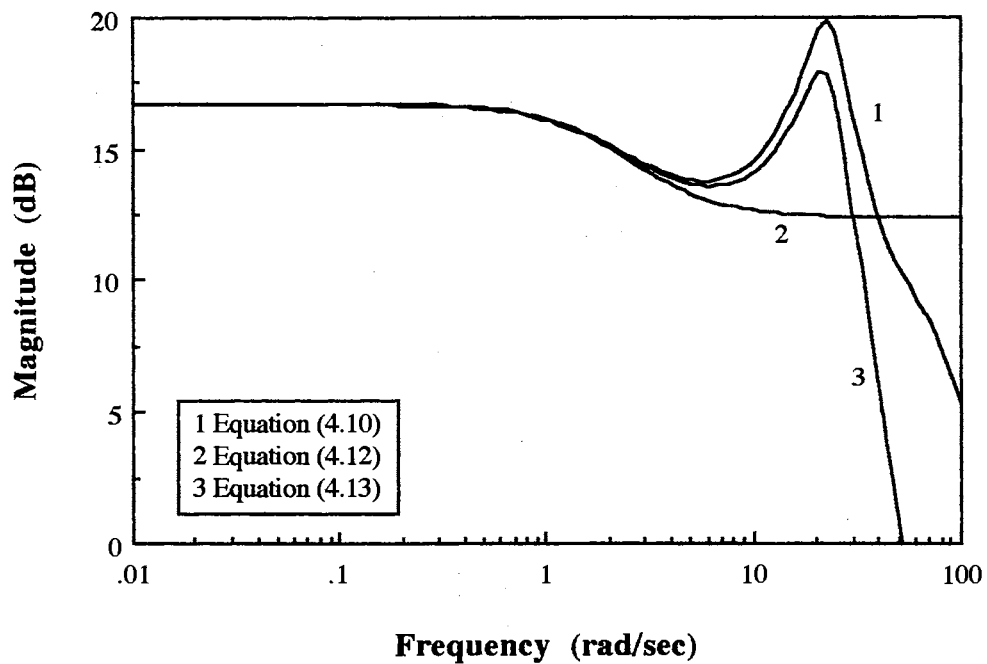


Figure 4.7. Magnitude Plot of Pilot Transfer Function (Velocity Control)

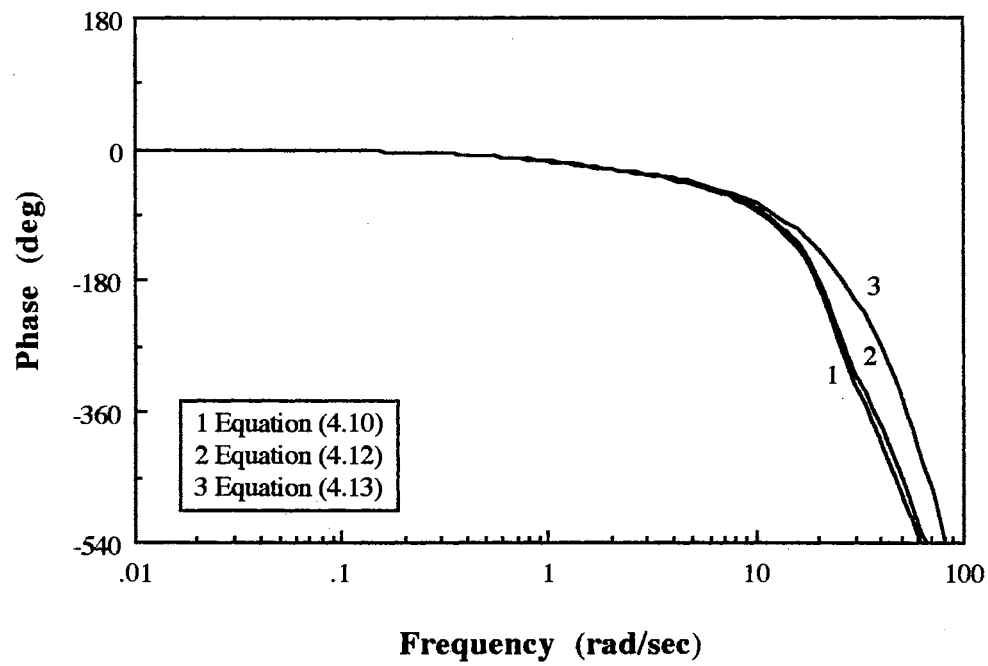


Figure 4.8. Phase Plot of Pilot Transfer Function (Velocity Control)



### 4.2.2 Acceleration Control Example

The controlled system and the external disturbance are represented by:

$$\begin{aligned} y(s) &= G_s(s) [u(s) + G_w(s) w(s)] \\ &= G_s(s)u(s) + G_s(s)G_w(s)w(s) \end{aligned} \quad (4.14)$$

where

$$G_s(s) = \frac{1}{s^2} \quad G_w(s) = \frac{1}{s+2} \quad (4.15)$$

The state space form of the system equation is:

$$\dot{x}_1(t) = x_2(t) \quad (4.16)$$

$$\dot{x}(t) = -x_1(t) + w(t) \quad (4.17)$$

$$\dot{x}_3(t) = x_4(t) \quad (4.18)$$

$$\dot{x}_4(t) = u(t) \quad (4.20)$$

$$y(t) = x_1(t) + x_3(t) \quad (4.21)$$

where  $w(t)$  is Gaussian white noise with a covariance  $W = 0.217$ .  $x_1(t)$  and  $x_3(t)$  are the system output due to the white noise and the control input, respectively. The error and error rate,  $y_e(t)$  and  $\dot{y}_e(t)$ , for the regulating task is defined as

$$y_e(t) = -y(t) = -x_1(t) - x_3(t) \quad (4.22)$$

$$\dot{y}_e(t) = -\dot{y}(t) = -x_2(t) - x_4(t) \quad (4.23)$$

The objective of the task is to minimize the following mean squared performance index

$$J(u) = E\{y_e^2\} + g E\{u^2\} \quad (4.24)$$

The input parameters for solving the optimal control model and results of the time domain performance are shown in TABLE 4.3 and TABLE 4.4, respectively.

TABLE 4.3

INPUT PARAMETERS OF ACCELERATION CONTROL EXAMPLE

W	$\tau_n$	$\tau$	$\rho_y$	$\rho_{\dot{y}}$	$\rho_u$	$q_1$	$q_2$	f	T <sub>1</sub>	T <sub>2</sub>
0.217	0.08	0.21	0.01	0.01	0.003	1	0	1	0	0

TABLE 4.4

TIME DOMAIN PERFORMANCE OF ACCELERATION CONTROL EXAMPLE

g	$\sigma_{y_e}^2$	$\sigma_{\dot{y}_e}^2$	$\sigma_u^2$	$\sigma_{\dot{u}}^2$	$\sigma_{\ddot{u}}^2$	J
0.000064	0.010(0.0014)	0.11(0.10)	1.33(1.43)	1.83	66.77	0.014

Figure 4.9.-4.11. shows the results of the frequency domain performance.

The pilot transfer function is:

$$G_p(s) = \frac{436.23(0)(0)(-0.46)(-2)(-2.38)(-3.84)(-9.99)(-10.01)}{(0)(0)(-2)(-2)(-3.82)(-9.99)(-9.99)[0.31,10.34]} \frac{[-0.96,28.78][-0.62,32.28]}{[0.55,32.15][0.92,37.82]} \quad (4.25)$$

The reduced pilot transfer function is:

$$G_p(s) = \frac{254.76(-0.46)(-2.38)}{(-2)[0.31,10.34]} e^{-0.195 s} \quad (4.26)$$

Equations (4.25) and (4.26) are compared in Figure 4.12. and 4.13.

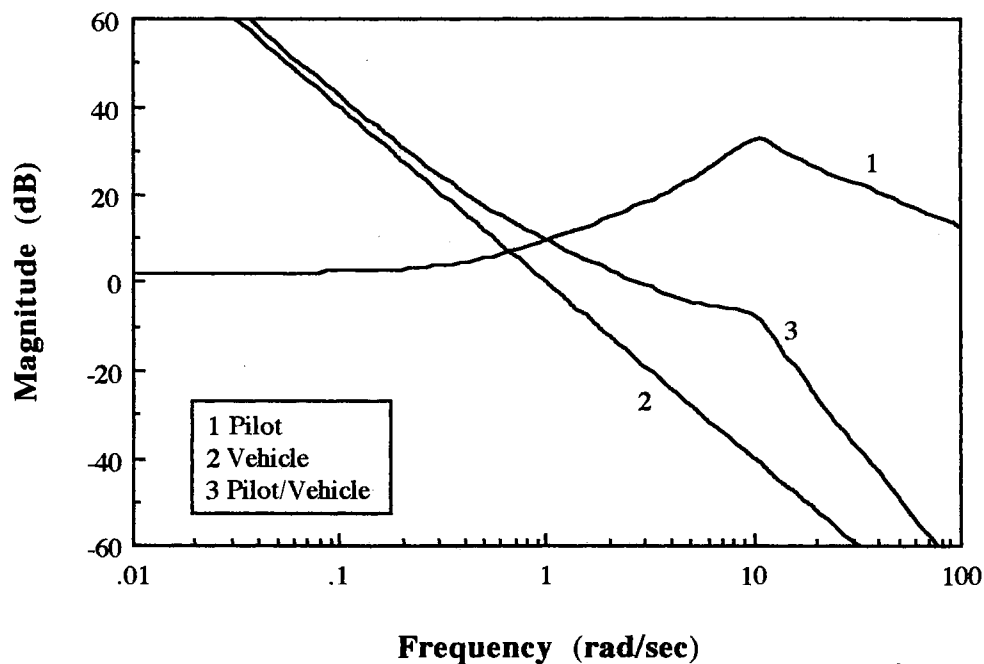


Figure 4.9. Magnitude Plot of Open Loop Response (Acceleration Control)

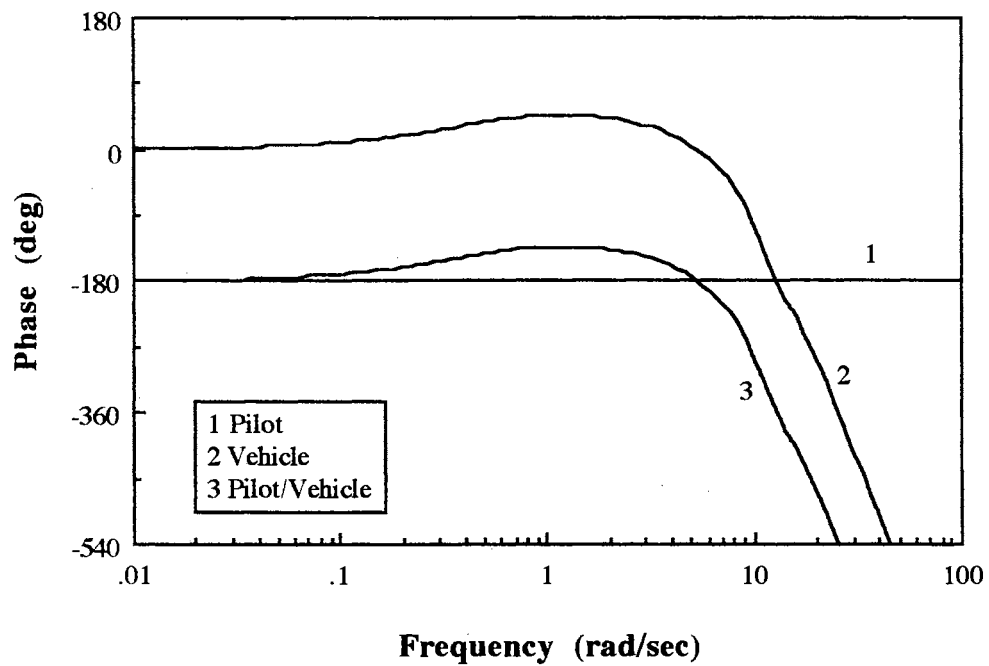


Figure 4.10. Phase Plot of the Open Loop Response (Acceleration Control)

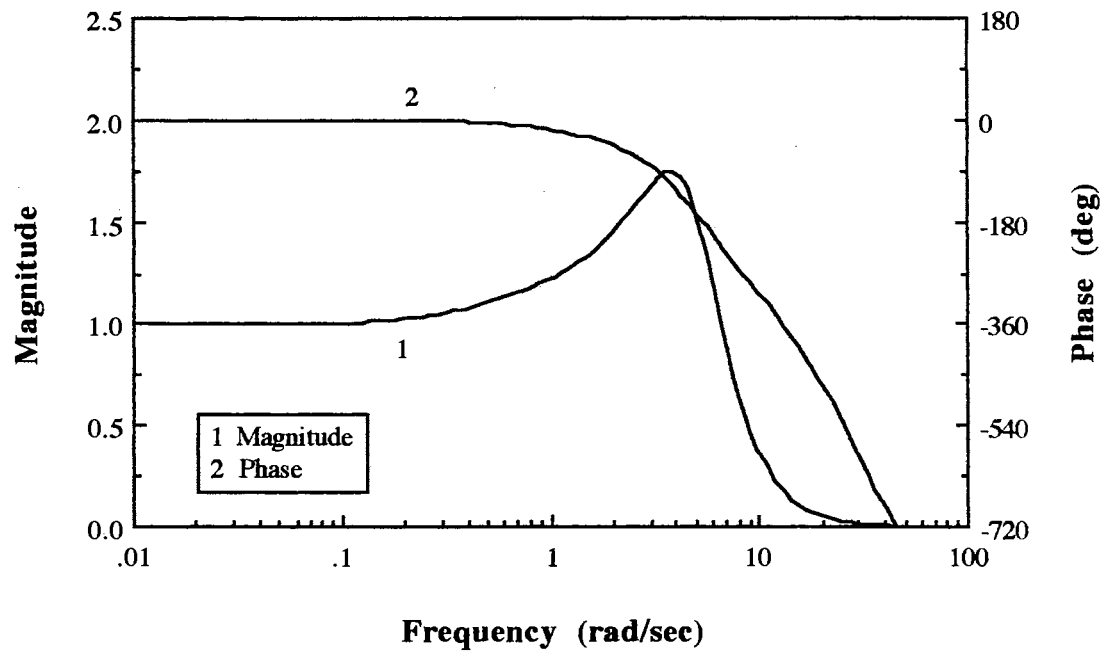


Figure 4.11. Closed Loop Response (Acceleration Control)

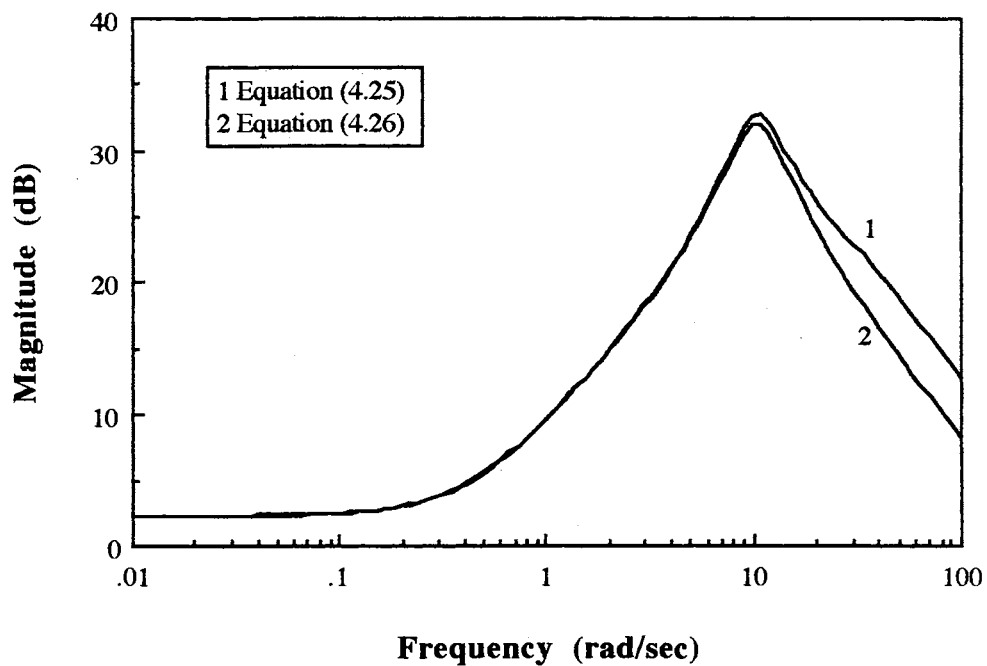


Figure 4.12. Magnitude Plot of the Pilot Transfer Function (Acceleration Control)

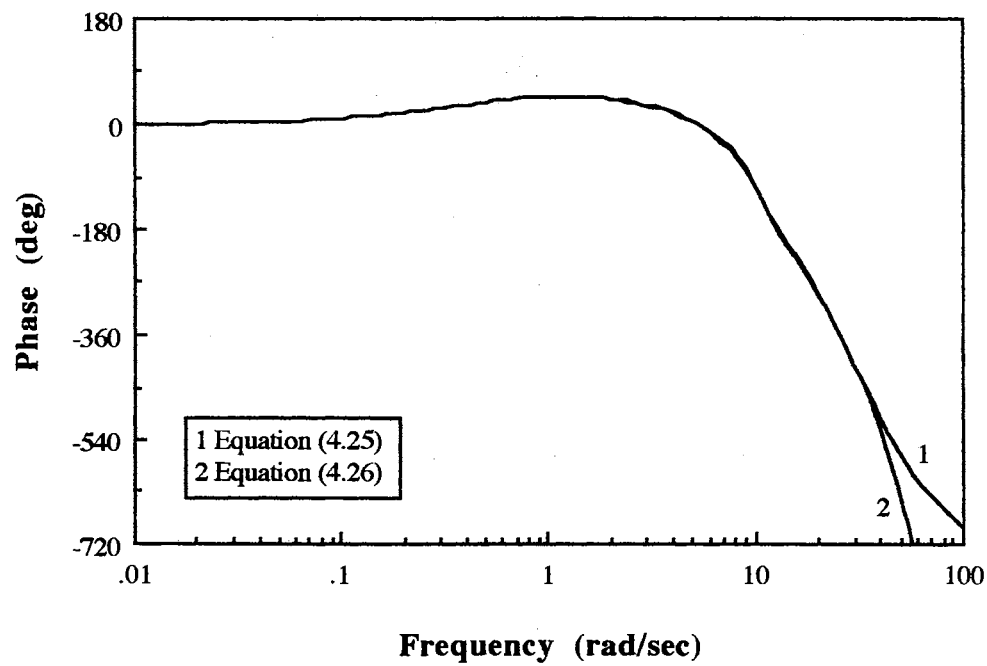


Figure 4.13. Phase Plot of Pilot Transfer Function (Acceleration Control)

### 4.3 Application for the Neal-Smith Data[8]

#### 4.3.1 Neal-Smith Tracking Task

In 1970, Neal and Smith investigated the longitudinal flying quality problems of fighter aircraft based on the experimental results of the USAF/CAL variable stability T-33 airplanes. This work was done for the following objectives:

- (1) To find the effects of the flight control system (FCS) in both the high order dynamics and the short period characteristics
- (2) To provide design criteria which can explain the handling qualities in performing a given task.

A total of 51 basic FCS/short period configurations were tested for the pitch tracking task in the combat phase of the fighter's mission. The pilot opinion rating, Cooper-Harper scale, representing an overall control and tracking ability of the airplane to perform a given task, was provided to each configuration through the actual flight test by a test pilot. Neal and Smith used a simple classical pilot model in the loop, which is shown in Figure 4.14., to explain the results of the experiments.

The control strategy for the tracking task based on the pilot comments is that the pilot wants to track a target quickly and predictably with a minimum overshoot and oscillation. Neal and Smith interpreted this strategy with following mathematical terms:

- (1) The pilot tries to achieve a certain open loop gain crossover frequency,  $\omega_c$ ,

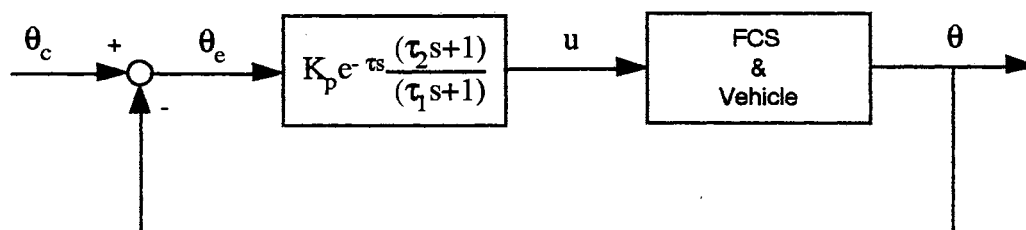


Figure 4.14. Neal-Smith Pitch Tracking (Classical Model)

- 2) The pilot tries to minimize the closed loop droop at  $\omega \leq \omega_c$ .
- 3) The pilot tries to maintain the high frequency stability by keeping the closed loop damping ratio greater than 0.35 and the phase margin of 60 to 110 degree.

In this mathematical interpretation of the pilot control strategy, (1) and (2) are related to the low frequency performance in the range,  $0.5 \leq \omega \leq 3$  rad/sec, roughly. The low frequency performance can be explained by the closed loop droop and the bandwidth, BW, defined in Figure 4.15., which means that the pilot wants to minimize the closed loop droop in the frequencies below BW. The Nichols chart is used to find the parameters of the pilot transfer function satisfying the tracking performance standard because it uses the gain and phase information of the open and closed loop in one plot.

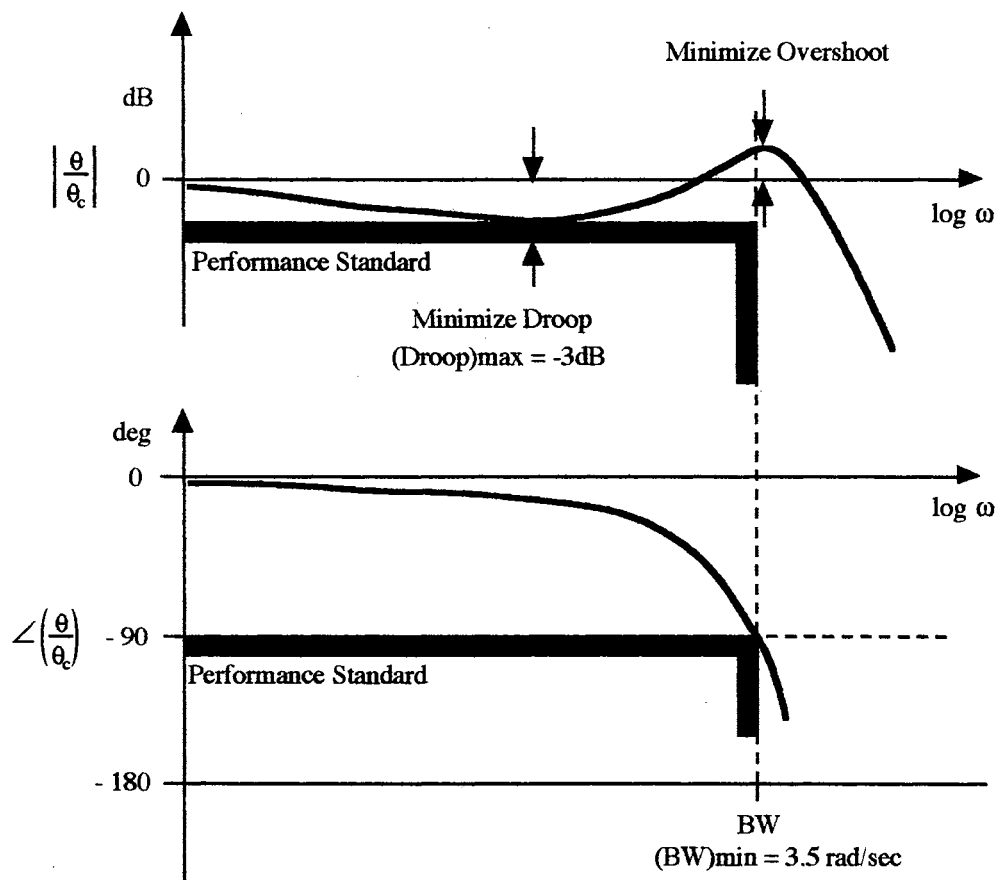


Figure 4.15. Neal-Smith Tracking Performance Standard

However, in the Neal-Smith methodology there are the following disadvantages:

- (1) There is no consideration of a driving noise, which can be defined for a given task, in generating the pilot transfer function.
- (2) Bandwidth, which may have critical importance to handling qualities, is fixed and predetermined for the various different controlled systems.
- (3) Defining the handling quality levels seems to be artistic.

In this thesis, the optimal control model technique is used to generate the pilot transfer function, which was explained in Section 3.4., and the frequency domain performance of the open loop transfer function is analyzed related to prediction of the pilot opinion ratings by the concept of the Bode ideal cutoff. The pilot transfer function is the frequency domain version of the optimal control model. So, the question is how the optimal control model works in the frequency domain in the presence of the driving noise (command signal) and the observation noise (sensor noise). This thesis is intended to answer to this question particularly. This attempt might provide more general understanding of the pilot model as well as the bridge between the frequency domain and time domain approach to pilot/vehicle analysis.

The vehicle dynamics are represented by the following transfer function [8]:

$$\frac{\theta(s)}{u(s)} = \frac{K_{\theta} (\tau_1 s + 1)(\tau_{\theta_2} s + 1)}{s (\tau_2 s + 1) \left( \frac{s^2}{\omega_3^2} + \frac{2\zeta_3}{\omega_3} s + 1 \right) \left( \frac{s^2}{\omega_{sp}^2} + \frac{2\zeta_{sp}}{\omega_{sp}} s + 1 \right)} \quad (4.27)$$

The corresponding parameters are listed with each configuration number and the gain,  $K_{\theta}$ , is defined as

$$K_{\theta} = \frac{57.3 \text{ g}}{V_T (F_s/n)} \quad F_s/n = 5 \text{ (lb/g)} \quad (4.28)$$



where  $V_T$  is the trimmed true airspeed (ft/sec), which is 480 in the configurations 1A-5E and 675 in the configurations 6A-8E, and  $g$  is the acceleration of gravity (ft/sec<sup>2</sup>).  $F_s/n$  is the steady stick force per unit normal acceleration change at constant speed (lb/g).

TABLE 4.5.

## NEAL-SMITH CONFIGURATIONS

Conf.	$1/\tau_1$	$1/\tau_{\theta_2}$	$1/\tau_2$	$\omega_{sp}/\zeta_{sp}$	$\omega_3/\zeta_3$	POR
1A	0.5	1.25	2	2.2/0.69	63/0.75	4-6
1B	2.0	1.25	5.0	2.2/0.69	63/0.75	3.5
1C	2.0	1.25	5.0	2.2/0.69	16/0.75	3.5-5
1D		1.25		2.2/0.69	75/0.67	3-5
1E		1.25	5.0	2.2/0.69	63/0.75	6
1F		1.25	2.0	2.2/0.69	63/0.75	8
1G		1.25	0.5	2.2/0.69	63/0.75	8.5
2A	2.0	1.25	5.0	4.9/0.70	63/0.75	4-4.5
2B	2	1.25	5	4.9/0.70	16/0.75	4-6
2C	5.0	1.25	12.0	4.9/0.70	63/0.75	3
2D		1.25		4.9/0.70	75/0.63	2.5-3
2E		1.25	12.0	4.9/0.70	63/0.75	4
2F		1.25	5.0	4.9/0.70	63/0.75	3
2G		1.25	5.0	4.9/0.70	16/0.75	7
2H		1.25	2	4.9/0.70	63/0.75	5-6
2I		1.25	2.0	4.9/0.70	16/0.75	8
2J		1.25	0.5	4.9/0.70	63/0.75	6
3A		1.25		9.7/0.63	75/0.67	4-5
3B		1.25	12	9.7/0.63	63/0.75	4.5
3C		1.25	5	9.7/0.63	63/0.75	3-4
3D		1.25	2	9.7/0.63	63/0.75	4
3E		1.25	0.5	9.7/0.63	63/0.75	4
4A		1.25		5.0/0.28	75/0.67	5-5.5
4B		1.25	12	5.0/0.28	63/0.75	7
4C		1.25	5	5.0/0.28	63/0.75	8.5
4D		1.25	2	5.0/0.28	63/0.75	8-9
4E		1.25	0.5	5.0/0.28	63/0.75	7.5
5A		1.25		5.1/0.18	75/0.67	5-7
5B		1.25	12	5.1/0.18	63/0.75	7
5C		1.25	5	5.1/0.18	63/0.75	7-9
5D		1.25	2	5.1/0.18	63/0.75	8.5-9

TABLE 4.5. (Continued)

5E		1.25	0.5	5.1/0.18	63/0.75	8
6A	0.8	2.4	3.3	3.4/0.67	63/0.75	5-6
6B	3.3	2.4	8	3.4/0.67	63/0.75	1-4
6C		2.4		3.4/0.67	75/0.67	4
6D		2.4	8	3.4/0.67	63/0.75	5.5
6E		2.4	3.3	3.4/0.67	63/0.75	7-8.5
6F		2.4	0.8	3.4/0.67	63/0.75	8-10
7A	3.3	2.4	8	7.3/0.73	63/0.75	2-5
7B	8	2.4	19	7.3/0.73	63/0.75	3
7C		2.4		7.3/0.73	75/0.69	1.5-4
7D		2.4	19	7.3/0.73	63/0.75	5.5
7E		2.4	8	7.3/0.73	63/0.75	5-6
7F		2.4	3.3	7.3/0.73	63/0.75	3-7
7G		2.4	2	7.3/0.73	63/0.75	5-6
7H		2.4	0.8	7.3/0.73	63/0.75	5
8A		2.4		16.6/0.69	75/0.67	4-5
8B		2.4	19	16.6/0.69	63/0.75	3.5
8C		2.4	8	16.6/0.69	63/0.75	3-3.5
8D		2.4	3.3	16.6/0.69	63/0.75	2-4
8E		2.4	0.8	16.6/0.69	63/0.75	2.5-5

In order to apply the optimal control model, three key elements are defined:

- (1) The objective function to be minimized
- (2) State space form representation of the system for the tracking task
- (3) The command signal to be tracked.

The objective function of the Neal-Smith pitch attitude tracking task is

$$J(u) = E\{y_e^2\} + g E\{\dot{u}^2\} \quad (4.29)$$

where the weighting matrix on the pitch error and error rate,  $Q$ , is selected as  $\text{diag}[1 \ 0]$  and the weighting on the control input,  $r$ , is 0. The tracking error,  $\theta_e$ , is defined as the difference between the commanded attitude,  $\theta_c$ , and the aircraft attitude,  $\theta$ . A pilot can

extract error as well as error rate from a single display. Thus,  $y$  is defined:

$$y^T(t) = [ \theta_e \quad \dot{\theta}_e ] \quad (4.30)$$

The vehicle states are augmented with the command signal states using the 2<sup>nd</sup> canonical form for the tracking task. The structure of the augmented system is:

$$\begin{bmatrix} \dot{x}_w \\ \dot{x} \end{bmatrix} = \begin{bmatrix} A_w & \mathbf{0} \\ \mathbf{0} & A_{veh} \end{bmatrix} \begin{bmatrix} x_w \\ x \end{bmatrix} + \begin{bmatrix} \mathbf{0} \\ B_{veh} \end{bmatrix} u + \begin{bmatrix} B_w \\ \mathbf{0} \end{bmatrix} w \quad (4.31)$$

$$y = [ I_2 \quad -I_2 \quad \mathbf{0} ] \begin{bmatrix} x_w \\ x \end{bmatrix} + v_y \quad (4.32)$$

$$x^T = [ \theta \quad \dot{\theta} ] \quad x_w^T = [ \theta_w \quad \dot{\theta}_w ] \quad (4.33)$$

It should be noted that the state vector,  $x$ , represents the pitch angle and the change of the pitch angle due to the pilot control input since this state space form is structured by the 2<sup>nd</sup> Canonical form.  $x_w$  represents the command pitch angle and its rate. The command signal is generated by a second-order shaping filter driven by the white noise to model the Neal-Smith pitch tracking experiment:

$$\ddot{\theta}_c + 0.5 \dot{\theta}_c + 0.25 \theta_c = 0.25 w(t) \quad (4.34)$$

where  $w(t)$  is a zero mean, Gaussian white noise with  $\sigma_w^2 = 64 \delta(t)$ .

$$\sigma_{\theta} = 4 \text{ deg}, \quad \sigma_{\dot{\theta}} = 2 \text{ deg/sec}$$

The second order model for the pitch tracking task is based on the actual discrete

instrument tracking task used in the Neal-Smith flight experiments. In the Neal-Smith experiments the evaluation pilot's task was to minimize this error, which required rapid and precise change of the pitch angle. Input parameters to solve the optimal control model are listed in TABLE 4.6, and Figure 4.16. shows the loop structure of the Neal-Smith pitch tracking task.

TABLE 4.6

## INPUT PARAMETERS FOR NEAL-SMITH PITCH TRACKING TASK

Observation vector	$y^T = [\theta_e \ \dot{\theta}_e]$	
Observation thresholds	$T_{\theta_e} = 0.05 \text{ deg}$	$T_{\dot{\theta}_e} = 0.18 \text{ deg/sec}$
Objective function weights	$Q_{ii} = [1 \ 0]$	$r = 0$
Observation noise ratio	$\rho_{y_i} = 0.01$	
Neuromuscular noise ratio	$\rho_{u_c} = 0.003$	
Fractional attention	$f = 1$	for single axis
Neuromuscular lag	$\tau_n = 0.1 \text{ sec}$	
Observation delay	$\tau = 0.2 \text{ sec}$	
Control input (Stick force)	$u \text{ (lbf)}$	

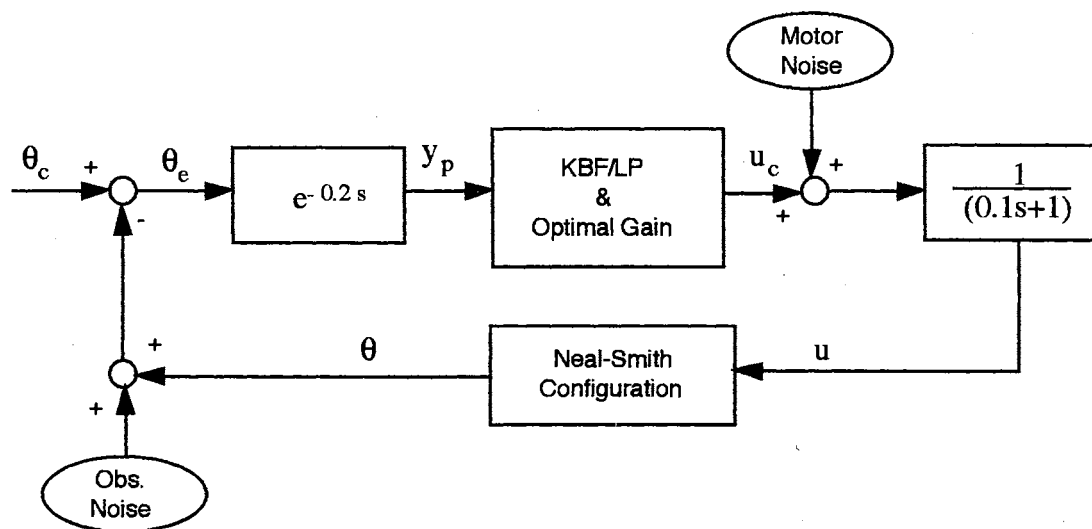


Figure 4.16. Neal-Smith Tracking Task (OCM)

### 4.3.3 Results and Discussions

The application of the ideal cutoff analysis to the 51 Neal-Smith short period/FCS configurations for the prediction of the handling qualities resulted in the POR/feedback correlation of Figure 4.17. and POR/sensor noise cutoff frequency correlation of Figure 4.18. where  $x$  and  $y$  represent the  $x$ -axis and  $y$ -axis variable, respectively, and  $R$  represents the coefficient of correlation. The correlation of the POR and the feedback at a disturbance cutoff frequency is based on the tracking ability of the human operator in performing a given task. In the Neal-Smith pitch tracking task, the pilot working band is  $0 \leq \omega \leq 0.5$  rad/sec, which is the frequency band of the actual pitch attitude command signal in the experiment and also the cutoff frequency of the shaping filter mathematically. Tracking error, covariance of the pitch angle error, is compared with the feedback gain of the open loop transfer function at the disturbance cutoff frequency in Figure 4.19. It shows that good tracking performance, small covariance, is proportional to the large gain at the disturbance cutoff frequency.

The sensor noise cutoff frequency is another important factor of handling qualities, which is closely related to the closed loop response time. As mentioned in Section 3.5, if the human can observe the high frequency signal information under the given situations, the resulting response of the closed loop system is relatively fast. However, there are distinct limitations of the human for processing signals in the optimal control model. The gain and phase plot of the pilot transfer function at the sensor noise cutoff frequency for the attenuation of the observation noise is shown in Figure 4.20. and Figure 4.21. They show a trend of decreased pilot gain and decreased (more negative) pilot phase with increased sensor noise cutoff frequency, which is a human's physical limitation for the high frequency signal in the manual control. Specifically it should be noted that pilot phase shift is linearly proportional to the sensor noise cutoff frequency and heavily dependent on the controlled system dynamics. If the vehicle dynamics have good high frequency performance, a pilot can operate the vehicle relatively easily with a

large time lag. If the vehicle dynamics are bad in the high frequency range, a pilot will struggle to make the vehicle stable with relatively small phase lag, which means that he has to react quickly to achieve the stability criteria. It may also cause pilot induced oscillations (PIO).

The pilot phase shift of the high frequency performance in the optimal control model is expressed in the range of  $6 \leq \omega \leq 18$  (rad/sec):

$$(\text{Pilot Phase}) = (95.7) - (19.4) \times (\text{Sensor Noise Cutoff Frequency}), [\text{deg}] \quad (4.35)$$

Mathematically it can be explained that this phase limitation of the high frequency performance is the sum of the pure perceptual time delay, neuromuscular lag and the phase of KBF/LP. Figure 4.22. shows that the phase lead of the KBF/LP decreases as the input frequency increases. It means that the prediction ability of the pilot decreases for the high frequency signals.

From the above discussions of the two significant factors, feedback and sensor cutoff frequency, we can obtain the final results for the prediction of the pilot opinion ratings. Figure 4.23. shows the result of the 51 Neal-Smith configurations and Figure 4.24. is the interpretation of the frequency domain performance related to the prediction of the pilot opinion ratings.

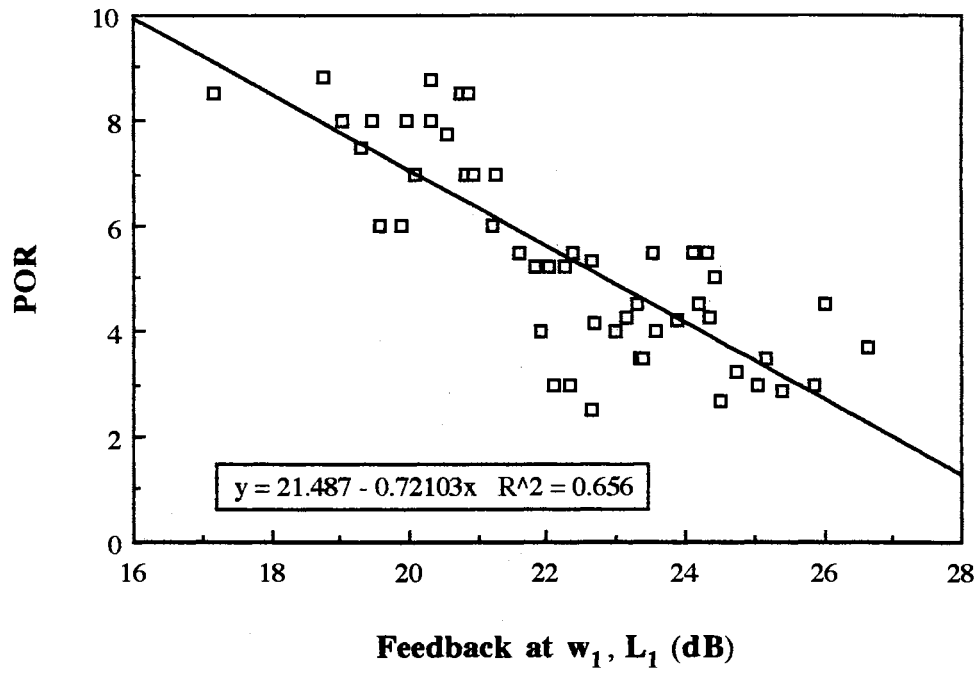


Figure 4.17. POR/Feedback Correlation

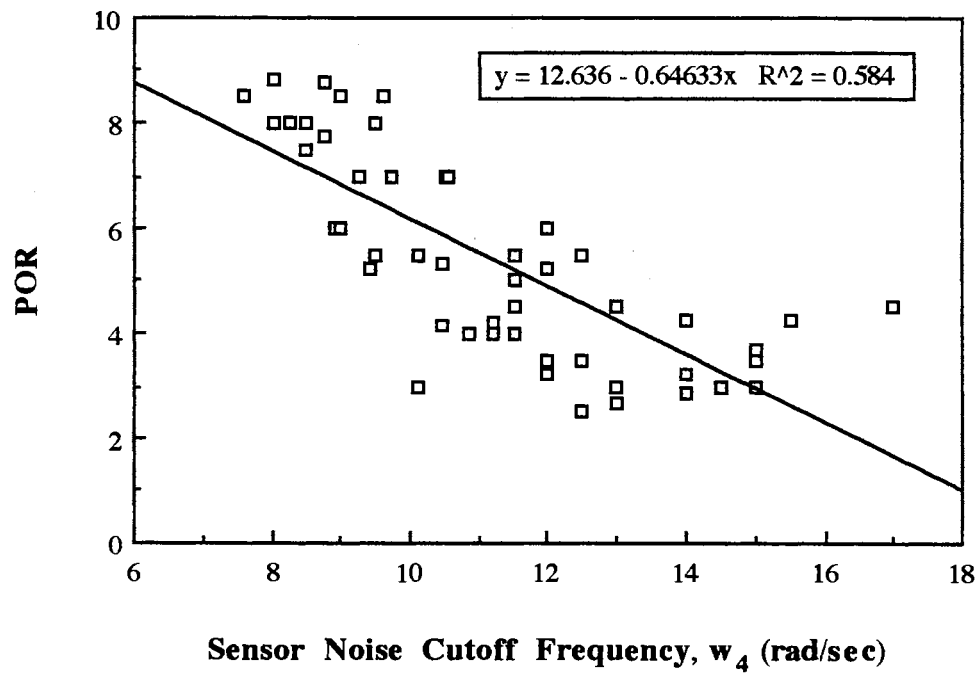


Figure 4.18. POR/Sensor Cutoff Correlation

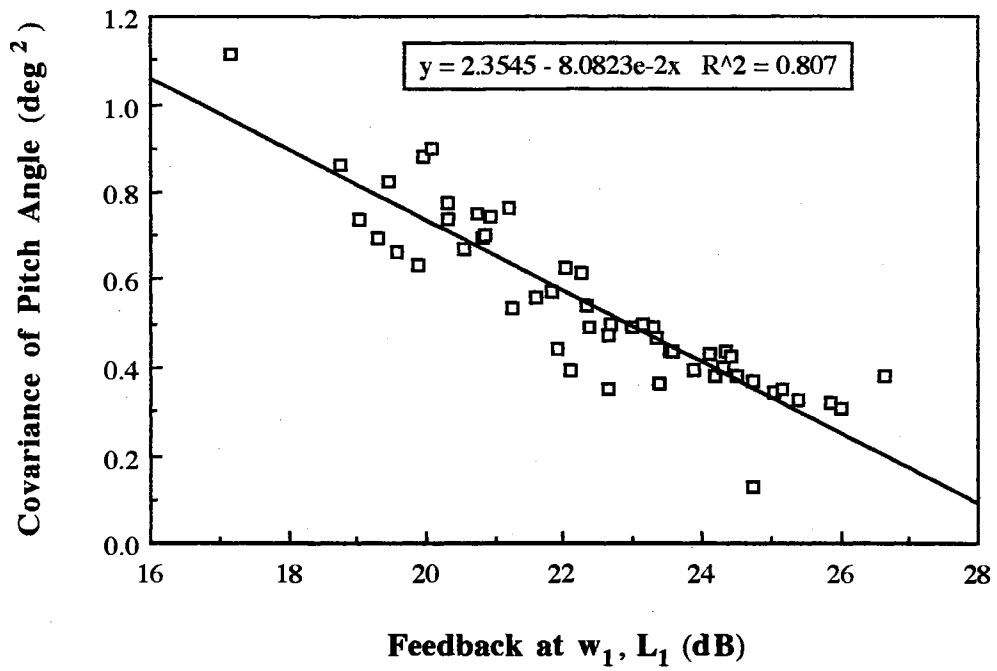


Figure 4.19. Feedback/Tracking Error Correlation

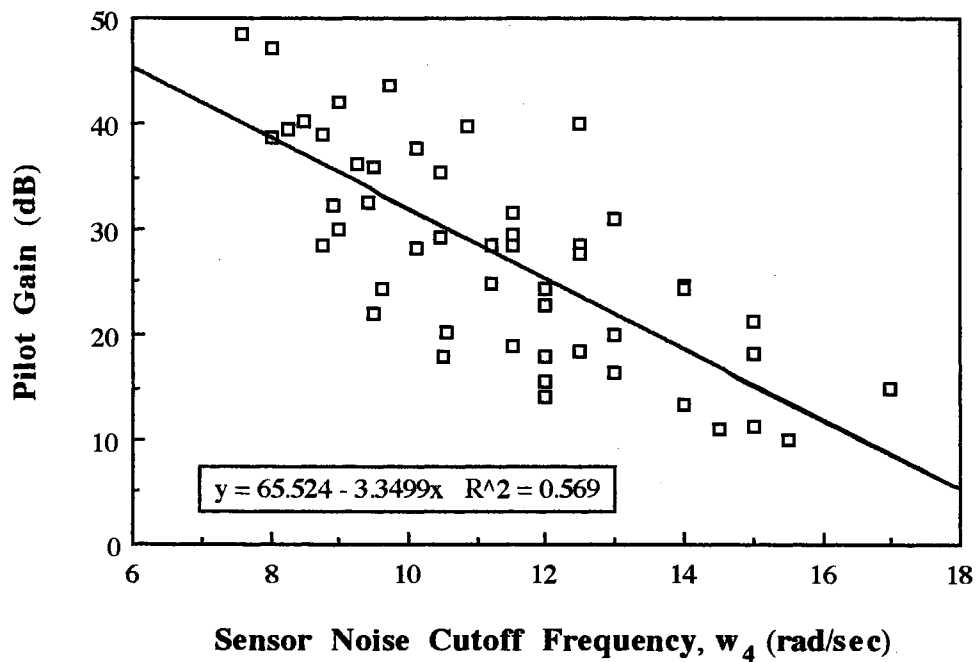


Figure 4.20. Limitation of Human Sensing (Gain)



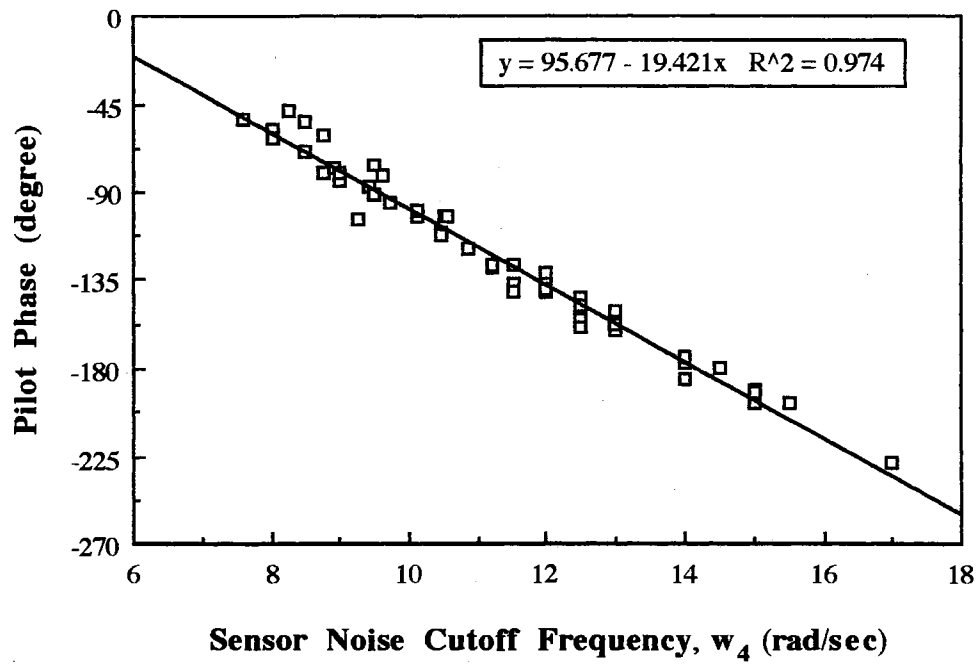


Figure 4.21. Limitation of Human Sensing (Phase)

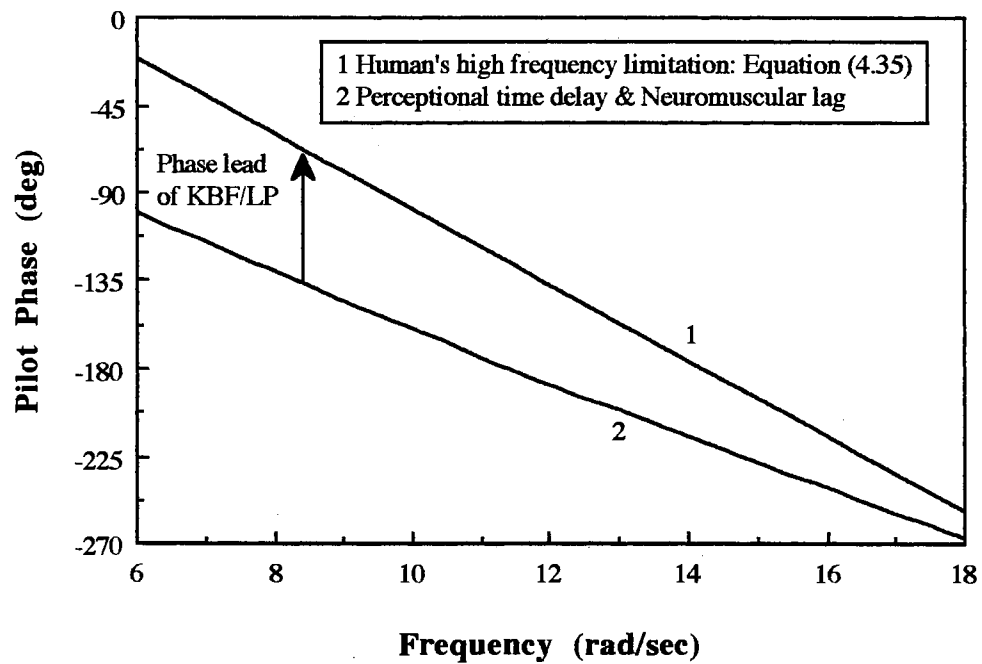


Figure 4.22. Interpretation of High Frequency Performance of OCM (Phase)

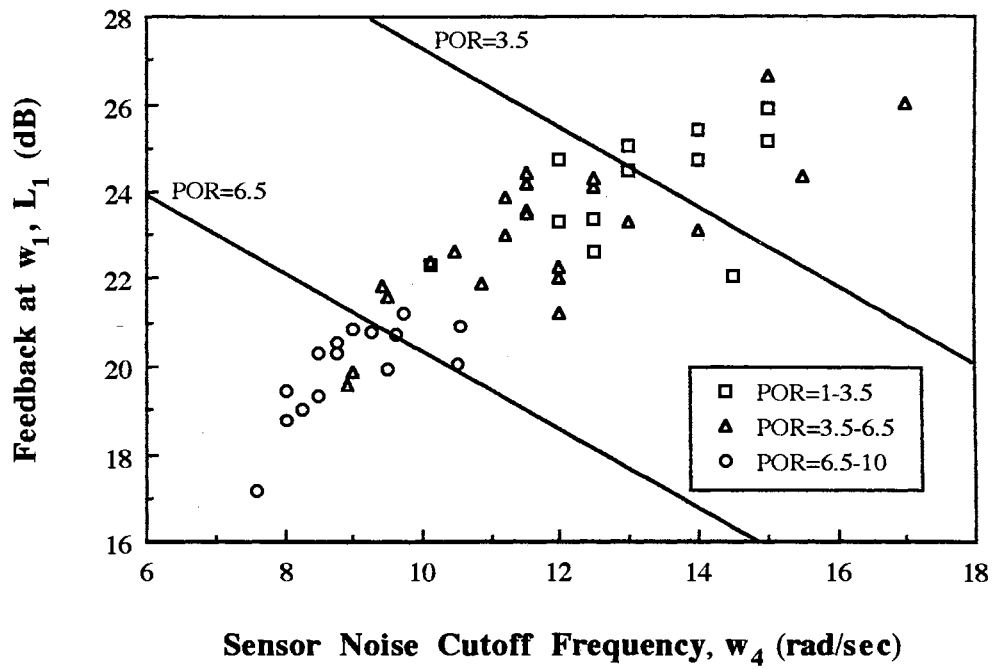


Figure 4.23. POR of Neal-Smith Configurations

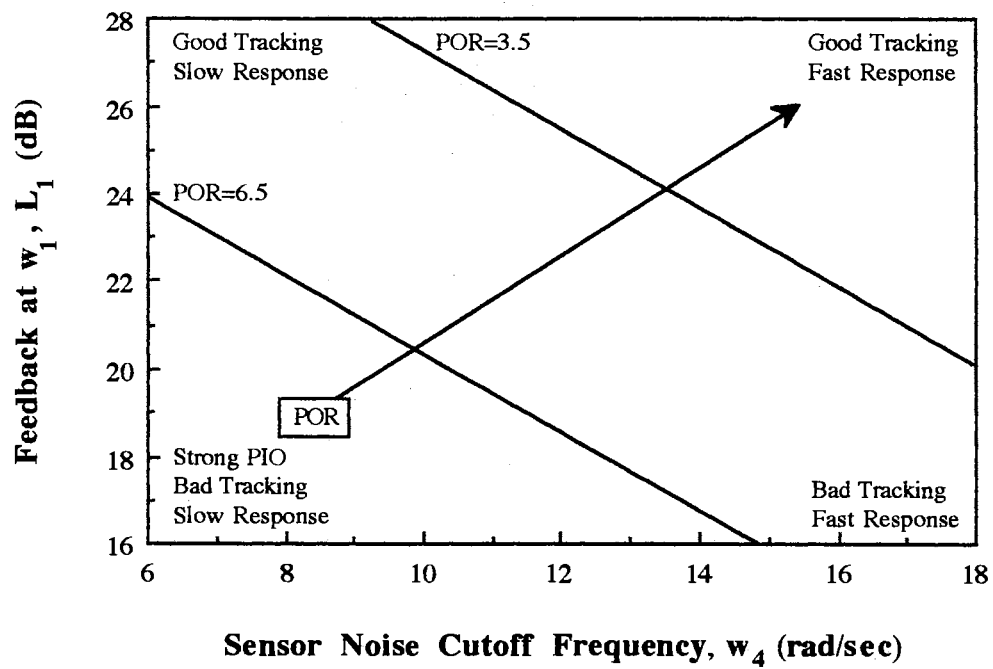


Figure 4.24. Interpretation of POR Criteria

For the detail discussions of the Bode ideal cutoff analysis in the optimal control model several Neal-Smith configurations are selected and divided into 3 groups. The configurations of each group are listed in Table 4.7.

### Group 1

Group 1 is a good example of the Bode ideal cutoff analysis in analyzing the effects of the high frequency vehicle performance to the optimal control model. The only difference in the pilot transfer function of Group 1 lies in the short period frequency of the vehicle, but they have almost the same damping ratio. The magnitude and phase of Group 1 are almost the same in the pilot working band,  $0 \leq \omega \leq 0.5$  rad/sec, but the vehicle dynamics are quite different in the high frequency range. Figure 4.25 shows the results of POR of Group 1. The magnitude and phase plot of the vehicles, pilot transfer functions and open loop transfer functions are shown in Figure 4.26.-4.30. and the arrows of the each plot indicate the direction of good handling qualities increasing short period frequency and also corresponding lines of the configurations presented in Figure 4.25., which means the arrow moves from 1D to 3A in Figure 4.26.-4.30.

The objective of the optimal control model is to find the optimal control strategy which minimizes the tracking error in the working band and also stabilizes the system in

TABLE 4.7

### GROUP SUMMARY

Index	Configuration	Description
Group 1	1D, 2D, 3A	Different short period freqs.
Group 2	2F, 4C, 5C	Different damping ratio
Group 3	1E, 1F, 1G	Different phase lag

the high frequency range. For the configurations of Group 1, which have the same low frequency performance and quite different high frequency performance, the tracking ability of a pilot is the same in the working band, but the high frequency compensation to stabilize the each vehicle are quite different. So, a pilot tries to compensate for the vehicle's high frequency performance to meet the high frequency stability in Figure 4.26. Mathematically, for a good high frequency performance vehicle, 3A in Group 1, a pilot can control the vehicle with a relatively small gain and large phase lag in the high frequency range and also attenuate the observation noise at a relatively high sensor noise cutoff frequency, comparing 1D and 2D in Figure 4.26. and 4.28. It means that a pilot can control a vehicle smoothly and the resulting closed loop pilot/vehicle system has relatively fast response. It is noted that the pilot phase of 3A in the high frequency is almost flat in Figure 4.29., which explains that a pilot can control very smoothly in his task. Figure 4.27. and 4.30. show the resulting open loop characteristics of Group 1.

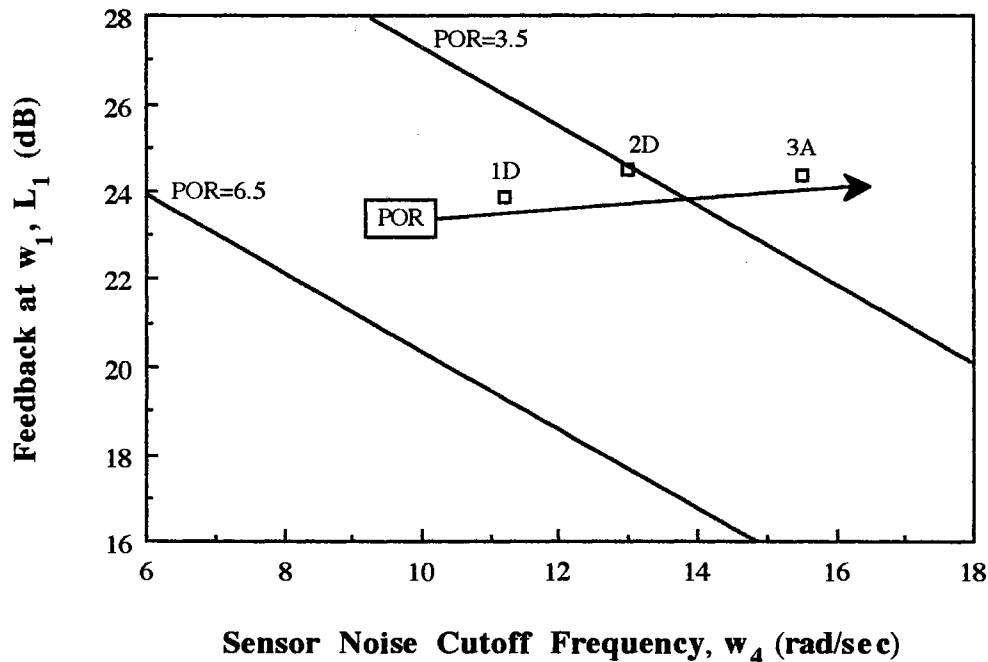


Figure 4.25. Results of POR (Group 1)

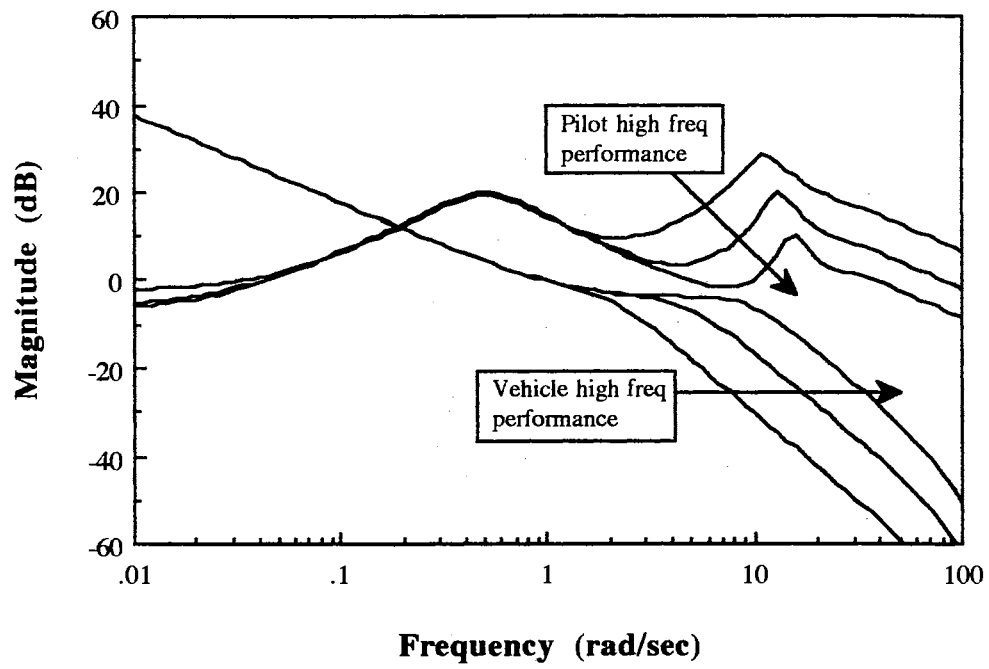


Figure 4.26. Magnitude Plot of Vehicle and Pilot Transfer Function (Group 1)

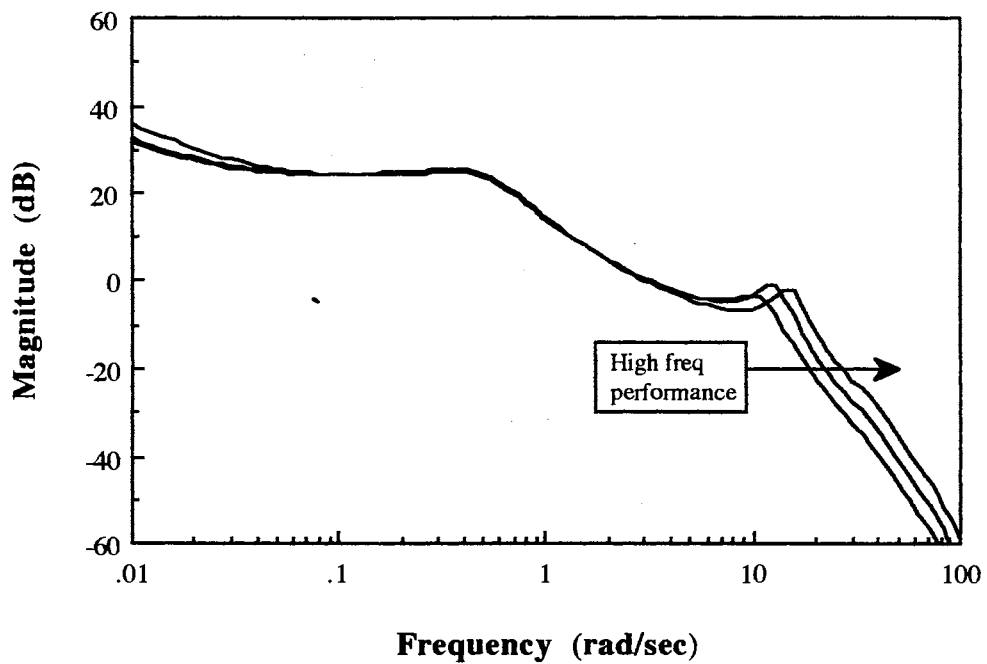


Figure 4.27. Magnitude Plot of Open Loop Transfer Function (Group 1)

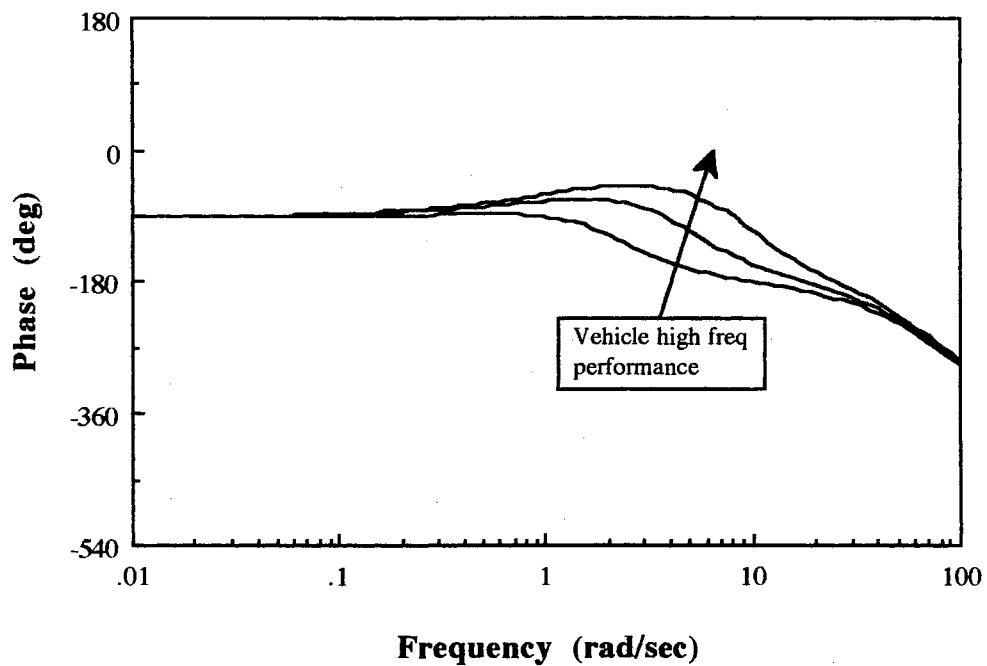


Figure 4.28. Phase Plot of Vehicle Transfer Function (Group 1)

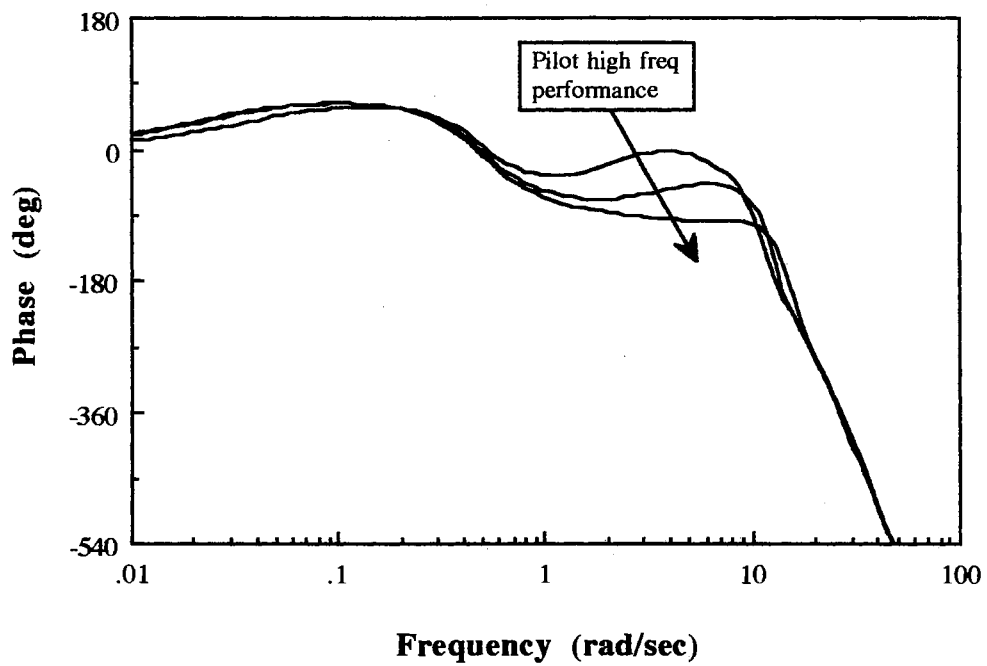


Figure 4.29. Phase Plot of Pilot Transfer Function (Group 1)

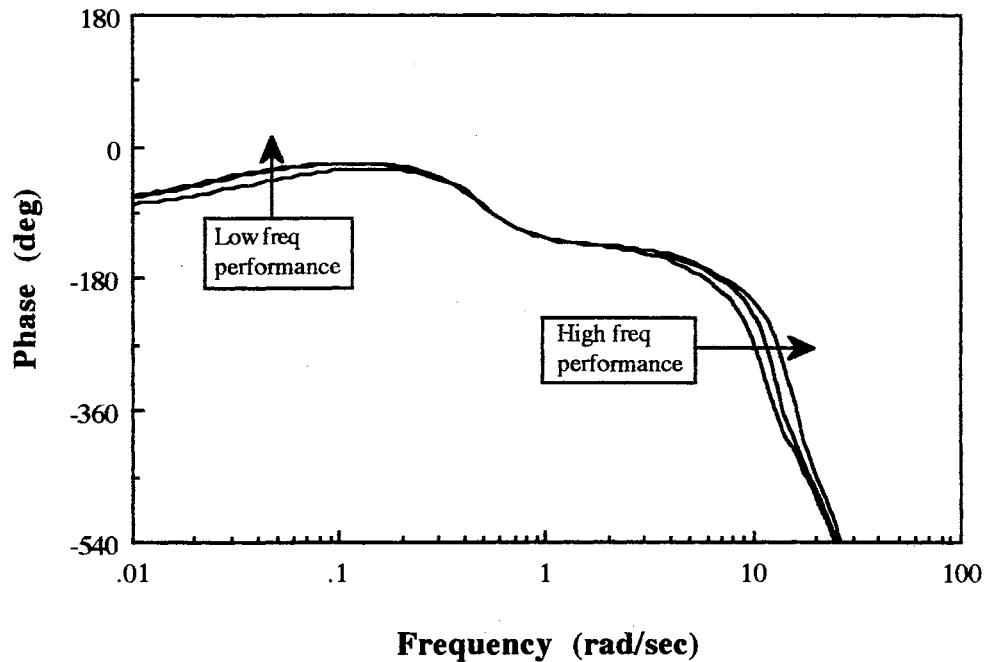


Figure 4.30. Phase Plot of Open Loop Transfer Function (Group 1)

## Group 2

Group 2 is chosen to analyze the effects of the damping ratio in the vehicle's short period dynamics to the optimal control model. The vehicle dynamics of each configuration are shown in Figure 4.32., and the peak of the magnitude plot in the high frequency affects the pilot's tracking ability in the working band as well as the high frequency performance in Figure 4.33. In the configuration of 5C, the high frequency phase compensation of the pilot is changed abruptly from the negative value (lag) to the positive value (lead) to meet the high frequency stability in Figure 4.36., which means that a pilot is required to move relatively fast to attenuate the high frequency sensor noise and to stabilize the vehicle explained in Group 1. The pilot comments of the Neal-Smith experiments say that the pilot cannot track a target without PIO problems in 5C. Thus, the PIO problem is strongly related to the high frequency phase compensation of a pilot for high frequency stability.

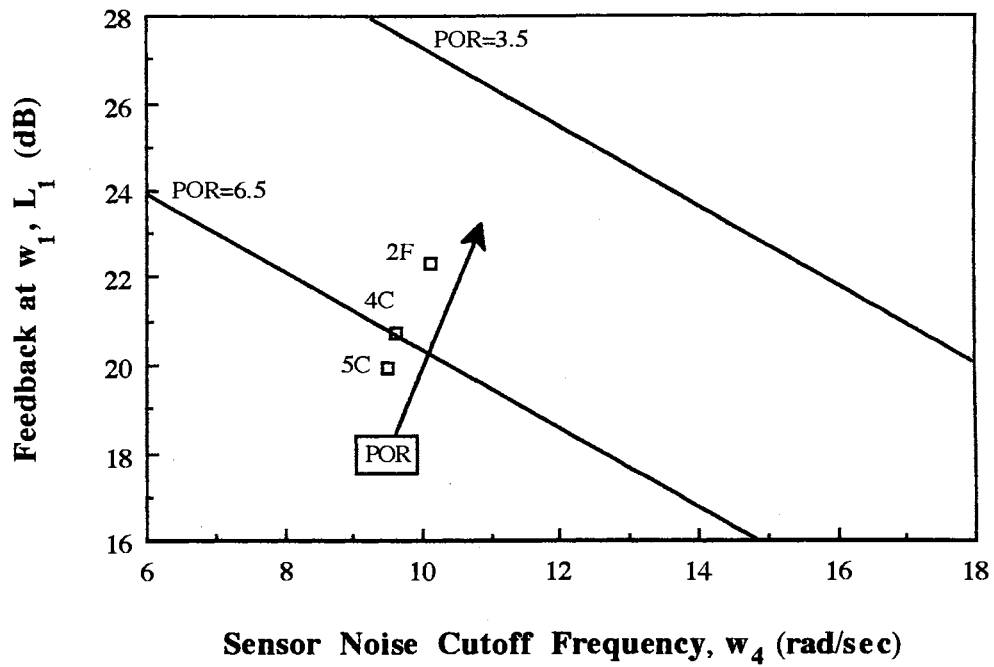


Figure 4.31. Results of POR (Group 2)

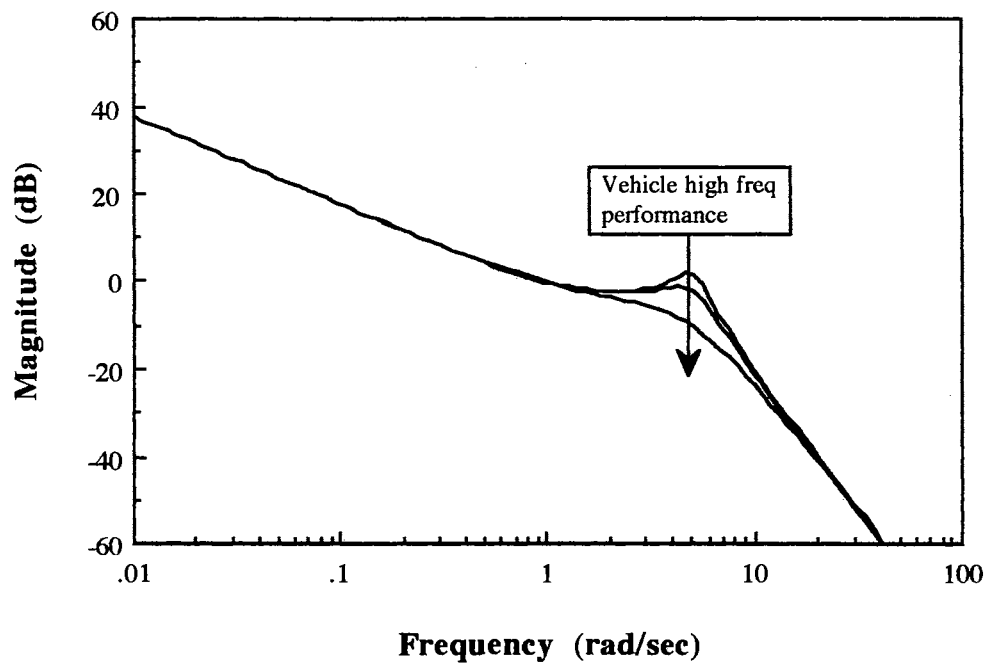


Figure 4.32. Magnitude Plot of the Vehicle Transfer Function (Group 2)



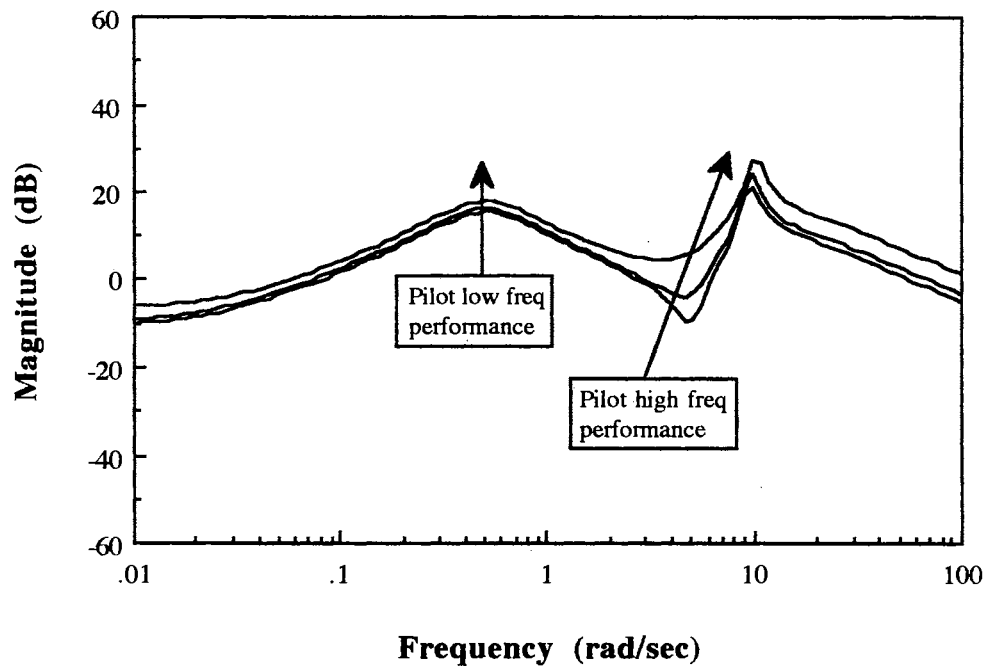


Figure 4.33. Magnitude Plot of Pilot Transfer Function (Group 2)

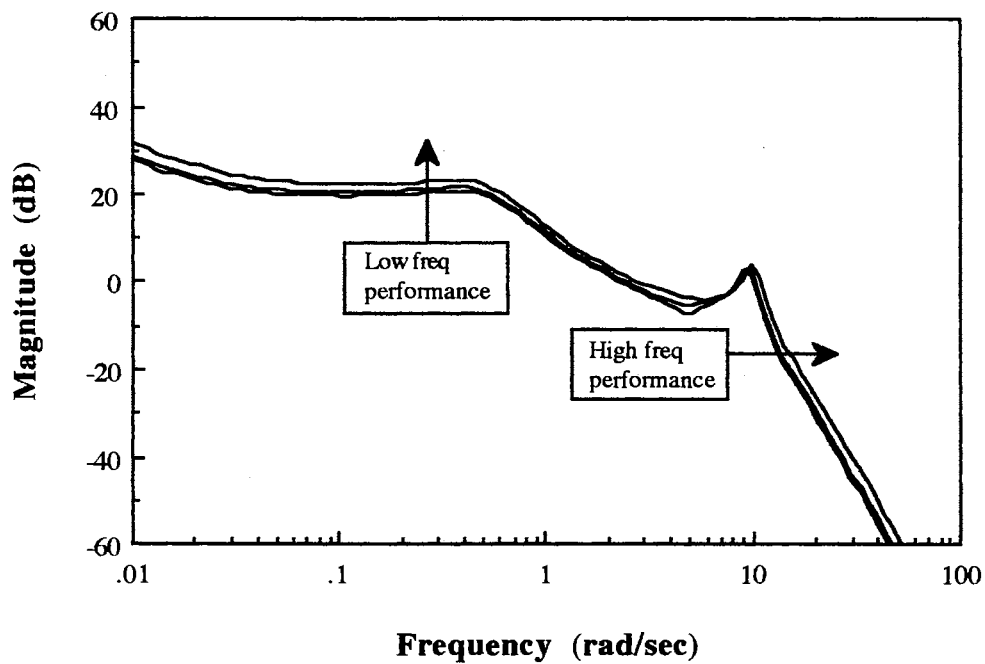


Figure 4.34. Magnitude Plot of Open Loop Transfer Function (Group 2)

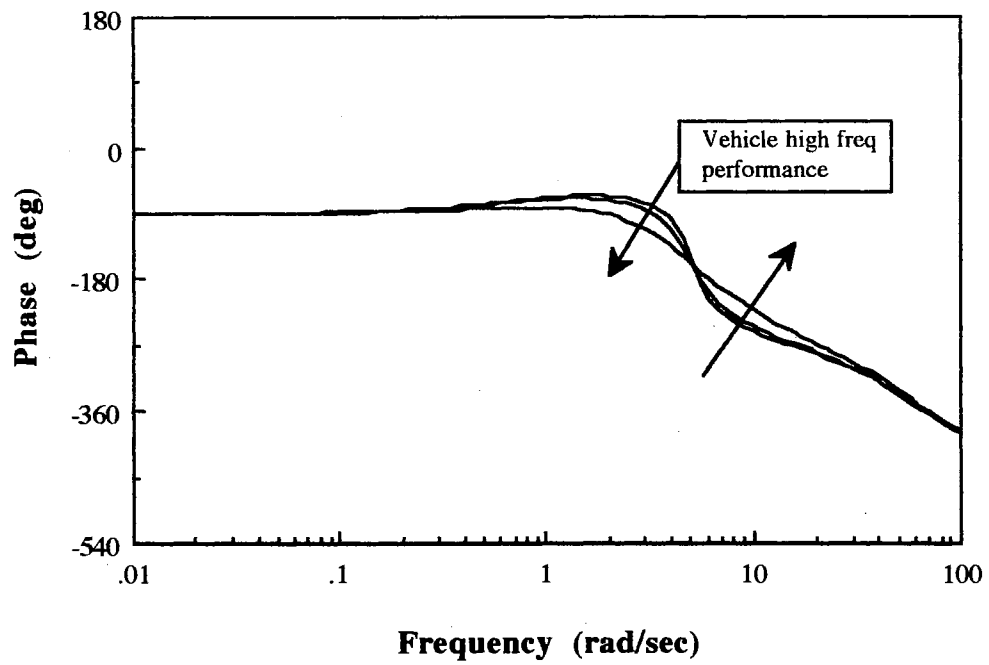


Figure 4.35. Phase Plot of Vehicle Transfer Function (Group 2)

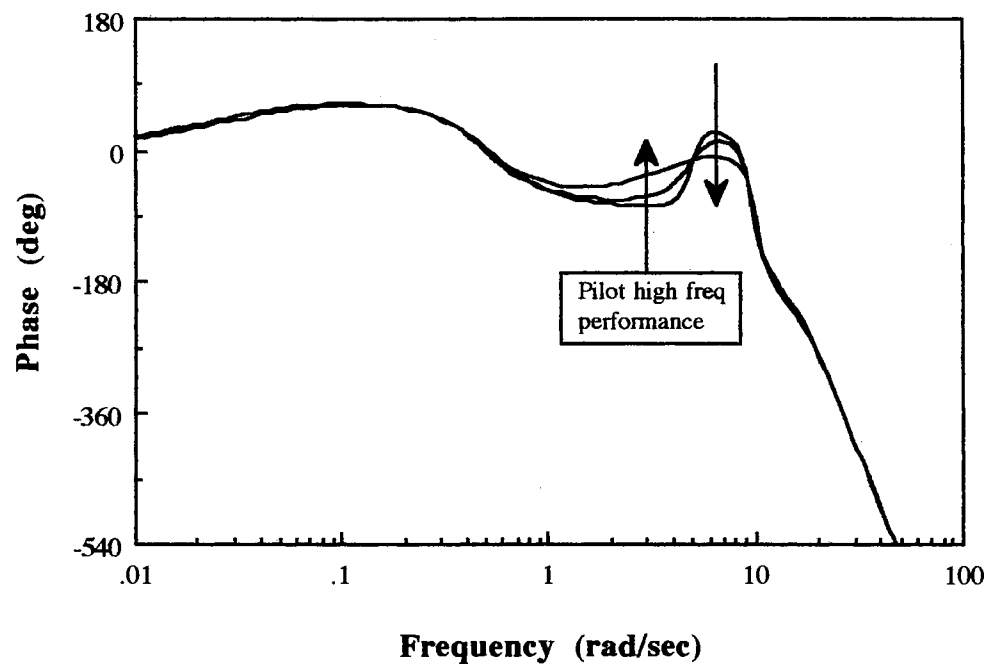
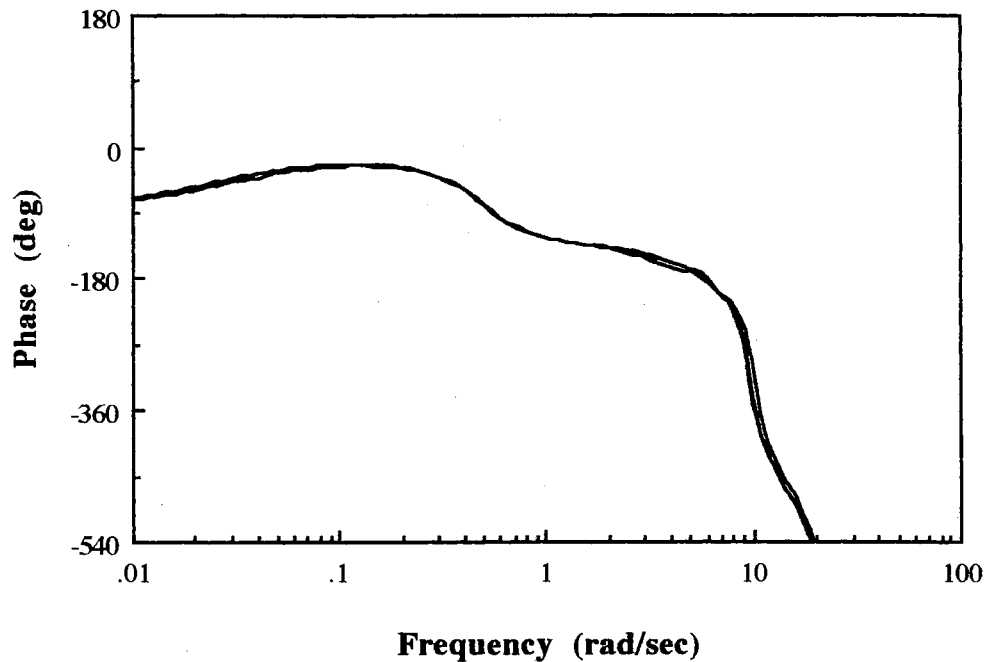


Figure 4.36. Phase Plot of Pilot Transfer Function (Group 2)



4.37. Phase Plot of Open Loop Pilot Transfer Function (Group 2)

### Group 3

Group 3 is selected to analyze how the lag of the vehicle dynamics affects the optimal control model. The phase of the vehicle dynamics in Figure 4.41. are decreased by the effects of this lag compared to Group 1 in Figure 4.28. in the high frequency range. For these configurations of Group 3, the magnitude and phase of a pilot are increased to meet the high frequency stability, which means that a pilot should control the vehicle with relatively small phase lag or even lead and also excessive gain in the high frequency range as mentioned earlier. This is interpreted as a pilot cannot control the vehicle without PIO problems. Thus, the major source of the PIO problems comes from the pilot's phase lag in the high frequency range to meet the high frequency stability requirement. From the Neal-Smith experiments, the POR of the 1E, 1F and 2G are very poor, 6, 8 and 8.5 , respectively, and they have also bad PIO problems.

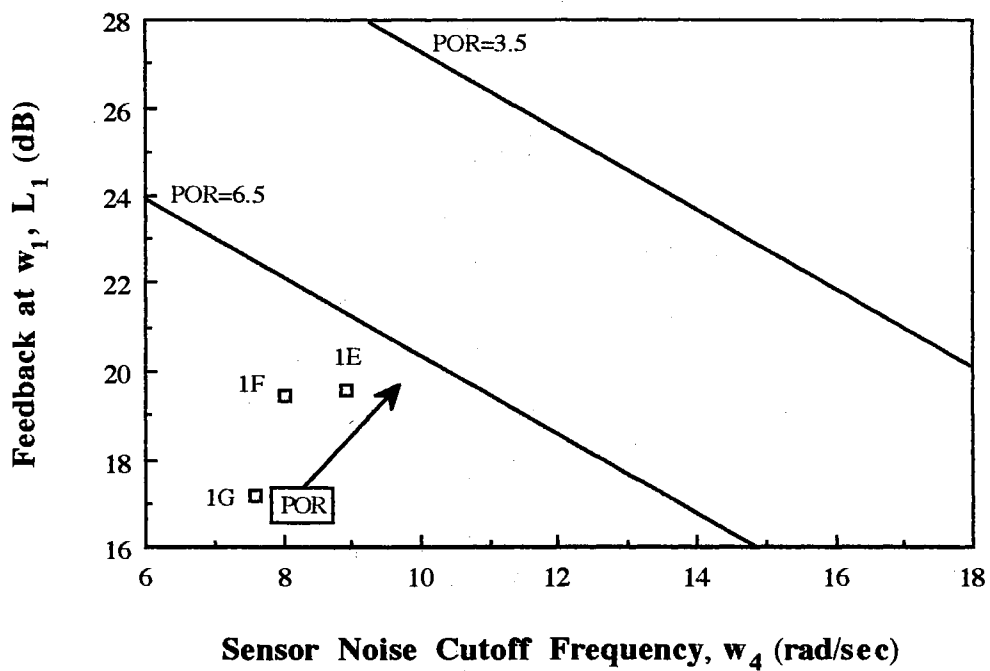


Figure 4.38. Results of POR (Group 3)

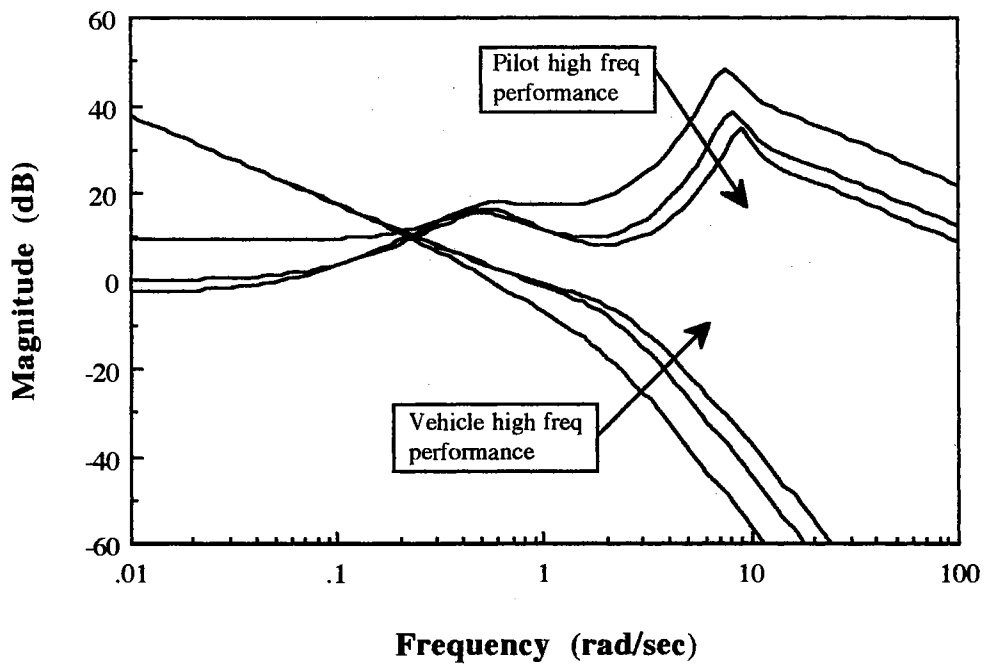


Figure 4.39. Magnitude Plot of Vehicle and Pilot Transfer Function (Group 3)

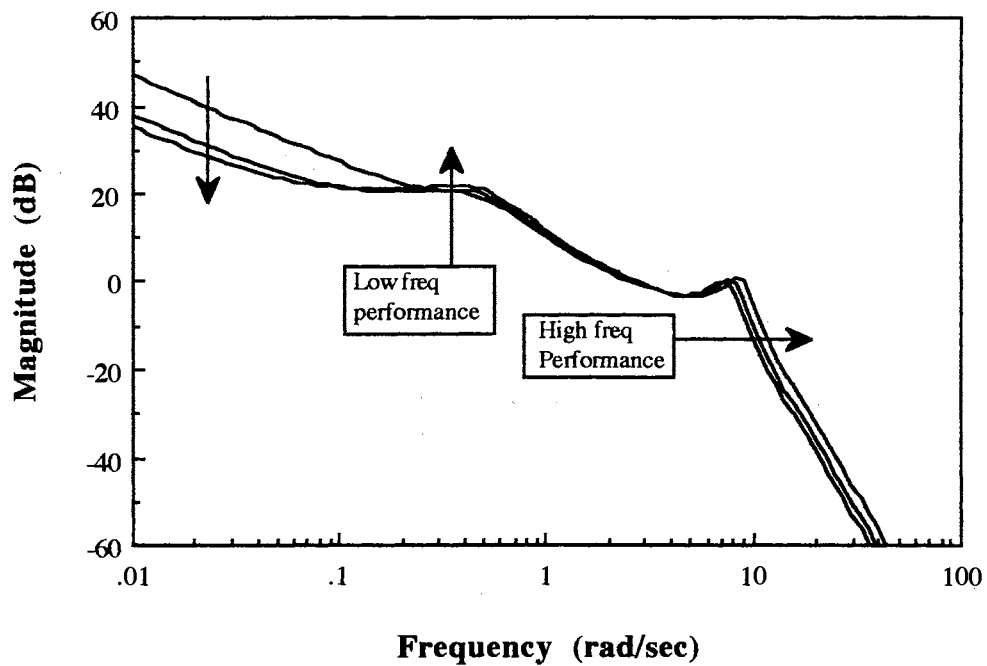


Figure 4.40. Magnitude Plot of Open Loop Transfer Function (Group 3)

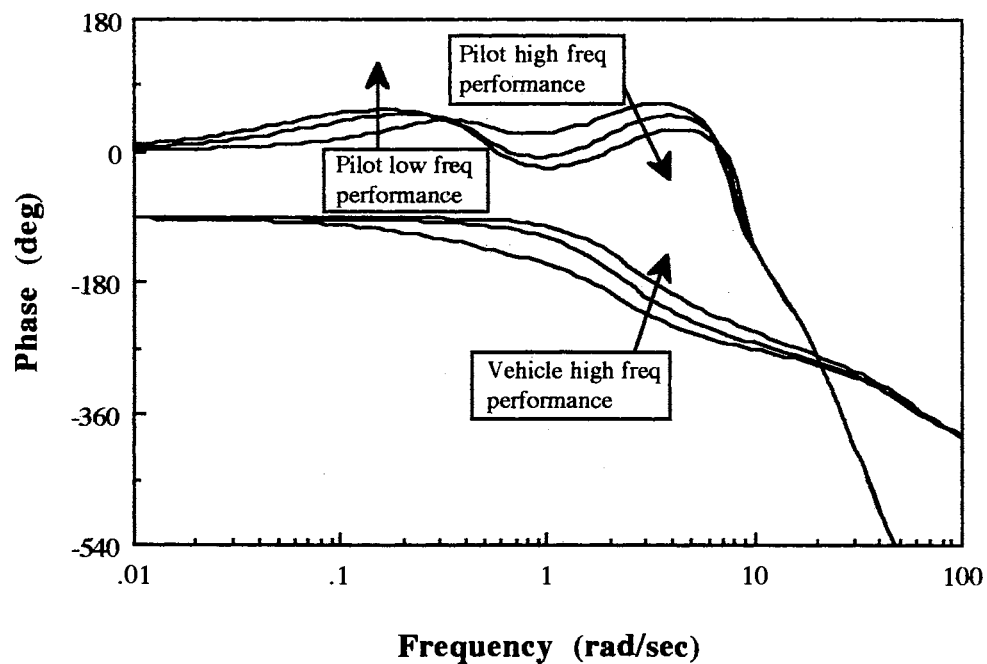


Figure 4.41. Phase Plot of Vehicle and Pilot Transfer Function (Group 3)

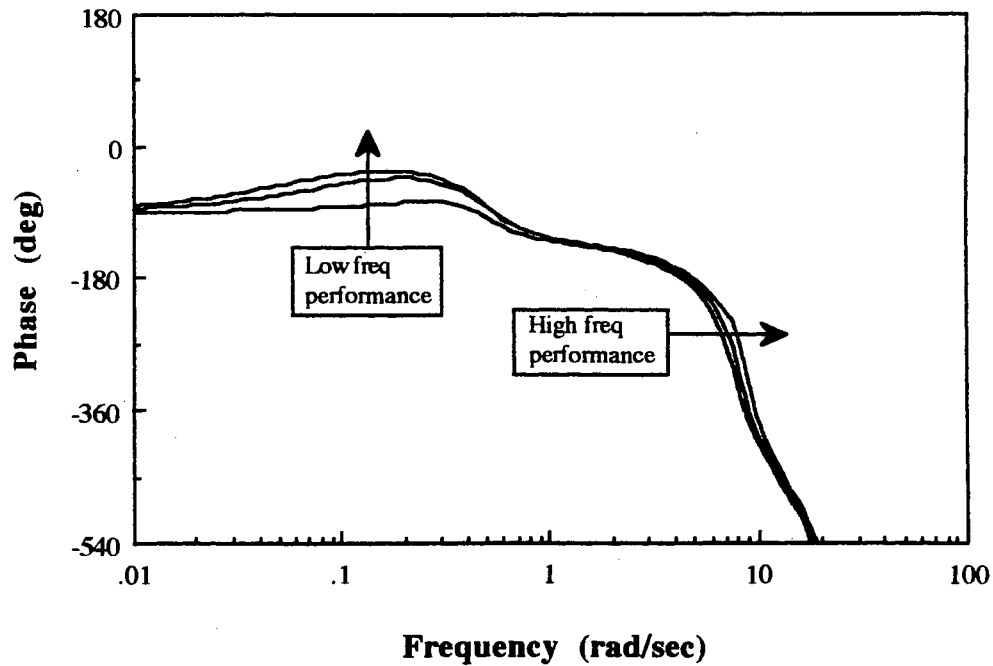


Figure 4.42. Phase Plot of Open Loop Transfer Function (Group 3)

The order of the pilot transfer function for the Neal-Smith configuration 2D and 1G is 21 and 23, respectively, which can be reduced by the exact and close pole/zero cancellations. The reduced pilot transfer function of configuration 2D (POR=2.5-3) as explained in Section 4.2. is

$$G_p(s) = \frac{30.81(-0.03)(-1.528)[0.70,4.74]}{[0.5,0.5](-1.26)[0.15,12.87]} e^{-0.16 s} \quad (4.36)$$

The reduced pilot transfer function of configuration 1G (POR=8-8.5) is

$$G_p(s) = \frac{72.85[0.86,0.36](-1.04)[0.71,2.24]}{[0.5,0.5](-1.25)[0.14,7.40]} e^{-0.22 s} \quad (4.37)$$

The equivalent perceptual time delay in these two equations is recovered from the

shifted Pade approximation for the human's perceptual delay, 0.2 seconds. The above two equations show that the equivalent perceptual time delay is related to the human's sensing ability to attenuate the sensor noise. Sensor noise cutoff frequencies of 2D and 1G are 13 and 7.6 rad/sec, respectively, which indicates the sensor working band. Thus, the human can perceive the vehicle's output signal relatively fast for configuration 2D compared to 1G.

The most difficult part in the analysis of the pilot/vehicle system is to find the absolute values to characterize the system, which is also one of the general issues in control theory. Bode ideal cutoff analysis gives us this absolute standard, maximum available feedback. So, we can relate the maximum available feedback to the feedback at the disturbance cutoff frequency to explain the error between the optimal case with the human's limitations and ideal case. As an example, consider configuration 2D. The frequency performances for 2D, which are calculated from the open loop transfer function, are

- |     |                                |   |
|-----|--------------------------------|---|
| (1) | Gain margin:                   | $x = 4.49$ dB                               |
| (2) | Phase margin:                  | $y \pi = 37.88$ deg = 0.661 rad, $y = 0.21$ |
| (3) | Working band frequency:        | $w_1 = 0.5$ rad/sec                         |
| (4) | Gain crossover frequency:      | $w_2 = 5.16$ rad/sec                        |
| (5) | Sensor noise cutoff frequency: | $w_4 = 13$ rad/sec                          |
| (6) | Bode step frequency:           | $w_3 = 7.64$ rad/sec                        |
|     |                                | $w_3$ is calculated by equation (3.73)      |
| (7) | Feedback at $w_1$              | $L_1 = 24.52$ dB                            |
| (8) | Maximum available feedback:    | $L_{\max} = 32.82$ dB                       |

The performance of the optimal control model for configuration 2D under the Neal-Smith pitch attitude tracking task is 58 percent of the maximum available feedback at disturbance cutoff frequency. It is explained that a pilot tries to maximize the feedback to reduce the tracking error in the working band, but he cannot achieve the ideal

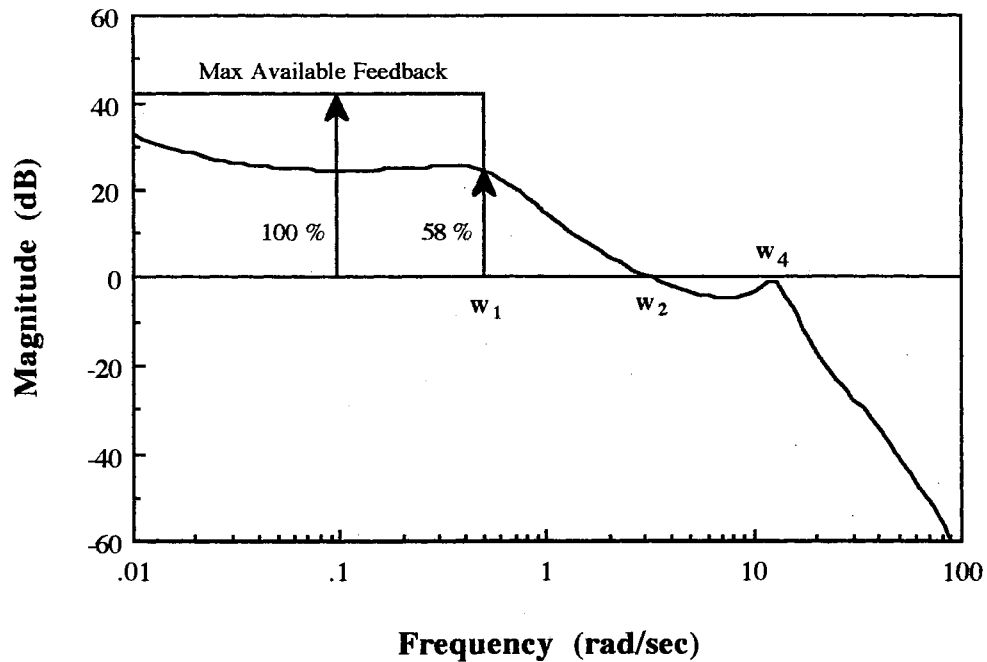


Figure 4.43. Magnitude Plot of Open Loop Transfer Function with 0.2 sec Delay (2D)

maximum feedback due to the his psycho-physical limitations. Figure 4.43 illustrates the maximum available feedback in the working band.

Finally, Table 4.6 summarizes the effects of the perceptual time delay which can give critical effects in evaluating handling qualities for configuration 2D.  $\tau = 0.2$  sec is accepted to simulate the optimal control model for the Neal-Smith tracking task in this thesis. A pilot with faster perception ( $\tau = 0.1$  sec) in a tracking task produces a larger feedback in the working band (better tracking ability) as well as a higher sensor noise cutoff frequency (faster response) in Figure 4.44. Conversely, a pilot with slower perception ( $\tau = 0.3$  sec) produces a lower sensor cutoff frequency which may violate the high frequency stability due to the high frequency magnitude peak. It is also shown that the phase of the pilot behavior ( $\tau = 0.3$  sec) is almost flat and more negative in the high frequency range compared to the pilot ( $\tau = 0.1$  sec) tracking in Figure 4.45., which is the



pattern of the smooth flight as mentioned earlier. It is interesting to note that the perceptual time delay does not significantly effect on the pilot's phase compensation ability in the working band in Figure 4.45., which means that the pilot's prediction ability in the low frequency range is not effected by the perceptual time delay. However, extensive investigation related to the effects of the perceptual time delay is required in the handling quality research, particularly at frequencies outside the working band.

TABLE 4.6

## SUMMARY OF EFFECTS OF PERCEPTUAL TIME DELAY (2D)

$\tau$	$x$	$y\pi$	$w_1$	$w_2$	$w_3$	$w_4$	$L_1$	$L_{\max}$	%
0.1	5.32	39.7	0.5	4.0	9.9	16	27.8	44.3	63
0.2	4.47	37.9	0.5	3.2	7.6	13	24.5	42.3	58
0.3	4.19	36.6	0.5	2.7	6.4	11	21.9	40.5	54

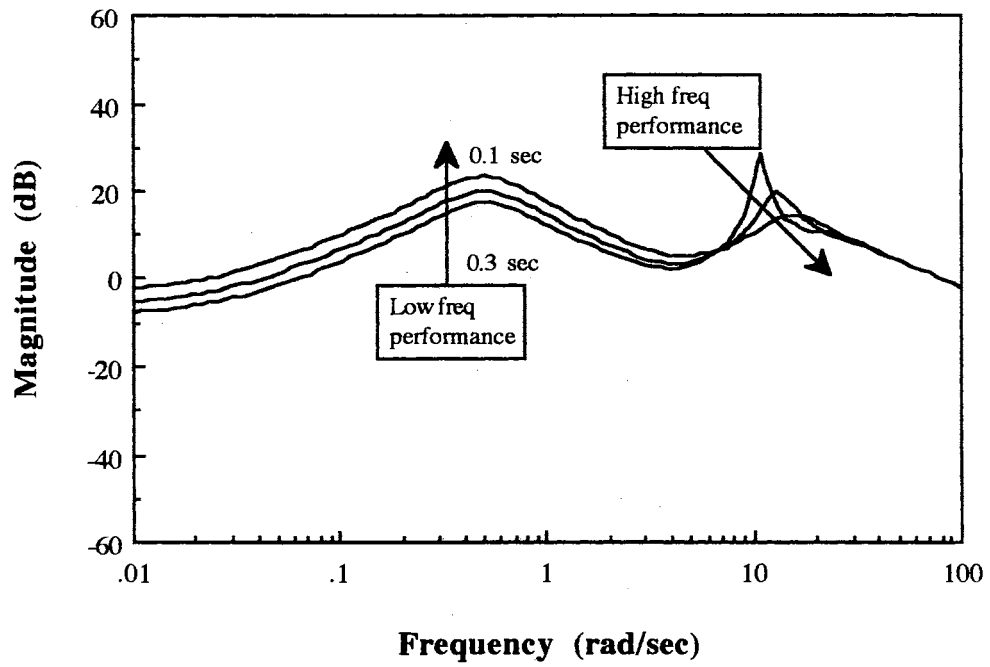


Figure 4.44. Magnitude Plot of Pilot Transfer Function (2D)

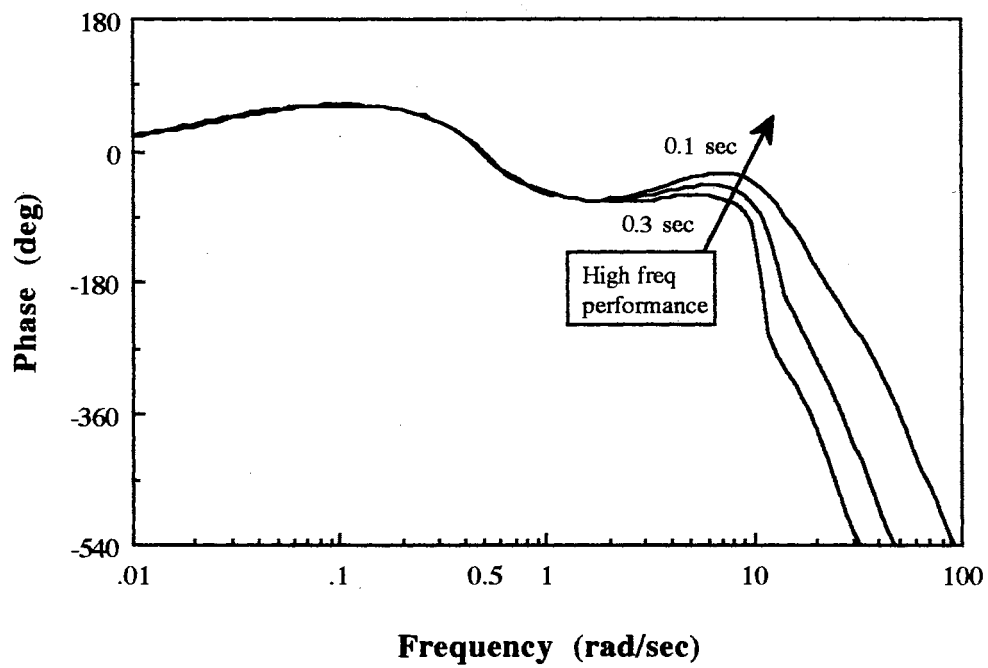


Figure 4.45. Phase Plot of Pilot Transfer Function (2D)

## CHAPTER V

### SUMMARY AND CONCLUSIONS

The Bode ideal cutoff analysis was successfully applied to predict the pilot opinion ratings of the 51 Neal-Smith short period/FCS configurations for the pitch attitude tracking task. The pilot opinion rating was correlated with the low frequency performance term, feedback at a disturbance cutoff frequency, as well as the high frequency performance term, sensor noise cutoff frequency, in the open loop transfer function of the pilot/vehicle system. In this proposed technique, the handling quality problem was interpreted based on the tracking error and the response speed of the closed loop system, which are the fundamental measures of the closed loop performance to quantify the general tracking control problems.

The results obtained in this study are summarized as follows:

- (1) Pilot opinion rating is a strong function of the gain of the open loop transfer function, feedback, at a disturbance cutoff frequency and a sensor noise cutoff frequency at which a pilot attenuates the observation noise.
- (2) Feedback at a disturbance cutoff frequency is a measure of the pilot's tracking ability in a pilot working band which is defined by a given task.
- (3) Sensor noise cutoff frequency is a measure of the pilot's observing ability in the high frequency range. If a pilot attenuates the observation noise at the relatively high frequency, the response of the closed loop pilot/vehicle system is also relatively fast.
- (4) The major source of the pilot induced oscillation problem is due to the small phase lag or phase lead of the pilot in a high frequency range, which are required to meet

the high frequency stability. It means that rapid movements of a pilot are required to stabilize a vehicle in a high frequency range.

Future work in this area will include an extension of this study to the analysis of the complex multiloop high-order systems, and study possible extension of the results presented in this thesis to the formulation of a general pilot opinion rating system.

## REFERENCES

1. Bacon, B. J. and Schmidt, D. K., "An Optimal Control Approach to Pilot/Vehicle Analysis and the Neal-Smith Criteria," *Journal of Guidance and Control*, Vol. 6, No. 5, Sep.-Oct., 1983, pp. 339-347.
2. Anderson, M. R. and Schmidt, D. K., "Closed-Loop Pilot Vehicle Analysis of the Approach and Landing Task," *Journal of Guidance and Control*, Vol. 10, No. 2, Mar.-Apr., 1987, pp. 187-194.
3. Thompson, P. T. and McRuer, D. T., "Comparison of the Human Optimal Control and Crossover Models," *AIAA Guidance, Navigation and Control Conference*, Minneapolis, Minnesota, August, 1988, AIAA paper No. 88-4183.
4. McRuer, D. T. and Schmidt, D. K., "Pilot-Vehicle Analysis of Multi-Axis Tasks," *Journal of Guidance and Control*, Vol. 13, No. 2, Mar.-Apr., 1990, pp. 348-355.
5. Kleinman, D.L., "Optimal Linear Control for Systems with Time Delay and Observation Noise," *IEEE, Trans. Auto. Control*, October 1969, pp. 524-527.
6. Kleinman, D. L., Baron, S. and Levison, W. H., "An Optimal Control Model of Human Response, Parts I and II," *Automatica*, Vol.6, 1970, pp. 357-383.
7. Cooper, G. E. and Harper, R. P., "The Use of Pilot Rating in the Evaluation of Aircraft Handling Qualities," NASA TN-D-5153, 1969.
8. Neal, T. P. and Smith, R. E., "An Inflight Investigation to Develop System Design Criteria for Fighter Airplanes," Air Force Flight Dynamics Laboratory, WPAFB, Ohio, AFFDL TR-70-74, Dec. 1970.
9. Graham, E. S., Krendel, E. S., McRuer, D. T. and Reisener, W., "Human Pilot Dynamics in Compensatory System: Theory, Models and Experiments with Controlled-Element and Forcing Function Variation," AFFDL TR-65-15, 1965.
10. Magdaleno, R., McRuer, D. T. and Stepelford, R. L., "Pilot Describing Function Measurements in a Multiloop Tasks," NASA CR-542, 1966.
11. McRuer, D. T., Ashkenas, I. L. and Guerre, C. L., "A Systems Analysis View of Longitudinal Flying Qualities," WPAFB, Ohio: Air Force Flight Dynamics Laboratory, WADD-TR-60-15, 1960.
12. Anderson, R. O., "A New Approach to the Specification and Evaluation of Flying Qualities," WPAFB, Ohio: Air Force Flight Dynamics Laboratory, AFFDL-TR-69-120, 1970.
13. Onstott, E. D., "Prediction and Evaluation of Flying Qualities in Turbulence,"

- Proceedings of the 8th Annual Conference on Manual Control*, University of Michigan, 1972, pp. 435-446.
14. Adams, J. J. and Moore, F. L., "An Analytical Study of Aircraft Lateral-Directional Handling Qualities Using Pilot Models," NASA TN D-8103, 1976.
  15. Dillow, J. D. and Picha, G. P., "Application of the Optimal Pilot Model to the Analysis of Aircraft Handling Qualities," WPAFB, Ohio: Air Force Institute of Technology, AFIT-TR-75-4, 1975.
  16. Phatak, A., Weinert, H. Segall, I., and Day, C., "Identification of a Modified Optimal Control Model for the Human Operator," *Automatica*, Vol. 12, 1976, pp. 31-41.
  17. Hess, R. A., "A Method for Generating Numerical Pilot Opinion Ratings Using the Optimal Pilot Model," NASA TM X-73, 101, 1976.
  18. Hess, R. A., "Prediction of Pilot Opinion Ratings Using an Optimal Pilot Model," *Human Factors*, 1977, 19(5), pp. 459-475.
  19. Schmidt, D. K., "On the Use of the OCM's Objective Function as a Pilot Rating Metric," *Proceedings of 17th Annual Conference on Manual Control*, Los Angeles, Calif., June 1981.
  20. Elkind, J. I., "Characteristics of Simple Manual Control Systems.", M.I.T. Lincoln Lab., Lexington, MA, 1956.
  21. Krendel, E. S. and McRuer, D. T., "Dynamic Response of Human Operator," Wright Air Development Center, Wright Patterson AFB, Dayton, 1957.
  22. Gram, D., Krendel, E. S., McRuer, D. T., and Reisner, W., "Human Pilot Dynamics in Compensatory Systems: Theory, Models and Experiments with Controlled Element and Forcing Function Variations," AFFDL-TR-65-15, July, 1965.
  23. Baron, S., Levison, W. H., and Kleinman, D. T., "A Model for Human Controller Remnant," *IEEE, Trans. Man-Machine System*, Vol. 10, 1969.
  24. Bode, H. W., "Relation Between Attenuation and Phase in Feedback Amplifier Design," *Bell System Technical Journal*, July 1940.
  25. Lurie, B. J., *Feedback Maximization*, Artech House, Inc., Dedham, MA, 1986.
  26. Horwitz, I. M., *Synthesis of Feedback Systems*, Academic Press, NY, 1963.
  27. Kissel, G., "The Bode integrals and Wave Front Tilt Control," *AIAA Guidance Navigation and Control Conference*, Portland, OR, August, 1990. AIAA Paper No. 90-3421.

## APPENDIX

### MATLAB PROGRAM FOR THE OPTIMAL CONTROL MODEL

```
% fname: PILOT.M
% This program is developed for solving the OCM.
% This should be executed externally by the user in the Matlab.
% Mfile and function
% HEAD      : descriptions of program
% COMFLOW   : computation flow for solving OCM
% INPUTSYS  : Enter system and shaping filter data
% TRANSF    : Enter transfer function data
% GETEQN    : transform transfer function to state space eqn
% CANON2    : 2nd canonical form
% SYSEQN    : Enter state space data
% OPTIMAL   : Computation of OCM in time domain
% SOLVELQR  : LQR problem
% SOLVEKBF  : KBF/IP problem
% MATITG    : Analytical solution of special matrix integration
% FDOMAIN   : Generate pilot transfer function
% CUTOFF    : Bode ideal cutoff analysis
% MAXMIN1   : Calculation of max or min value
% MAXMIN2   : Calculation of max or min value
% CHECKIN   : Check input data and parameters
% RESULTS   : Show results
% TFRESULT  : Time and frequency domain performance
% BODEPLOT  : Bode plot
% PTF       : Pilot transfer function
% OUTPUT    : Write results in data file
```

```
HEAD;
while 1
    COMFLOW;
    if MenuNo==1
        INPUTSYS;
    elseif MenuNo==2
        OPTIMAL;
    elseif MenuNo==3
        FDOMAIN;
    elseif MenuNo==4
        CUTOFF;
    elseif MenuNo==5
        CHECKIN;
    elseif MenuNo==6
        RESULTS;
    elseif MenuNo==7
        OUTPUT;
    elseif MenuNo==8
        clear MenuNo
        break;
    end
end
```

```
% fname: HEAD.M
% general descriptions of the program.

clc
fprintf('> PREDICTION OF PILOT OPINION RATINGS (POR)\n')
fprintf('. This program was developed for solving the OCM.\n')
fprintf('. All input parameters should be entered with [ ].\n')
fprintf('. Bode ideal cutoff analysis is used for the prediction of\n')
fprintf(' the POR (Cooper-Harper rating) in the frequency domain.\n\n')
fprintf('. Robert L. Swaim & Jounguk Kim\n')
fprintf(' School of Mechanical and Aerospace Engineering\n')
fprintf(' Oklahoma State University\n')
fprintf(' July, 1993\n\n')
fprintf('> Hit any key to continue :\n ')
pause;
```



```
% fname: COMFLOW.M
% sequence in computation of OCM

fprintf('\n')
clc;
fprintf('> Computation flow\n')
fprintf(' 1. Input system equation \n')
fprintf(' 2. Solve human optimal control model \n')
fprintf('    LQR (Linear Quadratic Regulator) \n')
fprintf('    KBF (Kalman Bucy Filter)/LP(Linear Predictor)\n')
fprintf(' 3. Frequency domain performance \n')
fprintf(' 4. Bode ideal cutoff anaysis \n')
fprintf(' 5. Check input data\n')
fprintf(' 6. Show output data\n')
fprintf(' 7. Write output data \n')
fprintf(' 8. Quit \n')
fprintf('> Select a number : ')
MenuNo=input(' ');
```

```
% fname: INPUTSYS.M
% Enter system equation
% (transfer function or state space equation)

while 1
    fprintf('\n')
    clc;
    fprintf('> Input system equation\n')
    fprintf(' 1. Transfer function \n')
    fprintf(' 2. State space equation \n')
    fprintf(' 3. quit\n')
    fprintf('> Select a number : ')
    No=input(' ');
    if No==1
        TRANSF;
    elseif No==2
        SYSEQN;
    elseif No==3
        clear No
        break;
    end
end
```

```

% fname: TRANSF.M
% Enter input data for vehicle and filter transfer function
% 1.  $y(s) = G_s(s)u(s) + G_w(s)w(s)$ 
% 2.  $y(s) = -G_s(s)u(s) + G_w(s)w(s)$ 
%    $G_s(s)$ : vehicle transfer function
%    $G_w(s)$ : filter transfer function
%    $u(s)$ : optimal input
%    $w(s)$ : white noise
%    $y(s)$ : error to the command signal
% IMPORTANT
% (order of denominator)-(order of numerator) >= 1 in  $G_s(s)$ 
% (order of denominator)-(order of numerator) >= 2 in  $G_w(s)$ 
% variables
% nSystem, dSystem      : numerator, denominator of  $G_s(s)$ 
% gSystem, zSystem, pSystem : gain, zero, pole of  $G_s(s)$ 
% nFilter, dFilter      : numerator, denominator of  $G_f(s)$ 
% gFilter, zFilter, pFilter : gain, zero, pole of  $G_f(s)$ 
% A, B, C, D, E        : system matrix of state space eqn

clear
yes=1;
while (yes)
    fprintf('\n')
    clc;
    fprintf('> Enter vehicle and filter transfer function.\n')
    fprintf(' 1.  $y(s) = G_s(s)u(s) + G_w(s)w(s)$ \n')
    fprintf(' 2.  $y(s) = -G_s(s)u(s) + G_w(s)w(s)$  \n')
    fprintf(' 3. quit\n')
    fprintf(' IMPORTANT\n')
    fprintf('   u(s) : Optimal control input\n')
    fprintf('   w(s) : White noise\n')
    fprintf('   y(s) : Error to the command signal\n')
    fprintf('    $G_s(s)$  : Vehicle transfer function\n')
    fprintf('    $G_w(s)$  : Filter transfer function\n');
    fprintf('   order(den)-order(num) >= 1 in  $G_s(s)$ \n')
    fprintf('   order(den)-order(num) >= 2 in  $G_w(s)$ \n')
    fprintf('> Select a number : ')
    case=input(' ');
    if case==1 | case==2
        fprintf('          K(N1s+N2) (N3s+N4) (N5s+N6) (N7s+N8) (M1s^2+M2s+M3)\n')
        fprintf(' (M4s^2+M5s+M6)\n')
        fprintf('  $G_s(s) =$ -----\n')
        fprintf(' -----\n')
        fprintf('          (D1s+D2) (D3s+D4) (D5s+D6) (D7s+D8) (E1s^2+E2s+E3)\n')
        fprintf(' (E4s^2+E5s+E6)\n')
        fprintf(' Integrator should have its own block. (ex) N1=D2=0, N2=D1=1\n')
        fprintf(' order(den)>=order(num) at each block.\n')
        fprintf('> Enter num of  $G_s(s)$  in [ K N1 N2 N3 N4 N5 N6 N7 N8 ] :')
        nSystem1=input(' ');
        fprintf('> Enter num of  $G_s(s)$  in [ M1 M2 M3 M4 M5 M6 ] :')
        nSystem2=input(' ');
        fprintf('> Enter den of  $G_s(s)$  in [ D1 D2 D3 D4 D5 D6 D7 D8 ] :')
        dSystem1=input(' ');
        fprintf('> Enter den of  $G_s(s)$  in [ E1 E2 E3 E4 E5 E6 ] :')
        dSystem2=input(' ');
        fprintf('          K(N1s^2+N2s+N3)\n')
        fprintf('  $G_f(s) =$ -----\n')
        fprintf('          (D1s^2+D2s+D3)\n')
        fprintf('> Enter num of  $G_w(s)$  in [ K N1 N2 N3 ] :')
        nFilter1=input(' ');
        fprintf('> Enter den of  $G_w(s)$  in [ D1 D2 D3 ] :')
        dFilter1=input(' ');
        fprintf('> Input data is correct ? (y/n) : ')
        s=input(' ','s');
    end
end

```

```

    if s=='Y'|s=='y'
        yes=0;
    else
        yes=1;
    end
elseif case==3
    fprintf('> Use state space form for input data.\n')
    fprintf('> Hit any key to continue : \n ')
    pause;
    break;
end
end
fprintf(' processing...\n ')
while(case~=3)
    K=nSystem1(1);
    N1=nSystem1(2);N2=nSystem1(3);N3=nSystem1(4);N4=nSystem1(5);
        N5=nSystem1(6);N6=nSystem1(7);N7=nSystem1(8);N8=nSystem1(9);
    M1=nSystem2(1);M2=nSystem2(2);M3=nSystem2(3);
    M4=nSystem2(4);M5=nSystem2(5);M6=nSystem2(6);
    D1=dSystem1(1);D2=dSystem1(2);D3=dSystem1(3);D4=dSystem1(4);
    D5=dSystem1(5);D6=dSystem1(6);D7=dSystem1(7);D8=dSystem1(8);
    E1=dSystem2(1);E2=dSystem2(2);E3=dSystem2(3);
    E4=dSystem2(4);E5=dSystem2(5);E6=dSystem2(6);
    [As,Bs,Cs,Ds]=linmod('System');
    K=nFilter1(1);
    N1=nFilter1(2);N2=nFilter1(3);N3=nFilter1(4);
    D1=dFilter1(1);D2=dFilter1(2);D3=dFilter1(3);
    N4=K*[N1 N2 N3];
    D4=[D1 D2 D3];
    [Af,Bf,Cf,Df]=tf2ss(N4,D4);
    [zSystem,pSystem,gSystem]=ss2zp(As,Bs,Cs,Ds,1);
    [zFilter,pFilter,gFilter]=ss2zp(Af,Bf,Cf,Df,1);
    clc;
    fprintf('> System transfer function : Gs(s)')
    fprintf('\n Gain : %g\n',gSystem)
    fprintf(' Zeros : \n')
    s=size(zSystem);
    imax=s(1,1);
    for i=1:imax,..
        fprintf('          (%15.7f) + (%15.7f)j\n',real(zSystem(i)),..
            imag(zSystem(i)));..
    end
    s=size(pSystem);
    imax=s(1,1);
    fprintf(' Poles : \n')
    for i=1:imax,..
        fprintf('          (%15.7f) + (%15.7f)j\n',real(pSystem(i)),..
            imag(pSystem(i)));..
    end
    fprintf('> Hit any key to continue : \n ');
    pause
    fprintf('\n> Filter transfer function : Gw(s)')
    fprintf('\n')
    fprintf(' Gain : %g\n',gFilter)
    fprintf(' Zeros : \n')
    s=size(zFilter);
    imax=s(1,1);
    for i=1:imax,..
        fprintf('          (%15.7f) + (%15.7f)j\n',real(zFilter(i)),..
            imag(zFilter(i)));..
    end
    fprintf(' Poles : \n')
    s=size(pFilter);
    imax=s(1,1);

```

```

for i=1:imax,..
    fprintf('          (%15.7f) + (%15.7f)j\n',real(pFilter(i)),..
            imag(pFilter(i)));..
end
fprintf('> Gs(s) and Gw(s) are correct ? : (y/n)');
s=input(' ','s');
if s=='n' | s=='N'
    break
end
fprintf(' Processing...')
[nSystem3,dSystem3]=ss2tf(As,Bs,Cs,Ds,1);
[nFilter2,dFilter2]=ss2tf(Af,Bf,Cf,Df,1);
sizeS=max(size(dSystem3));
sizeF=max(size(dFilter2));
for i=1:sizeS
    if nSystem3(i)>0.00001
        nSystem=nSystem3(i:sizeS)*dSystem3(1);
        break
    end
end
for i=1:sizeF
    if nFilter2(i)>0.00001
        nFilter=nFilter2(i:sizeF)*dFilter2(1);
        break
    end
end
dSystem=dSystem3/dSystem3(1);
dFilter=dFilter2/dFilter2(1);
% transfer function to state space equation (system eqn)
if case==1
    index=1;
else case==2
    index=-1;
end
[Ao,BEo,Co,Do]=GETEQN(nSystem,dSystem,nFilter,dFilter,index);
[A,BE,C,D]=minreal(Ao,BEo,Co,Do);
B=BE(:,1);
E=BE(:,2);
D=D(:,1);
% original state eqn matrix
Bo=BEo(:,1);
Eo=BEo(:,2);
Do=Do(:,1);
size1=max(size(Ao));
size2=max(size(A));
fprintf('\n')
clc;
fprintf('> State space equation \n')
fprintf(' dx(t) = Ao x(t) + Bo u(t) + Eo w(t)\n')
fprintf(' y(t) = Co x(t) + Do u(t)\n')
Ao
fprintf('> Hit any key to continue : \n ')
pause;
Bo
fprintf('> Hit any key to continue : \n ')
pause;
Eo
fprintf('> Hit any key to continue : \n ')
pause;
Co
fprintf('> Hit any key to continue : \n ')
pause;
Do
fprintf('> Hit any key to continue : \n ')

```

```

pause;
% reduced state equation matrix
if size1 > size2
    fprintf('\n')
    clc;
    fprintf('> Reduced state space equation \n')
    fprintf(' dx(t) = A x(t) + B u(t) + E w(t)\n')
    fprintf(' y(t) = C x(t) + D u(t)\n')
    A
    fprintf('> Hit any key to continue : \n ')
    pause;
    B
    fprintf('> Hit any key to continue : \n ')
    pause;
    E
    fprintf('> Hit any key to continue : \n ')
    pause;
    C
    fprintf('> Hit any key to continue : \n ')
    pause;
    D
    fprintf('> Hit any key to continue : \n ')
    pause;
end
break
end
clear i s yes imax
clear nSystem1 nSystem2 nSystem3 nFilter1 nFilter2
clear dSystem1 dSystem2 dSystem3 dFilter1 dFilter2
clear As Bs Cs Ds Af Bf Cf Df BE BEO Ao Bo Co Do Eo
clear K N1 N2 N3 N4 N5 N6 N7 N8 M1 M2 M3 M4 M5 M6
clear D1 D2 D3 D4 D5 D6 D7 D8 E1 E2 E3 E4 E5 E6
clear k d1 d2 d3 d4 d5 d6 n1 n2 n3 n4 n5 n6
clear a b c d m q p iu iy nblocks sizeS sizeF size1 size2
save afile

```

```

% fname: GETEQN.M
% get state space equation from transfer function
% (order of denominator)-(order of numerator) >= 1 in Gs(s)
% (order of denominator)-(order of numerator) >= 2 in Gw(s)

function [Ac,BEc,Cc,Dc]=GETEQN(nSystem,dSystem,nFilter,dFilter,index)
[A1,B1,C1,D1]=CANON2(nFilter,dFilter);
[A2,B2,C2,D2]=CANON2(nSystem,dSystem);
k1=max(size(nFilter));
k2=max(size(dFilter));
m1=max(size(nSystem));
m2=max(size(dSystem));
n1=max(size(A1));
n2=max(size(A2));
Ac=[A1,zeros(n1,n2);
    zeros(n2,n1),A2];
Bc=[zeros(n1,1);B2];
Ec=[B1;zeros(n2,1)];
BEc=[Bc,Ec];
if (m2-m1)>1
    Cc=[eye(2),zeros(2,n1-2),index*eye(2),zeros(2,n2-2)];
    Dc=[zeros(2)];
elseif (m2-m1)==1
    if m2==2
        Cc=[eye(2),zeros(2,n2-2),index*[1 A2]'];
        Dc=[0 0; index*B2 0];
    elseif m2>2
        Cc=[eye(2),zeros(2,n1-2),index*eye(2),zeros(2,n2-2)];
        Dc=[0 0; index*B2(1) 0];
    end
end
end

```

```

% fname: CANON2.M
% second canonical form (phase variable)

function [A,B,C,D]=CANON2(num,den)
n1=max(size(num));
n2=max(size(den));
if n1>n2,..
    fprintf('> Error : order of numerator is greater than denominator\n');
    break;..
end
if n2==2 & n1==1
    A=-den(2);
    B=num/den(1);
    C=1;
    D=0;
elseif n2>2
    A=zeros(n2-1);
    A(1:n2-2,2:n2-1)=eye(n2-2);
    A(n2-1,:)=-den(n2:-1:2);
    if n2>n1,..
        NUM=zeros(1,n2);..
        NUM(1,n2-n1+1:n2)=num;..
    else,..
        NUM=num;..
    end
    b=zeros(n2,1);
    b(1)=NUM(1);
    for i=2:n2;..
        for j=1:i-1,..
            b(i)=-den(1+j)*b(i-j)+b(i);..
        end,..
        b(i)=b(i)+NUM(i);..
    end
    B=b(2:n2,1);
    C=zeros(1,n2-1);
    C(1,1)=1;
    D=b(1);
end
end

```



```

% filename: SYSEQN.M
% input system equation as state space form
% dx(t) = Ao x(t) + Bo u(t) + Eo w(t)
% y(t) = Co x(t) + Do u(t)

yes=1;
while(yes)
    clear;
    clc;
    fprintf('> Enter data for state space equation.\n')
    fprintf(' dx(t) = Ao x(t) + Bo u(t) + Eo w(t) \n')
    fprintf(' y(t) = Co x(t) + Do u(t) \n')
    fprintf('> Enter Ao matrix : ')
    Ao=input(' ');
    fprintf('> Enter Bo matrix : ')
    Bo=input(' ');
    fprintf('> Enter Fo matrix : ')
    Eo=input(' ');
    fprintf('> Enter Co matrix : ')
    Co=input(' ');
    fprintf('> Enter Do matrix : ')
    Do=input(' ');
    fprintf('> Input data is correct ? (y/n) : ')
    s=input(' ', 's');
    if s=='Y'|s=='y'
        yes=0;
    else
        yes=1;
    end
end
% original state equaiton matrix
BEo=[Bo,Eo];
DEo=[Do,zeros(2,1)];
[A,Bm,C,Dm]=minreal(Ao,BEo,Co,DEo);
B=Bm(:,1);
E=Bm(:,2);
D=Dm(:,1);
% reduced state equation matrix
size1=max(size(A));
size2=max(size(Ao));
if size1 < size2
    clc;
    fprintf('> Reduced state space equation \n')
    fprintf(' dx(t) = A x(t) + B u(t) + E w(t) \n')
    fprintf(' y(t) = C x(t) + D u(t)\n')
    A
    fprintf('> Hit any key to continue : \n ')
    pause;
    B
    fprintf('> Hit any key to continue : \n ')
    pause;
    E
    fprintf('> Hit any key to continue : \n ')
    pause;
    C
    fprintf('> Hit any key to continue : \n ')
    pause;
    D
    fprintf('> Hit any key to continue : \n ')
    pause;
    fprintf('\n')
end
[nSystem1,dSystem1]=ss2tf(A,B,C(1,:),D(1,:),1);
[nFilter1,dFilter1]=ss2tf(A,E,C(1,:),zeros(1),1);

```

```

[nSystem,dSystem]=minreal(nSystem1,dSystem1);
[nFilter,dFilter]=minreal(nFilter1,dFilter1);
[zSystem,pSystem,gSystem]=tf2zp(nSystem,dSystem);
[zFilter,pFilter,gFilter]=tf2zp(nFilter,dFilter);
if gSystem > 0
    case=1;
else
    case=2;
end
clc;
fprintf('> Transfer function of system and shaping filter\n')
fprintf(' y(s)= Gs(s)u(s) + Gw(s)w(s)\n')
fprintf(' Gs(s) : Vehicle transfer function\n')
fprintf(' Gw(s) : Filter transfer function\n')
gSystem
fprintf('> Hit any key to continue : \n ')
pause;
zSystem
fprintf('> Hit any key to continue : \n ')
pause;
pSystem
fprintf('> Hit any key to continue : \n ')
pause;
gFilter
fprintf('> Hit any key to continue : \n ')
pause;
zFilter
fprintf('> Hit any key to continue : \n ')
pause;
pFilter
fprintf('> Hit any key to continue : \n ')
pause;
clear yes s case No BEo DEo Bm Dm size1 size2 ;
clear nSystem1 dSystem1 nFilter1 dFilter1
save afile;

```

```
% fname: OPTIMAL.M
% This is a sequence of the calculation for optimal control model.

while 1
    fprintf('\n')
    clc;
    fprintf('> Solve human optimal control model\n')
    fprintf(' 1. solve L Q R\n')
    fprintf(' 2. solve K B F/linear predictor\n')
    fprintf(' 3. quit \n')
    fprintf('> Select a number : ')
    No=input(' ');
    if No==1
        SOLVELQR;
    elseif No==2
        SOLVEKBF;
    elseif No==3
        clear No;
        break;
    end
end
end
```

```

% fname: SOLVELQR.M
% Input
% [q1,q2]:weights on error (y1) and error rate (y2)
% Tn      :neuro-muscular time constant
% Output
% r: weight on input (u)
% G: weight on input rate (du/dt)
% To solve the Linear Quadratic Regurator (LQR) problem
% for a single input
% cost function:
%  $J=E[y'Qy + G(du/dt)^2]=[x_0'(C_0'QC_0)x_0 + G(du/dt)^2]$ 
% Q=weights on error(y1) and error rate(y2)
% augmented system equation:
%  $d(x_0)/dt = A_0 x_0 + B_0 du/dt$ 
%  $y = C_0 x_0$ 
%  $x_0=[x \ u]'$ ,  $A_0=[A \ B; 0 \ 0]$ ,  $B_0=[0 \ I]'$ ,  $C_0=[C \ D]$ 
%  $Q_0=C_0'QC_0$ 
% solution
%  $\dot{u}=-Lx_0$ 
%  $L=B_0'K_0/G$ 
%  $0=A_0'K_0+K_0A_0+Q_0-K_0B_0B_0'K_0/G$ 
% iteration to find G: Bisection method
%  $L=[L_1 \ L_2]$ 
%  $1/L_2=Tn$  : iteration stop

run=1;
while (run)
    fprintf('\n')
    clc;
    fprintf('> Solve linear quadratic regurator problem\n')
    fprintf(' cost func : J(u) = E[ q1 y1^2 + q2 y2^2 +'
    fprintf(' G (du/dt)^2 ]\n')
    fprintf(' y1 y2      : error and error rate for single axis\n')
    fprintf(' du/dt      : optimal pilot control rate\n')
    fprintf(' q1 q2      : weights on error and error rate\n')
    fprintf(' G          : weight on control rate \n')
    fprintf('> Enter the weights Q on [y1 y2] : [q1 q2]')
    q=input(' ');
    fprintf('> Enter the neuro-muscular time constant : [Tn]')
    Tn=input(' ');
    fprintf('> Use default range to solve G ? : (y/n)')
    yes=input(' ','s');
    if yes=='n' | yes=='N'
        fprintf(' Recommended initial range of G : [ 0.000001 1 ]\n')
        fprintf('> Enter the initial range for G : [ q1 q2 ]')
        rangeG=input(' ');
    else
        rangeG=[0.000001 1];
    end
    fprintf('> Input data is correct ? : (y/n)')
    yes=input(' ','s');
    if yes=='y' | yes=='Y'
        fprintf(' Processing...')
        Q=[q(1) 0 ;
           0 q(2)];
        G1=rangeG(1);
        G2=rangeG(2);
        ns=max(size(A));% no of states of A
        A0=[ A      B;
            zeros(1,ns) 0];
        B0=[zeros(1,ns) 1]';
        C0=[C D];
        Q0=C0'*Q*C0;
        r=Q0(3,3);
    end
end

```

```

for i=1:ns
    for j=1:ns
        if abs(Q0(i,j))<0.000000000001
            Q0(i,j)=0;
        end
    end
end
[L,K0]=LQR(A0,B0,Q0,G1);
F1=1/L(ns+1)-Tn;
[L,K0]=LQR(A0,B0,Q0,G2);
F2=1/L(ns+1)-Tn;
if F1*F2<0
    run=0;
    fprintf('\n Initial range of G is O.K.\n')
    fprintf('> processing')
else
    run=1;
    fprintf('\n Initial range of G is NOT appropriate for bisection')
    fprintf(' method.\n')
    fprintf('> Hit any key to continue : \n ')
    pause;
end
end
end
run=1;
while (run)
    [L,K0]=LQR(A0,B0,Q0,G1);
    F1=1/L(ns+1)-Tn;
    G3=(G1+G2)/2;
    [L,K0]=LQR(A0,B0,Q0,G3);
    F3=1/L(ns+1)-Tn;
    if F1*F3<0
        G2=G3;
        fprintf('.')
    else
        G1=G3;
        fprintf('.')
    end
    if abs((G1-G2)/G1)>0.01
        run=1;
    else
        run=0;
    end
end
end
G=G1;
L1=L(1:ns);
L2=L(ns+1);
fprintf('\n The weight on control rate : G = %g',G)
fprintf('\n> Hit any key to continue : \n ')
pause;
clear i j q run yes yes KO G1 G2 G3 rangeG F1 F2 F3 ;
save afile;

```

```

% fname: SOLVEKBF.M
% To solve the Kalman Bucy Filter and linear predictor problem.
% augmented system eqn
%  $d(x1)/dt = A1 x1 + B1 ua + w1$ 
%  $y = C1 x1$ 
%  $x1=[x u]'$ ,  $w1=[w (v)ua]'$ 
%  $A0=[A B;0 -L2]$ ,  $B0=[0 L2]'$ ,  $C1=[C D]$ 
%  $W1=[EWE' 0;0 L2VuaL2']$ 
% covariance matrix for noise : Vy, Vua, W

yes=1;
while (yes)
    fprintf('\n')
    clc;
    fprintf('> Solve Kalman Bucy filter/linear predictor\n')
    fprintf(' KBF/linear predictor estimates the state of\n')
    fprintf(' the controlled system augmented with the neuro-muscular\n')
    fprintf(' mode and driven by an additional white noise source.\n')
    fprintf('> Enter the pure perceptual time delay : [Td]');
    Td=input(' ');
    fprintf('> Enter the covariance of w(t) : [W]');
    W=input(' ');
    fprintf('> Enter the noise ratios for [y1 y2 ua] : [r1 r2 r3]');
    ratios=input(' ');
    fprintf('> Enter the observation thresholds for [y1 y2] : [T1 T2]');
    treshd=input(' ');
    fprintf('> Enter the fractional attention : [f]');
    f=input(' ');
    fprintf('> Input data is correct ? (y/n) : ')
    s=input(' ', 's');
    if s=='Y' | s=='y'
        yes=0;
    else
        yes=1;
    end
end
ratio1=ratios(1); ratio2=ratios(2); ratio3=ratios(3);
T1=treshd(1); T2=treshd(2);
% initial values for iteration
fprintf('\n')
clc;
fprintf('> Kalman Buch filter/linear predictor\n')
fprintf(' processing...\n')
check1=1;
while (check1)
    fprintf('> Do you want to try with default initial values\n')
    fprintf(' for [var(y1) var(y2) var(ua)] ? (y/n)')
    s1=input(' ', 's');
    if s1=='Y' | s1=='y'
        vary1=0.1; vary2=0.1; varua=0.1;
    else
        fprintf('> Enter initial values for [var(y1) var(y2) var(ua)] : ')
        invar=input(' ');
        vary1=invar(1); vary2=invar(2); varua=invar(3);
    end
    fprintf(' processing')
    check2=1;
    check3=0;
    count1=0;
    count2=0;
    while (check2)
%construct augmented matrix
        fprintf('.');
        count1=count1+1;

```

```

count2=count2+1;
erfc1=1-ERF(T1/(sqrt(2)*sqrt(vary1)));
erfc2=1-ERF(T2/(sqrt(2)*sqrt(vary2)));
Vy1=pi*ratio1*vary1/(f*erfc1^2);
Vy2=pi*ratio2*vary2/(f*erfc2^2);
Vy=[Vy1 0 ;
    0 Vy2];
Vua=pi*ratio3*varua;
A1=[ A B;
     zeros(1,ns) -L2];
B1=[zeros(1,ns) L2]';
C1=[C,D];
W1=[ E*W*E' zeros(ns,1);
     zeros(1,ns) L2*Vua*L2'];
E1=eye(ns+1);
[H1,sigma1]=LQE(A1,E1,C1,W1,Vy);
Lopt=[L1/L2 0];
Int=MATITG(A1,W1,Td);
E1=expm(A1*Td)*sigma1*expm(A1'*Td)+Int;
A3=A1-B1*Lopt;
W3=expm(A1*Td)*H1*Vy*H1'*expm(A1'*Td);
Xhat1=LYAP(A3,W3);
X1=E1+Xhat1;
Y=C1*X1*C1';
Ua=Lopt*Xhat1*Lopt';
if abs((vary1-Y(1,1))/max(vary1,Y(1,1))) > 0.005..
    | abs((vary2-Y(2,2))/max(vary2,Y(2,2))) > 0.005
    check2=1;
elseif abs((varua-Ua)/max(varua,Ua)) > 0.005
    check2=1;
else
    check1=0;
    check2=0;
    check3=1;
end
if count2==1
    temp1=vary1; temp2=vary2; temp3=varua;
elseif count2==2;
    temp4=vary1; temp5=vary2; temp6=varua;
end
vary1=Y(1,1); vary2=Y(2,2); varua=Ua;
if count2==3
    if (count1-2) < 10
        fprintf('\n iter no :          %g          %g          %g\n',...
            count1-2,count1-1,count1)
    else
        fprintf('\n iter no :          %g          %g          %g\n',...
            count1-2,count1-1,count1)
    end
    fprintf(' var(y1) :%15.7f%15.7f%15.7f\n',temp1, temp4, vary1)
    fprintf(' var(y2) :%15.7f%15.7f%15.7f\n',temp2, temp5, vary2)
    fprintf(' var(ua) :%15.7f%15.7f%15.7f\n',temp3, temp6, varua)
    count2=count2-3;
    fprintf('> Do you want more iterations ? (y/n)')
    s2=input(' ','s');
    if s2=='N' | s2=='n'
        check1=0;
        check2=0;
        fprintf('> Try with another set of initial values ? (y/n)')
        s3=input(' ','s');
        if s3=='Y' | s3=='y'
            fprintf('> Enter new initial values : [var(y1)')
            fprintf(' var(y2) var(ua)]');
            invar=input(' ');

```

```

        vary1=invar(1); vary2=invar(2); varua=invar(3);
        check1=1; check2=1;
        count1=0; count2=0;
        fprintf(' processing')
    end
    else
        fprintf(' processing')
    end
end
end
end
if check3==1
    n1=max(size(X1));
    U=X1(n1,n1);
    dUhat=L*Xhat1*L'+[zeros(1:ns),L2]*E1*[zeros(1:ns),L2]';
    J=trace(Y*Q)+trace(dUhat*G);
    fprintf('\n KBF/linear predictor was solved.\n')
    fprintf(' Covariance of u          (U)      : %g\n',U)
    fprintf(' Covariance of ye          (Y1,Y2) : %g %g\n',...
            Y(1,1),Y(2,2))
    fprintf(' Covariance of ua          (Ua)      : %g\n',Ua)
    fprintf(' Covariance of du/dt         (dUhat) : %g\n',dUhat)
    fprintf(' Optimal cost                 (J)      : %g\n',J)
    fprintf('> Hit any key to continue : \n ')
    pause;
end
clear yes Int s s1 s2 s3 i j ratios treshd invar;
clear erfc1 erfc2 sizeA xlsize n1 count1 count2 A3 W3;
clear check1 check2 check3 vary1 vary2 varua;
clear temp1 temp2 temp3 temp4 temp5 temp6;
save afile;

```



```
% fname: MATITG.M
% matrix integral with time delay

function [y]=matitg(A,W,delay)
[P,D]=eig(A,'nobalance');
invP=inv(P);
n=max(size(invP));
for i=1:n
    for j=1:n
        invPt(i,j)=invP(j,i);
        Pt(i,j)=P(j,i);
    end
end
PWPt=invP*W*invPt;
for i=1:n
    for j=1:n
        temp=D(i,i)+D(j,j);
        if abs(temp) > 0.00001
            Jd(i,j)=PWPt(i,j)/(temp)*(exp(temp*delay)-1);
        else
            Jd(i,j)=PWPt(i,j)*delay;
        end
    end
end
end
y=real(P*Jd*Pt);
```

```

% fname: FDOMAIN.M
% To find pilot transfer function
% 4th order Pade approximation of the pure observation delay

fprintf('\n')
clc;
fprintf('> Frequency domain response \n')
fprintf(' Classical studies of human operator models use transfer ')
fprintf('function models.\n')
fprintf(' Processing...')
[nPade,dPade]=pade(Td,4);
[zPade,pPade,gPade]=tf2zp(nPade,dPade);
[Ap,Bp,Cp,Dp]=tf2ss(nPade,dPade);
A2=zeros(2*ns+7);
A2(1:ns+1,1:2*ns+6)=[A1-H1*C1,-B1*Dp*Lopt,B1*Cp];
A2(ns+2:2*ns+2,1:2*ns+2)=[-expm(A1*Td)*H1*C1,A1-B1*Lopt];
A2(2*ns+3:2*ns+6,ns+2:2*ns+6)=[-Bp*Lopt, Ap];
A2(2*ns+7,ns+2:2*ns+7)=[-L2*Dp*Lopt,L2*Cp,-L2];
B2=zeros(2*ns+7,2);
B2(1:2*ns+2,1:2)=[H1;expm(A1*Td)*H1];
C2=zeros(1,2*ns+7);
C2(1,2*ns+7)=1;
E2=zeros(2*ns+5,1);
E2(2*ns+7,1)=L2;
A3=A2;
B3=B2(:,1)+A2*B2(:,2);
C3=C2;
D3=C2*B2(:,2);
% pilot transfer function
[nPilot,dPilot]=ss2tf(A3,B3,C3,D3,1);
[zPilot,pPilot,gPilot]=tf2zp(-index*nPilot,dPilot);
[nPilotM,dPilotM]=minreal(nPilot,dPilot,0.01);
[zPilotM,pPilotM,gPilotM]=tf2zp(nPilotM,dPilotM);
[Ac,Bc,Cc,Dc]=linmod('Closed1');
[zClosed,pClosed,gClosed]=ss2zp(Ac,Bc,Cc,Dc,1);
[zClosedM,pClosedM]=minreal(zClosed,pClosed,0.001);
[nClosed,dClosed]=ss2tf(Ac,Bc,Cc,Dc,1);
[nClosedM,dClosedM]=minreal(nClosed,dClosed,0.001);
fprintf(' Processing...\n');
omega=logspace(-2,2,100);
[magP,phaseP]=bode(-index*nPilot,dPilot,omega);
[magS,phaseS]=bode(nSystem,dSystem,omega);
[magC,phaseC]=bode(nClosedM,dClosedM,omega);
LmagP=20*log10(magP);
LmagS=20*log10(magS);
LmagC=20*log10(magC);
LmagO=LmagP+LmagS;
if phaseP(1)==180
    phaseP=phaseP-360;
end
if phaseS(1)==180
    phaseS=phaseS-360;
end
phaseO=phaseP+phaseS;
semilogx(omega,LmagP,omega,LmagS,omega,LmagO),grid,xlabel('w (rad/sec)');
ylabel('magnitude (dB)'),title('open-loop transfer function')
pause;
semilogx(omega,magC),grid,xlabel('w (rad/sec)');
ylabel('magnitude'),title('closed-loop transfer function')
%for ascii data
dat1=[omega',LmagP,LmagS,LmagO,LmagC,magC,phaseC];
dat2=[omega',phaseP,phaseS,phaseO,phaseC];
fprintf(' Frequency domain performance was solved.\n')
fprintf('> Hit any key to continue : \n ');

```

```
pause
save a.1 dat1 /ascii /tabs %magnitude Bode plot
save a.2 dat2 /ascii /tabs %phase Bode plot
clear dat1 dat2;
save afile;
```

```

% fname: CUTOFF.M
% Bode ideal cutoff analysis
% Wd : working band
% Wn : break frequency for sensor noise
clc;
fprintf('> Bode ideal cutoff analysis\n');
fprintf(' Find the break frequency for disturbance and sensor noise\n')
fprintf(' on the Bode diagram of the pilot transfer function.\n');
fprintf(' Wd : disturbance break frequency (1st peak)\n')
fprintf(' Wn : sensor noise break frequency (2nd peak)\n')
fprintf('> Hit any key to continue : ');
pause;
semilogx(omega,ImagP),grid,title('Pilot transfer function');
xlabel('w (rad/sec)'),ylabel('magnitude (dB)');
pause;
fprintf('\n Find disturbance break frequency (Wd)\n')
fprintf('> Enter No (local max=1, local min=2, no peak=3) : ')
no=input(' ');
%calculate working band (Wd)
if no==1 | no==2
    fprintf('> Enter subinterval for disturbance break freq : ')
    fprintf('[w1 w2] (rad/sec)');
    range1=input(' ');
    [mPWd,pPWd,Wd]=maxmin1(-index*nPilotM,dPilotM,range1,no);
%enter working band
elseif no==3
    fprintf('> Enter the working band (rad/sec) : ');
    Wd=input(' ');
    [mPWd,pPWd]=bode(-index*nPilotM,dPilotM,Wd);
end
fprintf(' 1st peak is at %g\n',Wd);
%Log magnitude of System and Pilot at Wd
[mSWd,pSWd]=bode(nSystem,dSystem,Wd);
if pSWd==180
    pSWd=-180;
end
ImPWd=20*log10(mPWd);
ImSWd=20*log10(mSWd);
%Feedback at working band (open loop)
ImPSWd=ImPWd+ImSWd;
pPSWd=pPWd+pSWd;
fprintf('> Hit any key to continue : ');
pause;
semilogx(omega,ImagP),grid,title('Pilot transfer function');
xlabel('w (rad/sec)'),ylabel('magnitude (dB)')
pause;
fprintf('\n Find sensor noise break frequency (Wn) \n')
fprintf('> Enter No (local max=1, local min=2, no peak=3) : ')
no=input(' ');
%calculate break frequency for sensor noise (Wn)
if no==1 | no==2
    fprintf('> Enter subinterval for sensor noise break freq : ')
    fprintf('[w1 w2] (rad/sec)');
    range2=input(' ');
    fprintf(' Processing...');
    [mPWn,pPWn,Wn]=maxmin1(-index*nPilotM,dPilotM,range2,no);
elseif no==3
    fprintf('> Enter break frequency for sensor noise (rad/sec) : ');
    Wn=input(' ');
    [mPWn,pPWn]=bode(-index*nPilotM,dPilotM,Wn);
end
if pPWn>0
    pPWn=pPWn-360;
end
end

```

```

fprintf('\n 2nd peak is at %g\n',Wn);
[mSWn,pSWn]=bode(nSystem,dSystem,Wn);
if pSWn>0
    pSWn=pSWn-360;
end
ImPWn=20*log10(mPWn);
ImSWn=20*log10(mSWn);
ImPSWn=ImPWn+ImSWn;
pPSWn=pPWn+pSWn;
%calculate peak of closed loop response
[mag,i]=max(magC);
range3=[omega(i-1) omega(i+1)];
[mPSWp,pPSWp,Wp]=maxmin2(nClosedM,dClosedM,range3,1);
ImPSWp=20*log10(mPSWp);
range4=[0.001 Wp];
[mPSWdr,pPSWdr,Wdr]=maxmin2(nClosedM,dClosedM,range4,2);
droop=1-mPSWdr;
ImPSWdr=20*log10(mPSWdr);
[Gm,Pmargin,Wcg,Wcp]=margin(magP.*magS,phaseO,omega);
Gmargin=20*log10(Gm);
% Bode Ideal Cutoff Analysis
XdB=Gmargin;
Yrad=Pmargin/180;
nWcp=Wcp/Wd;
nWn=Wn/Wd;
slope=-12*(1-Yrad);
highpole=1+abs(max(size(nSystem))-max(size(dSystem)));
%nWc=2*(1-Yrad)*nWn/highpole;
nWc=2^(XdB/(12*(1-Yrad)))+1;
Wc=nWc*Wcp;
maxFB=12*(1-Yrad)*(1+log10(Wc/Wd)/log10(2))-XdB;
pecFB=ImPSWd/maxFB*100;
fprintf(' Cutoff analysis was done.\n');
fprintf('> Hit any key to continue : \n ');
pause
clear i imax no s nWcp nWc XdB Yrad Gm mag
clear rangel range2 range3 range4
save afile

```

```
% fname: MAXMIN1.M
% Local minimum and maximum

function [m,p,w]=maxmin1(num,den,range,case)
yes=1;
while(yes)
    omega=range(1):(range(2)-range(1))/20:range(2);
    [mag,phase]=bode(num,den,omega);
    if case==1
        [m,i]=max(mag);
    elseif case ==2
        [m,i]=min(mag);
    end
    p=phase(i);
    w=omega(i);
    if (omega(i+1)-omega(i))/omega(i)<0.05
        yes=0;
    end
    range=[omega(i-1) omega(i+1)];
end
```

```
% fname: MAXMIN2.M
% Local maximum and minimum

function [m,p,w]=maxmin2(num,den,range,case)
yes=1;
while(yes)
    omega=range(1):(range(2)-range(1))/20:range(2);
    [mag,phase]=bode(num,den,omega);
    if case==1
        [m,i]=max(mag);
    elseif case ==2
        [m,i]=min(mag);
    end
    p=phase(i);
    w=omega(i);
    if i==1
        yes=0;
    else
        range=[omega(i-1) omega(i+1)];
    end
    if (omega(i+1)-omega(i))/omega(i)<0.05
        yes=0;
    end
end
end
```

```

% fname: CHECKIN.M
% check input data is correct or not to confirm results

clc;
fprintf('> System transfer function : Gs(s)')
fprintf('\n Gain : %g\n',gSystem)
fprintf(' Zeros : \n')
s=size(zSystem);
imax=s(1,1);
for i=1:imax,..
    fprintf('          (%15.7f) + (%15.7f)j\n',real(zSystem(i)),...
        imag(zSystem(i)));..
end
s=size(pSystem);
imax=s(1,1);
fprintf(' Poles : \n')
for i=1:imax,..
    fprintf('          (%15.7f) + (%15.7f)j\n',real(pSystem(i)),...
        imag(pSystem(i)));..
end
fprintf('> Hit any key to continue : \n ');
pause
fprintf('\n> Filter transfer function : Gw(s)')
fprintf('\n')
fprintf(' Gain : %g\n',gFilter)
fprintf(' Zeros : \n')
s=size(zFilter);
imax=s(1,1);
for i=1:imax,..
    fprintf('          (%15.7f) + (%15.7f)j\n',real(zFilter(i)),...
        imag(zFilter(i)));..
end
fprintf(' Poles : \n')
s=size(pFilter);
imax=s(1,1);
for i=1:imax,..
    fprintf('          (%15.7f) + (%15.7f)j\n',real(pFilter(i)),...
        imag(pFilter(i)));..
end
fprintf('> Hit any key to continue : \n ');
pause
fprintf('\n')
clc
fprintf('> Input parameters for OCM\n')
fprintf(' Covariance of disturbance (W)      : %9.4f\n',W)
fprintf(' Objective function weights (Q)      : [%9.4f %9.4f]\n',...
    Q(1,1),Q(2,2))
fprintf(' Neuromuscular lag (Tn)              : %9.4f\n',Tn)
fprintf(' Observation delay (Td)               : %9.4f\n',Td)
fprintf(' Observation noise ratio (r1)         : %9.4f\n', ratio1)
fprintf(' Neuromuscular noise ratio (r2)      : %9.4f\n', ratio3)
fprintf(' Observation threshold (T1,T2)       : [%9.4f %9.4f ]\n',T1,T2)
fprintf(' Fractional attention (f)            : %9.4f\n',f)
fprintf('> Hit any key to continue : \n ');
pause;

```



```
% fname: RESULTS.M
% Results menu for time domain and frequency domain performance

while 1
    fprintf('\n')
    clc;
    fprintf('> Simulation results\n')
    fprintf(' 1. Time/frequency domain performance \n')
    fprintf(' 2. Pilot transfer function\n')
    fprintf(' 3. Bode plot \n')
    fprintf(' 4. quit      \n')
    fprintf('> Select a number : ')
    No=input(' ');
    if No==1
        TFRESULT;
    elseif No==2
        PTF;
    elseif No==3
        BODEPLOT;
    elseif No==4
        break;
    end
end
```

```

% fname: TRESULTS.M
% Results of time and freq domain performance on the screen

clc;
fprintf('> Time domain performance\n')
fprintf('  Objevctive function weight (G)      : %15.7f\n',G)
fprintf('  Covariance of u          (U)          : %15.7f\n',U)
fprintf('  Covariance of ye        (Y1,Y2)      : [%15.7f %15.7f]\n',...
      Y(1,1),Y(2,2))
fprintf('  Covariance of ua        (Ua)         : %15.7f\n',Ua)
fprintf('  Covariance of d(uhat)/dt (dUdot)     : %15.7f\n',dUhat)
fprintf('  Optimal cost            (J)          : %15.7f\n',J)
fprintf('> Hit any key to continue : \n ');
pause;
clc;
fprintf('\n> Open loop \n')
fprintf('  Gain crossover frequency (Wcg)       : %15.7f\n',Wcg)
fprintf('  Gain margin              (Gm)        : %15.7f\n',Gmargin)
fprintf('  Phase crossover frequency (Wcp)      : %15.7f\n',Wcp)
fprintf('  Phase margin             (Pm)        : %15.7f\n',Pmargin)
fprintf('> Closed loop\n')
fprintf('  Peak frequency          (Wp)         : %15.7f\n',Wp)
fprintf('  [gain phase] at Wp      : [%15.7f %15.7f]\n',...
      LmPSWp, pPSWp)
fprintf('  Droop frequency         (Wdr)        : %15.7f\n',Wdr)
fprintf('  [gain phase] at Wdr    : [%15.7f %15.7f]\n',...
      LmPSWdr, pPSWdr)
fprintf('> Hit any key to continue : \n ');
pause;
clc;
fprintf('\n> Cutoff analysis\n')
fprintf('  Working band            (Wd)         : %15.7f\n',Wd)
fprintf('  [gain phase] of pilot  at Wd        : [%15.7f %15.7f]\n',...
      LmPWd, pPWd)
fprintf('  [gain phase] of system at Wd        : [%15.7f %15.7f]\n',...
      LmSWd, pSWd)
fprintf('  [gain phase] of Pilot/system at Wd : [%15.7f %15.7f]\n',...
      LmPSWd, pPSWd)
fprintf('  Noise cutoff frequency (Wn)         : %15.7f\n',Wn)
fprintf('  [gain phase] of pilot  at Wn        : [%15.7f %15.7f]\n',...
      LmPWn, pPWn)
fprintf('  [gain phase] of system at Wn        : [%15.7f %15.7f]\n',...
      LmSWn, pSWn)
fprintf('  [gain phase] of pilot/system at Wn : [%15.7f %15.7f]\n',...
      LmPSWn, pPSWn)
fprintf('  Max available feedback (maxFB)      : %15.7f\n',maxFB)
fprintf('  Percent feedback at Wd (pecFB)      : %15.7f\n',pecFB)
fprintf('  Gain slope at Wcp      (slope)      : %15.7f\n',slope)
fprintf('  Ideal phase crossover freq (Wc)     : %15.7f\n',Wc)
fprintf('> Hit any key to continue : ');
pause;

```

```

% fname: TRESULTS.M
% Results of time and freq domain performance on the screen

clc;
fprintf('> Time domain performance\n')
fprintf(' Objective function weight (G)      : %15.7f\n',G)
fprintf(' Covariance of u          (U)          : %15.7f\n',U)
fprintf(' Covariance of ye         (Y1,Y2)       : [%15.7f %15.7f]\n',...
        Y(1,1),Y(2,2))
fprintf(' Covariance of ua        (Ua)          : %15.7f\n',Ua)
fprintf(' Covariance of d(uhat)/dt (dUdot)       : %15.7f\n',dUhat)
fprintf(' Optimal cost            (J)           : %15.7f\n',J)
fprintf('> Hit any key to continue : \n ');
pause;
clc;
fprintf('\n> Open loop \n')
fprintf(' Gain crossover frequency (Wcg)       : %15.7f\n',Wcg)
fprintf(' Gain margin              (Gm)        : %15.7f\n',Gmargin)
fprintf(' Phase crossover frequency (Wcp)      : %15.7f\n',Wcp)
fprintf(' Phase margin             (Em)        : %15.7f\n',Pmargin)
fprintf('> Closed loop\n')
fprintf(' Peak frequency          (Wp)         : %15.7f\n',Wp)
fprintf(' [gain phase] at Wp      : [%15.7f %15.7f]\n',...
        LmPSWp, pPSWp)
fprintf(' Droop frequency         (Wdr)        : %15.7f\n',Wdr)
fprintf(' [gain phase] at Wdr    : [%15.7f %15.7f]\n',...
        LmPSWdr,pPSWdr)
fprintf('> Hit any key to continue : \n ');
pause;
clc;
fprintf('\n> Cutoff analysis\n')
fprintf(' Working band            (Wd)         : %15.7f\n',Wd)
fprintf(' [gain phase] of pilot  at Wd        : [%15.7f %15.7f]\n',...
        LmPWd, pPWd)
fprintf(' [gain phase] of system at Wd        : [%15.7f %15.7f]\n',...
        LmSWd, pSWd)
fprintf(' [gain phase] of Pilot/system at Wd : [%15.7f %15.7f]\n',...
        LmPSWd, pPSWd)
fprintf(' Noise cutoff frequency (Wn)         : %15.7f\n',Wn)
fprintf(' [gain phase] of pilot  at Wn        : [%15.7f %15.7f]\n',...
        LmPWn, pPWn)
fprintf(' [gain phase] of system at Wn        : [%15.7f %15.7f]\n',...
        LmSWn, pSWn)
fprintf(' [gain phase] of pilot/system at Wn : [%15.7f %15.7f]\n',...
        LmPSWn, pPSWn)
fprintf(' Max available feedback (maxFB)       : %15.7f\n',maxFB)
fprintf(' Percent feedback at Wd (pecFB)       : %15.7f\n',pecFB)
fprintf(' Gain slope at Wcp      (slope)       : %15.7f\n',slope)
fprintf(' Ideal phase crossover freq (Wc)      : %15.7f\n',Wc)
fprintf('> Hit any key to continue : ');
pause;

```

```
% fname: BODEPLOT.M
% open loop and closed loop Bode plot on the screen

semilogx(omega,ImagP,omega,ImagS,omega,ImagO),grid,xlabel('w (rad/sec)');
ylabel('magnitude (dB)'),title('open-loop transfer function')
pause;
semilogx(omega,phaseP,omega,phaseS,omega,phaseO),grid,xlabel('w (rad/sec)');
ylabel('phase (degree)'),title('open-loop transfer function')
pause
semilogx(omega,magC),grid,title('closed-loop transfer function')
xlabel('w (rad/sec)'),ylabel('magnitude')
pause
semilogx(omega,ImagC),grid,title('closed-loop transfer function')
xlabel('w (rad/sec)'),ylabel('magnitude (dB)')
pause
semilogx(omega,phaseC),grid,title('closed-loop transfer function')
xlabel('w (rad/sec)'),ylabel('phase (degree)')
pause
```

```
% fname: PTF.M
% Show pilot transfer function on the screen.

clc;
fprintf('> Pilot transfer function : Gpilot(s)\n')
fprintf(' Gain : %g\n',gPilot)
fprintf(' Zeros : ')
s=size(zPilot);
imax=s(1,1);
for i=1:imax,..
    fprintf('\n          (%15.7f) + (%15.7f)j',real(zPilot(i)),..
        imag(zPilot(i))),..
end
fprintf('\n> Hit any key to continue : ')
pause
clc;
fprintf('\n Poles : ')
s=size(pPilot);
imax=s(1,1);
for i=1:imax,..
    fprintf('\n          (%15.7f) + (%15.7f)j',real(pPilot(i)),..
        imag(pPilot(i))),..
end
fprintf('\n> Hit any key to continue : ')
pause
```

```

% fname: OUTPUT.M
% write output data file

clc;
fprintf('> Write output data on the output data file. \n')
fprintf('> Enter the title of this problem : ')
confNo=input(' ','s');
fprintf('> Enter the output file name : ')
fn=input(' ','s');
fprintf(' processing...')
sizeNo=size(confNo);
n=max(sizeNo);
fprintf(fn,'\nTitle : ')
fprintf(fn,confNo)
if index==1
    fprintf(fn,'\n y(s) = Gs(s) u(s) + Gw(s) w(s) \n')
elseif index==-1
    fprintf(fn,'\n y(s) = -Gs(s) u(s) + Gw(s) w(s) \n')
end
fprintf(fn,' y      : tracking error \n')
fprintf(fn,' u      : pilot control input \n')
fprintf(fn,' w      : plant processing driving noise \n')
fprintf(fn,' Gs(s) : system transfer function \n')
fprintf(fn,' Gw(s) : filter transfer function \n\n')
fprintf(fn,'System transfer function : Gs(s)\n')
fprintf(fn,' Gain : %g\n',gSystem)
fprintf(fn,' Zeros : \n')
s=size(zSystem);
imax=s(1,1);
for i=1:imax,..
    fprintf(fn,' (%15.7f) + (%15.7f)j\n',real(zSystem(i)),..
        imag(zSystem(i)));..
end
s=size(pSystem);
imax=s(1,1);
fprintf(fn,' Poles : \n')
for i=1:imax,..
    fprintf(fn,' (%15.7f) + (%15.7f)j\n',real(pSystem(i)),..
        imag(pSystem(i)));..
end
fprintf(fn,'\nFilter transfer function : Gw(s)\n')
fprintf(fn,' Gain : %g\n',gFilter)
fprintf(fn,' Zeros : \n')
s=size(zFilter);
imax=s(1,1);
for i=1:imax,..
    fprintf(fn,' (%15.7f) + (%15.7f)j\n',real(zFilter(i)),..
        imag(zFilter(i)));..
end
fprintf(fn,' Poles : \n')
s=size(pFilter);
imax=s(1,1);
for i=1:imax,..
    fprintf(fn,' (%15.7f) + (%15.7f)j\n',real(pFilter(i)),..
        imag(pFilter(i)));..
end
fprintf(fn,'\nInput parameters for OCM\n')
fprintf(fn,' Covariance of disturbance (W)      : %9.4f\n',W)
fprintf(fn,' Objective function weights (Q)      : [%9.4f %9.4f]\n',..
    Q(1,1),Q(2,2))
fprintf(fn,' Neuromuscular lag (Tn)              : %9.4f\n',Tn)
fprintf(fn,' Observation delay (Td)              : %9.4f\n',Td)
fprintf(fn,' Observation noise ratio (r1)        : %9.4f\n', ratio1)
fprintf(fn,' Neuromuscular noise ratio (r2)     : %9.4f\n', ratio3)

```

```

fprintf(fn,' Observation threshold      (T1,T2) : [%9.4f %9.4f]\n',T1,T2)
fprintf(fn,' Fractional attention      (f)      : %9.4f\n\n',f)
fprintf(fn,'Time domain performance\n')
fprintf(fn,' Objective function weight (G)      : %15.7f\n',G)
fprintf(fn,' Covariance of u                (U)      : %15.7f\n',U)
fprintf(fn,' Covariance of y                (Y1,Y2) : [%15.7f %15.7f]\n',...
        Y(1,1),Y(2,2))
fprintf(fn,' Covariance of ua            (Ua)      : %15.7f\n',Ua)
fprintf(fn,' Covariance of d(uhat)/dt      (dUhat) : %15.7f\n',dUhat)
fprintf(fn,' Optimal cost                    (J)      : %15.7f\n\n',J)
fprintf(fn,'Open loop\n')
fprintf(fn,' Crossover frequency            (Wcg)    : %15.7f\n',Wcg)
fprintf(fn,' Gain margin                     (Gm)     : %15.7f\n',Gmargin)
fprintf(fn,' Crossover frequency            (Wcp)    : %15.7f\n',Wcp)
fprintf(fn,' Phase margin                    (Pm)     : %15.7f\n\n',Pmargin)
fprintf(fn,'Closed loop\n')
fprintf(fn,' Peak frequency                  (Wp)     : %15.7f\n',Wp)
fprintf(fn,' [gain phase] at Wp              : [%15.7f %15.7f]\n',...
        LmPSWp, pPSWp)
fprintf(fn,' Droop frequency                 (Wdr)    : %15.7f\n',Wdr)
fprintf(fn,' [gain phase] at Wdr             : [%15.7f %15.7f]\n\n',...
        LmPSWdr, pPSWdr)
fprintf(fn,'Bode ideal cutoff analysis\n')
fprintf(fn,' Working band                    (Wd)     : %15.7f\n',Wd)
fprintf(fn,' [gain phase] of pilot at Wd     : [%15.7f %15.7f]\n',...
        LmPWd, pPWd)
fprintf(fn,' [gain phase] of system at Wd    : [%15.7f %15.7f]\n',...
        LmSWd, pSWd)
fprintf(fn,' [gain phase] of Pilot/system at Wd : [%15.7f %15.7f]\n',...
        LmPSWd, pPSWd)
fprintf(fn,' Noise cutoff frequency          (Wn)     : %15.7f\n',Wn)
fprintf(fn,' [gain phase] of pilot at Wn     : [%15.7f %15.7f]\n',...
        LmPWn, pPWn)
fprintf(fn,' [gain phase] of system at Wn    : [%15.7f %15.7f]\n',...
        LmSWn, pSWn)
fprintf(fn,' [gain phase] of pilot/system at Wn : [%15.7f %15.7f]\n',...
        LmPSWn, pPSWn)
fprintf(fn,' Max available feedback          (maxFB)  : %15.7f\n',maxFB)
fprintf(fn,' Percent feedback at Wd          (pecFB)  : %15.7f\n',pecFB)
fprintf(fn,' Gain slope at Wcp               (slope)  : %15.7f\n',slope)
fprintf(fn,' Ideal phase crossover freq (Wc) : %15.7f\n',Wc)
fprintf(fn,' \nPadé approximation for observation delay : Gpade(s)\n')
fprintf(fn,' Gain : 1\n')
fprintf(fn,' Zeros : \n')
s=size(zPade);
imax=s(1,1);
for i=1:imax,..
    fprintf(fn,' (%15.7f) + (%15.7f)j\n',real(zPade(i)),imag(zPade(i))),..
end
fprintf(fn,' Poles : \n')
s=size(pPade);
imax=s(1,1);
for i=1:imax,..
    fprintf(fn,' (%15.7f) + (%15.7f)j\n',real(pPade(i)),imag(pPade(i))),...
end
fprintf(fn,' \nPilot Transfer function : Gpilot(s)\n')
fprintf(fn,' Gain : %g\n',gPilot)
fprintf(fn,' Zeros : ')
s=size(zPilot);
imax=s(1,1);
for i=1:imax,..
    fprintf(fn,' \n (%15.7f) + (%15.7f)j',real(zPilot(i)),...
        imag(zPilot(i))),..
end

```

```
fprintf(fn, '\n Poles : ')\ns=size(pPilot);\nimax=s(1,1);\nfor i=1:imax,..\n    fprintf(fn, '\n (%15.7f) + (%15.7f)j', real(pPilot(i)),..\n        imag(pPilot(i))),..\nend\nfprintf('\n Writing was completed in ')\nfprintf(fn)\nfprintf('\n> Hit any key to continue : \n ')\npause;\nclear i imax s fn fn1 fn2 d1 d2;\nclc;
```



2

VITA

Jounguk Kim

Candidate for the Degree of

Doctor of Philosophy

Thesis: BODE IDEAL CUTOFF ANALYSIS FOR PREDICTION OF  
PILOT OPINION RATING

Major Field: Mechanical Engineering

Biographical:

Personal Data: Born in Pusan, Korea, May 5, 1958, the son of Mr. Sou-Bong  
Kim and Mrs. Joung-Suk Pyo

Education: Received the Bachelor of Science degree in Production Engineering  
from Pusan National University in February, 1982; received the Master of  
Science degree in Mechanical Engineering from Oklahoma State  
University in 1988; completed the requirements for the Doctor of  
Philosophy degree at Oklahoma State University in December, 1993

Professional Experience: Graduate Teaching Assistant, School of Mechanical  
and Aerospace Engineering, Oklahoma State University, 1988-1992